universität wien

MASTERARBEIT / MASTER'S THESIS

Titel der Masterarbeit / Title of the Master's Thesis

„**E.T.** The **Evaluation** of **Toxin-producing potential**. A monitoring system for cyanobacteria in bathing waters via amplicon sequencing."

verfasst von / submitted by

Magdalena Sabine Purker, BSc

angestrebter akademischer Grad / in partial fulfilment of the requirements for the degree of

Master of Science (MSc)

Wien, 2021 / Vienna, 2021

Studienkennzahl lt. Studienblatt / degree programme code as it appears on the student record sheet:	UA 066 830
Studienrichtung lt. Studienblatt / degree programme as it appears on the student record sheet:	Masterstudium Molekulare Mikrobiologie, Mikrobielle Ökologie und Immunbiologie
Betreut von / Supervisor:	Mag. Dr. Rainer Kurmayer, Privatdoz.

Abstract

Cyanobacterial blooms are a major problem in freshwater systems as they have an impact on whole ecosystems and can cause serious health problems in humans. Nevertheless, factors influencing the development of cyanobacterial harmful blooms are not well understood. According to Article 8 of the Bathing Waters Directive (2006/7/EC), a monitoring pipeline based on High Throughput Sequencing should be applied, which observes the bacterial species composition over the season and work as early warning system.

The aim of this master thesis was to elaborate a workflow for the monitoring of cyanobacteria in Austrian bathing waters. Therefore, planktonic and benthic samples were obtained from 20 bathing waters during 2020 and analyzed with general bacterial and specific cyanobacterial 16S primers. Next to this, correlations with the cyanobacterial read numbers, toxin concentration as well as abiotic and biotic factors were applied. Finally, benthic mats were collected to estimate the origin of toxins from benthic filamentous cyanobacterial colonies.

The results indicate that the number of cyanobacterial reads and cyanotoxin production were correlated with water surface temperature. Furthermore, it was demonstrated that amplicon sequencing offers great insight into the bacterial community, allowing monitoring and prediction of cyanobacterial harmful algal blooms in bathing waters. Analysing the sequence data revealed higher cyanobacterial numbers when clustering into Amplicon Sequence Variants, compared to Operational Taxonomic Units. Using in-situ fluorescence measurements, a rough quantitative estimate of the cyanobacterial community was obtained. The collected benthic mats were often dominated by potentially toxic cyanobacteria, but toxin production could not be found.

Keywords: Bathing water, Harmful algal bloom, Cyanotoxin, High Throughput Sequencing, AlgaeTorch

Acknowledgement

Throughout the writing of this master thesis I have received great support and assistance.

I would first like to thank my supervisors, Dr. Rainer Kurmayer and Dr. Peter Hufnagl, whose expertise was indispensable in formulating my research questions, methodology and professional consultation. I would also like to acknowledge Dr. Stefanie Dobrovolny, who supported me during lab work and data analysis. A big thanks to my colleagues at AGES IMED Linz for performing the chemical analyses and answering my questions in no time at all.

I would also like to thank Dr. Karin Pall and the team of systema. I have learned a lot during my time with you and always got great support for all my projects and ideas.

Especially, I would like to thank my parents, Barbara and Peter Purker, my sister Anna Purker and my grandparents, Heidemarie and Hermann Pusch, who have motivated and supported me since I was born.

Finally, I would never have been able to complete this master's thesis without the support of Christian Cupak, who not only provided his computer power, language skills and scientific understanding but always has a sympathetic ear for me. The same goes for all my friends who always take my mind off things and made me the person I am today.

This master thesis was founded by AGES (Austrian Agency for Health and Food Safety).

Table of Contents

1 Introduction

1.1 The incredible properties of Cyanobacteria

Cyanobacteria, commonly known as blue-green algae, are photosynthetic, gram-negative bacteria. They are morphologically diverse, as they occur solitary as free-living cells, or as colonies or filaments (Catherine et al., 2013). Beside, cyanobacteria can be part of symbiotic interactions with higher plants, bryophytes (Adams & Duggan, 2008), fungi or sponges (Rai et al., 2002).

Cyanobacteria are one of the oldest living entities on earth. Stromatolite-fossils, as shown in Figure 1, discovered in Australia and North America have been traced back their origin to 2.7 billion years ago. Probably due to this long evolutionary history, cyanobacteria have successfully inhabited nearly every ecosystem worldwide: From the arctic (Trout-Haney et al., 2016) to arid regions (Isichei, 1990), from freshwater to marine systems as well as environmentally extreme habitats, like hypersaline and alkaline lakes (Rampelotto, 2013), or under rapidly changing conditions (Lüttge, 1997).

Fig. 1: Stromatolites. **Source:** Oliver Roetz: https://www.zdf.de/dokumentation/terra-x/stromatolithen-in-westaustralien-100.html.

The rather extreme or variable conditions can be handled due to various physiological adaptations. Beside storage of starch via oxidative photosynthesis of CO_2, some species are also able to fix atmospheric nitrogen (N_2). This pathway is localized in specialized cells, called heterocytes (Muro-Pastor & Hess, 2012), which is indicated by the arrow in Figure 2, where the oxygen-sensitive enzyme nitrogenase is located (Herrero, Muro-Pastor, & Flores, 2001). Heterocytes are, therefore, additionally

covered by a glycolipid- and polysaccharide layer to prevent diffusion of oxygen into the cell (Wolk et al., 1994).

Fig. 2: *Dolichospermum* sp. filament with one heterocyte (signaled by the arrow), originating from a plankton sample from the Old Danube (2018). To prevent contact to oxygen, these cells are lacking photosystem II, thus no photosynthesis is carried out. Instead, carbon compounds are supplied by neighbouring cells, which can be used as an energy source for N_2-fixation. To fix 1 mole of N_2, 16 ATP molecules are needed, from which two moles of NH_3 result. Furthermore, heterocytes contain cyanoglobin, a form of myoglobin, with a high affinity to oxygen, in case of a contamination by oxygen. From supplied carbon compounds cyclic phosphorylation can be carried out, which also results in the production of ATP (Lee, 2008).

These N_2 fixing species, so-called diazotrophics, like *Aphanizomenon, Cylindrospermopsis, Dolichospermum* (former *Anabaena*), *Nodularia* and *Nostoc*, have a competitive advantage over non-diazotrophics (e.g., *Microcystis* (Figure 3), *Oscillatoria* (Figure 4) or *Synechococcus*) in nitrogen-limited ecosystems. Other cyanobacteria, lacking of heterocytes, like *Cyanothece* and *Lyngbia*, use temporal instead of spatial separation to segregate the two metabolic pathways (Berman-Frank et al., 2003). In detail, this means that photosynthesis is carried out during day, whereas at night the metabolism switches to N_2 fixation. Furthermore, Akinetes are present in heterocystous cyanobacteria. These cells are characterized by a thickened cell wall and are filled with cyanophycin, a nitrogen and carbon reserve polymer (Watzer & Forchhammer, 2018), and polyphosphates (Lee, 2008).

Cyanobacteria are able to perform vertical migration with the help of intracellular proteinaceous vacuoles, so-called gas vesicles, which favour cell migration to the surface. This ability gives cyanobacteria a competitive advantage against other (non-motile) phytoplankton species, especially under eutrophic conditions, as they can harvest light at the surface more efficiently, whereby causing shading effects for phototrophic species below (Porat, 2001).

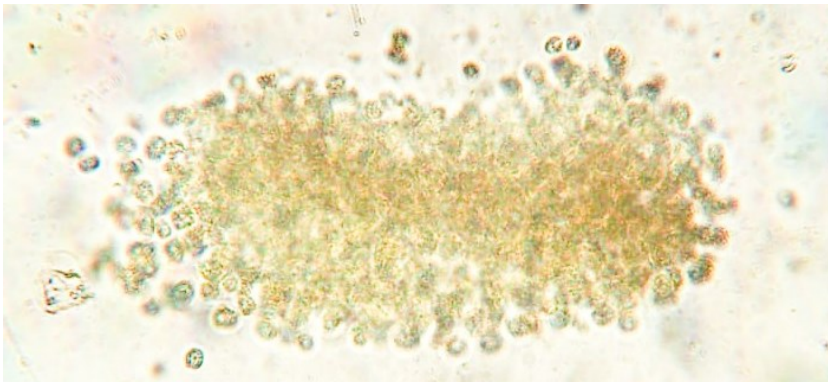

Fig. 3: *Microcystis* sp. colony which does not form heterocytes and is a non-nitrogen fixing organism. The colony-forming organism is responsible for blooms in many lakes and reservoirs worldwide (Xiao et al., 2018). The Genus is eponymous to the frequent cyanotoxin, microcystin.

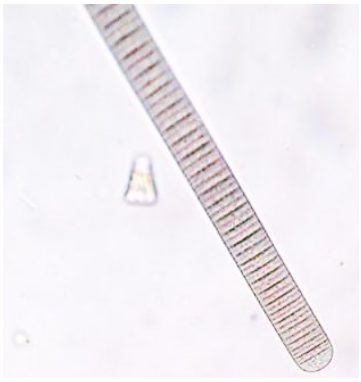

Fig. 4: Non-nitrogen fixing *Oscillatoria* sp. A filamentous species which is named after their oscillating way of movement.

The main light-harvesting pigment of cyanobacteria, which is present in all algal species is chlorophyll a, constituting so-called light reaction centres, embedded in the thylakoid membrane. Additionally, cyanobacteria (except prochlorophytes) possess antenna protein complexes, called phycobilisomes, which are arranged hemidiscoidal on the outer side of the thylakoid membrane, as drawn in Figure 5 (Grigoryeva, 2019). These proteins have their absorption maxima at approximately 560 nm (phycoerythrin), 620 nm (phycocyanin) and 650 nm (allophycocyanin), respectively (Meriluoto et al., 2017). Due to this spectrum shift into the green coloured spectrum, the efficiency of photosynthesis in cyanobacteria is greatly enhanced (Figure 6). As a result, positive net growth can be achieved in even greater depths characterised by prevailing green shaded low light conditions (Dodds & Whiles, 2010).

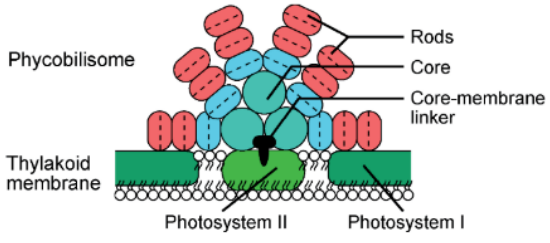

Fig.5: Schematic structure of the phycobilisomes. **Source:** Grigoryeva, 2019

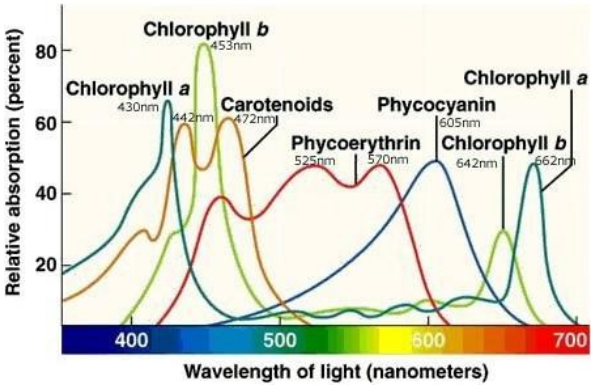

Fig. 6: Absorbing spectrum of various photosynthetic pigments. **Source**: https://algaeresearchsupply.com/pages/lighting-for-algae-cultures

However, cyanobacteria are also considered as cause of the first mass extinction event, since the oxygenation of earth`s atmosphere led to a rapid change in its chemical composition and to the formation of the stratospheric ozone layer. This event is known as Great Oxidation Event (GOE) during the Proterozoic era (2.5 -2.3 Ga[1]) (Schirrmeister, Gugger & Donoghue, 2015). The ability of photosynthesis originated in cyanobacteria and was obtained by other organisms, like eukaryotic algae and plants, through endosymbiosis. The evolution of chloroplasts is widely known as the Archaeplastida hypothesis and goes back to Mereschkowsky (1905). It involves the uptake of a photosynthetic cyanobacterium by a bi-flagellated phagotrophic eukaryotic cell (Sagan, 1967), as shown in Figure 7. This early stage of a stable symbiotic interaction is called Archaeplastid and is supported by the fact that chloroplasts as we know them today have a double cell membrane (Jackson et al., 2015).

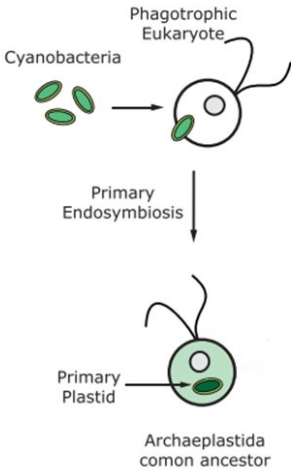

Fig. 7: Schema of the Archaeplastida evolution. **Modified** after Jackson (2015).

Fig. 8: *Microcystis* sp. bloom in Lower Austria.

In marine ecosystems the cyanobacterial species, *Phormidium correlyticum*, is the cause of a coral disease, called Black Band Disease. The cyanobacterial biofilm is visible as a black band around the coral, which kills the healthy tissue and leaves back the dead calcium skeleton (Frias-Lopez et al., 2003). Another fact about marine cyanobacteria is that *Trichodesmium erythraeum*, a bloom forming species containing

[1] Giga annum, meaning a billion of years

phycoerythrin, is responsible for the eponymous colouring of the Red Sea (Ehrenberg, 1830).

1.2 When cyanobacteria form blooms

As mentioned above, cyanobacteria occupy various ecological niches globally, sometimes appearing in form of extensive blooms, as shown in Figure 8. However, there is not an official definition of blooms. In the classical sense, an algal bloom is defined when the algal biomass can be seen with the naked eye (Reynolds & Walsby, 1975). Alternatively, it is called an algal bloom if the total amount of chlorophyll exceeds 20 µg L^{-1} or the vast majority (>50%) of the phytoplankton community belongs to the phylum cyanobacteria (Molot et al., 2014).

Nevertheless, these blooms have a negative effect on water quality and its inhabitants, as turbidity increases and mats floating on the surface cause shading, which limits the growth of macrophytes and other algal species. In addition, large stocks of algae can lead to oxygen depletion, as dead cells sediment and are decomposed under oxygen consumption. This hypoxic zones can cause death of fish and benthic invertebrates (Huisman et al., 2018).

1.3 Cyanobacteria`s response to environmental factors and climate change

Cyanobacterial harmful algal blooms have been reported since many decades (Francis, 1878) and were even mentioned in the drama “The Merchant of Venice” by W. Shakespeare (Huisman et al., 2005). Since then, a lot of research has been done to better understand correlations between abiotic and biotic factors, the occurrence of cyanobacterial blooms and the production of cyanotoxins. Nevertheless, many results are still contradictory or inconclusive (Mantzouki et al., 2018). What is for sure, is the fact that higher water temperature (over 20°C) and nutrient levels (mainly N and P), as well as sunlight and physically stratified water columns support occurrence of cyanobacterial harmful algal blooms (Chorus & Welker, 2021; Davis et al., 2009; Dokulil & Teubner, 2000; Harke et al., 2016; Hudnell, 2008; Vézie et al., 2002). Furthermore, Visser et al. (2016) highlighted that the major driver of climate change, the rising atmospheric CO_2 level, will favour harmful cyanobacterial blooms as the increase in C influx allows even higher levels of productivity.

1.4 Cyanotoxins in detail

In consequence to these blooms, hazardous substances produced by cyanobacteria are resulting in so-called cyanobacterial harmful algal blooms (CHAB`s) (Huisman et al., 2018; Neilan et al., 2013). It is generally accepted that the occurrence of these CHAB`s have increased dramatically in recent decades (Chorus & Bartram, 1999; Hudnell, 2008). For example, the ratio of cyanobacteria to eukaryotic phytoplankton increased since 1945 (Taranu et al., 2015).

In general, two groups of secondary metabolites are produced during a cyanobacterial bloom: (i) cyanotoxins, as well as (ii) taste and odour compounds (Watson et al., 2008). Both groups have negative impact on the function of bathing waters as recreational areas, while, particular attention is paid to cyanotoxins as they can cause health problems for animals and humans (Kaloudis et al., 2017). Even in summer 2020 during sampling activity in the course of this thesis, newspapers reported about the mysterious death of more than 350 elephants in the Okavango Delta, Botswana. Later, the hypothesis was confirmed that a neurotoxin, produced by cyanobacteria, was the cause, as the deaths stopped towards the end of June 2020 which coincided with drying out of the water puddles (Swails & Rahim, 2020). But also, cases of human deaths caused by cyanotoxins are known. During 1996 in Caruaru, Brazil, a total of 76 dialysis patients died after routine renal dialysis treatment due to microcystin and cylindrospermopsin contaminated water (Carmichael et al., 2001).

The original function of cyanotoxin production is not completely known (Holland & Kinnear, 2013), but is thought to act primarily as allelopathic[2] substance by reducing feeding pressure as well as interspecific and intraspecific competition (Jang et al., 2006). By reducing competition the availability of limiting nutrients increases for cyanobacteria (Legrand et al., 2003). Other authors report that these allelopathic substances help in the defence against predators of higher taxonomic levels (Berry, 2008).

Interestingly, not all cyanobacterial genera have the ability to produce cyanotoxins, while others, however, are forming multiple types of them. To make it more complex,

[2] Allelopathy describes the phenomenon where chemical substances released by one organism have an (positive or negative) effect on another organism (Lampert & Sommer, 1997).

nearly all cyanobacterial species are composed of toxic and non-toxic strains (Chorus & Bartram, 1999). Thus individuals either contain genes responsible for toxin-production, or don't (i.e, lacking the respective genes indicative of toxin synthesis) (Davis et al., 2009).

The most common genera that produce toxins are *Aphanizomenon, Chroococcus, Cylindrospermopsis, Dolichospermum, Lyngbya, Microcystis, Merismopedia, Nodularia, Oscillatoria, Planktothrix, Phormidium, Synechococcus* (Codd et al., 2005; Singh & Dhar, 2013). Normally, the toxins are inside the cell. However, when the organism dies and the cell envelope degrades, the toxins are rapidly released (Kurmayer et al., 2017).

Due to the threat of cyanotoxins on humans and animals, the WHO set the life-time upper limit for microcystin-LR concentration in drinking waters at 1 µg L^{-1} (24 µg L^{-1} for recreational waters) and for cylindrospermopsin at 0.7 µg L^{-1} (6 µg L^{-1} for recreational waters). For anatoxin-a, the calculated guideline value in recreational waters is defined as 60 µg L^{-1}, while for saxitoxin a value of 30 µg L^{-1} is assessed (Chorus & Welker 2021). The various types of toxins have different consequences on mammals and are going to be shortly discussed in the following.

1.4.1 Microcystin (MC)

Microcystins are cyclic heptapeptides, where over 200 structural variants have been identified (Puddick et al., 2014). They mostly differ in the 2nd and/or 4th amino acid. For example, the most frequently occurring one, microcystin-LR (Vezie et al., 1997), contains leucin (L) and arginin (R) at the 2nd and 4th position, respectively (Carmichael et al., 1988). The chemical structure, as well as the variable amino acids are demonstrated in Figure 9.

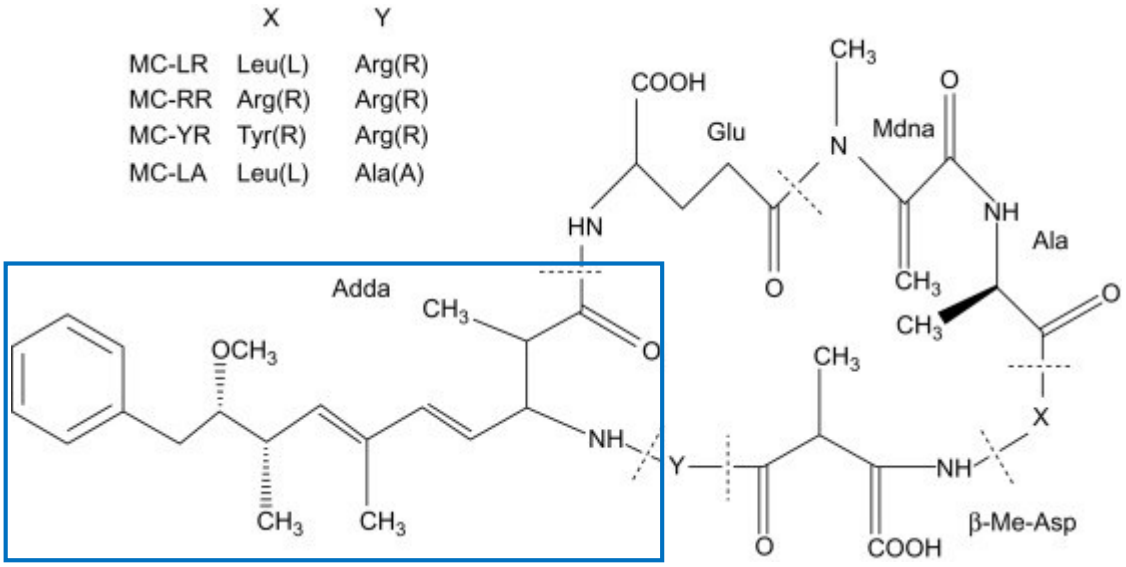

Fig. 9: Chemical structure of microcystin. At position X and Y, the amino acids are variable, as summarized in the table in the upper left corner. The blue box highlights the conserved structure among microcystin and nodularin. **Modified** after Wang & Chen (2019).

Genera known to produce microcystin are *Microcystis, Planktothrix* and *Dolichospermum* (former Anabaena).

The acute toxicity of microcystin-LR was estimated in several studies (Dittmann et al., 2013), and revealed LD_{50}[3] values of 50 to 60 µg kg^{-1} body weight (Chorus & Bartram, 1999). For microcystin-RR and other structural variants of microcystin higher LD_{50} values around 500 µg kg^{-1} were reported (Chorus & Bartram, 1999).

Microcystin is a hepatotoxin, which causes damage in the digestive tract and liver (Elliott, 2012) and long-time exposure is associated with liver and colorectal cancer in humans (Davis et al., 2009). Furthermore, microcystin is known of being an inhibitor of the eukaryotic protein phosphatases types 1 and 2A and is linked to work as tumour promoter (Codd et al., 2005).

There is evidence, that microcystins have a photo-protective effect on the cyanobacterial cell by binding to proteins under high light conditions (Alexova et al. 2011) and can, therefore, help to manage oxidative stress (Zilliges et al., 2011). Furthermore, the expression of microcystin is linked to the global nitrogen

[3] Refers to the lethal doses (LD) of a substance. It describes the dose, where 50% of the laboratory animals die. Therefore, specifying the animal-species and type of application is necessary for comparability. All LD_{50} values given in this text are based on evaluation by mice experiments via intra-peritoneal (i.p.) application.

transcriptional regulator, NtcA, which indicates an influence of nutrients on toxin production (Alexova et al., 2011). NtcA triggers heterocytes formation in filamentous cyanobacteria and thus is activated, when ammonium, the preferred N-source, is absent (Herrero et al., 2004).

1.4.2 Nodularin (NOD)

The hepatotoxin nodularin is named after the genus *Nodularia*. Nodularin is closely related to microcystin and also inhibits the eukaryotic protein phosphatases 1 and 2A. Interestingly, there exist multiple congeners of microcystin, but only seven naturally-occurring isoforms of nodularin (Pearson et al., 2010). However, all have in common a conserved unique amino acid, 3-amino-9-methoxy-2,6,8-trimethyl-10-phenyldeca-4,6-dienoic acid (adda) side chain, which is highlighted by the blue box in Figure 9 and 10, respectively. Rantala et al. (2004) was able to demonstrate that nodularin synthase encoding genes evolutionary derived from microcystin synthase encoding ones through gene deletion.

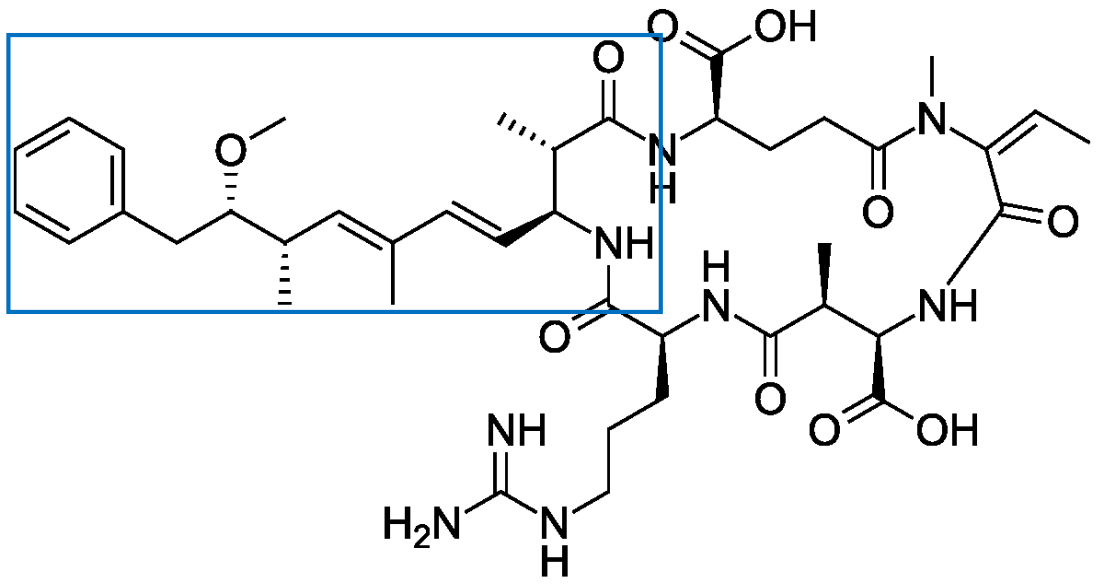

Fig. 10: Chemical structure of nodularin. The blue box highlights the conserved structure among nodularin and microcystin. **Source:** https://en.wikipedia.org/wiki/Nodularin#/media/File:Nodularin_R.svg

LD_{50} values are ranging from 30-50 µg kg^{-1} body weight (Chorus et al., 2000).

1.4.3 Cylindrospermopsin (CYN)

Cylindrospermopsin belongs to the cytotoxins, neurotoxins and hepatotoxins (Ohtani et al., 1992). It is a cyclic sulphated guanidine alkaloid and was first reported in 1979

at the Palm Island (Queensland, Australia) outbreak of hepato-enteritis (Bourke et al., 1983), commonly known as Palm-Island Mystery Disease. In this time 148 people were hospitalized due to hepatitis-like syndromes, as dehydration and bloody diarrhoea. In 1983, only Bourke et al. were able to trace back the cause of the symptoms to a *Raphidiopsis* (former *Cylindrospermopsis*) *raciborskii* bloom and the resulting toxin contamination.

The chemical structure of cylindrospermopsin is illustrated in Figure 11. Originally, this toxin was named after *Cylindrospermopsis raciborskii*, but is additionally known to be synthesized by genera like *Dolichospermum, Aphanizomenon, Umezakia, Oscillatoria* and *Lyngbya*. According to Dittmann et al. (2013), *Raphidiopsis raciborskii* is predominantly producing toxins in tropical and subtropical regions, whereas *Aphanizomenon* (*Chrysosporum ovalisporum*) is mostly the origin of cylindrospermopsin in the temperate regions of the Northern hemisphere.

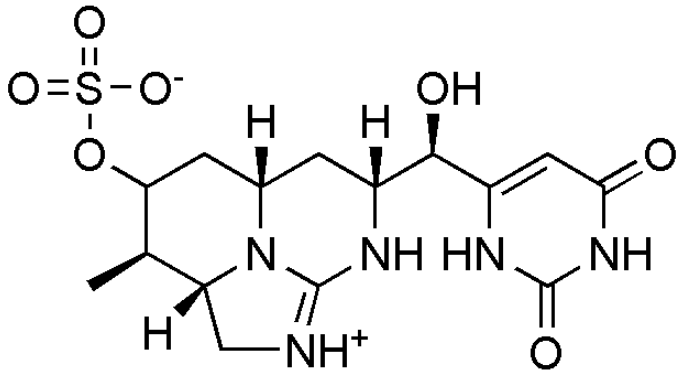

Fig. 11: Chemical structure of cylindrospermopsin. **Source:** https://commons.wikimedia.org/wiki/File:Cylindrospermopsin.png

A LD_{50} value of 200 µg kg^{-1} body weight was determined after 5-6 days (Chorus & Bartram, 1999). Cylindrospermopsin has no specific target which is inhibited, but it is known to inhibit protein synthesis, the function of glutathione, as well as the cytochrome P450 complex and furthermore interact directly with the DNA (Dittmann et al., 2013).

1.4.4 Anatoxin (ATX)

Anatoxin-a acts as neurotoxin (Kurmayer et al., 2017) and was the first chemically and functionally described cyanobacterial toxin back in 1972 (Huber, 1972). It is an alkaloid and was named after *Anabaena flos-aquae* (now *Dolichospermum flos-aquae)*, while

the toxin was first isolated by Devlin et al. (1977). Except Homoanatoxin, no other structural variants were found. The chemical structure of anatoxin-a is shown in Figure 12. Anatoxin is predominantly produced by genera including *Dolichospermum, Oscillatoria, Aphanizomenon, Phormidium* and *Tychonema* (John et al., 2019).

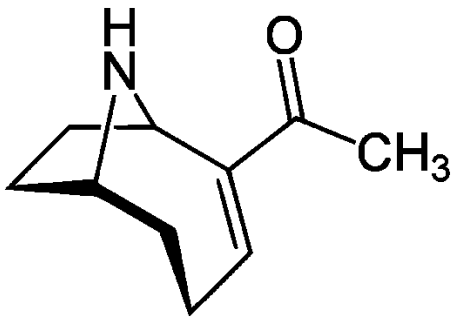

Fig. 12: Chemical structure of anatoxin-a. **Source:** https://de.wikipedia.org/wiki/Anatoxin_A.

Anatoxin-a is known to mimic the neurotransmitter acetylcholine, leading to dysfunction of signal transmission between neurons and muscles (Devlin et al., 1977). Symptoms caused by anatoxin-a contamination are asphyxia and muscular paralysis in mammal species (Carmichael et al., 1975). A LD_{50} value of 375 µg kg^{-1} body weight was reported (Chorus & Bartram, 1999).

1.4.5 Saxitoxin (SXT)

Saxitoxin is also known as neurotoxin (Kurmayer et al., 2017) and belongs to the group of carbamate alkaloid toxins (Schantz et al., 1975), with the chemical structure shown in Figure 13. In marine ecosystems saxitoxin is the principal toxin causing Paralytic Shellfish Poisoning (PSP). They are produced by marine dinoflagellates which are accumulated in filter-feeding invertebrates, like shellfish and fish, which are further transported into higher levels of the food chain (Ikawa et al., 1982).

In freshwater ecosystems, genera like *Dolichospermum, Aphanizomenon* and *Raphidiopsis* are known to produce saxitoxin (Dittmann et al., 2013).

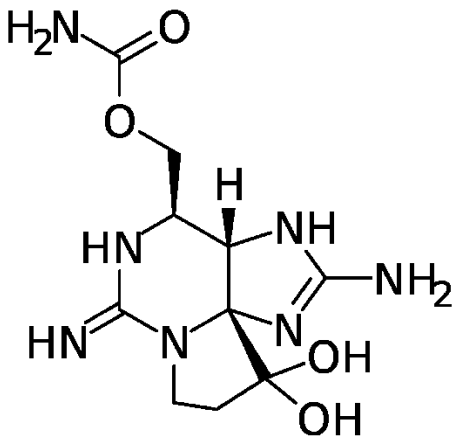

Fig. 13: Chemical structure of saxitoxin. **Source:** https://en.wikipedia.org/wiki/Saxitoxin#/media/File:Saxitoxin_neutral.svg

LD_{50} value of saxitoxin is comparably low and a literature value of 10 µg kg^{-1} body weight was found (Oshima, 1995). It is known to bind to voltage-gated sodium channels causing interruptions of the nerve transmission system and can lead to death due to respiratory paralysis (Cusick & Sayler, 2013).

1.5 EU Bathing Water Directive (2006/7/EC)

According to the EU Bathing Water Directive (2006/7/EC) two parameters are currently measured to monitor and assess the quality of bathing waters (except for swimming pools and spa pools) and for classification of the status:

- Number of intestinal *Enterococci*
- Number of *Escherichia coli*

These two parameters are indices for fecal contamination and can be counted by two individual methods. On the one hand, variable volumes of water samples are transferred into tubes containing a liquid medium. Corresponding to the positive tubes, the Most Probable Number (MPN) of *Enterococci* or *E. coli*, respectively, is calculated. On the other hand, the water samples are filtered using a 0.45 µm pore-size membrane and inoculated on a solid medium. The number of colonies is counted and are considered as the quantity of bacteria present at the time of inoculation.

Accredited water laboratories, like AGES IMED Wien, Währingerstr. 25A, use BIO RAD MUS/SF Microplates Kit (for *Enterococci* or *E. coli*, respectively). The principle is based on the property that an *Enterococci* (or *E. coli*) specific enzyme is detected.

Within the microplate wells, the substrate is already present in dehydrated form. In case of presence of the enzyme, a fluorescence signal can be detected under UV-light (BIO-RAD, 2020).

Article 8 of the Bathing Waters Directive (2006/7/EC) states that additional monitoring programmes should be applied on bathing waters which pose an increased risk of cyanobacterial blooms.

1.6 High Throughput Sequencing (HTS)

Currently, phytoplankton species are monitored according to the water framework directive (WFD) (2000/60/EG), which is usually done based on taxonomic analysis by microscopic observation, followed by calculation of the total volume and abundances to estimate the so-called “biovolume”. However, using only microscopy it is often difficult to differentiate among taxa (Moreira et al., 2014) as well as to distinguish between a toxic and non-toxic strain (Kurmayer et al., 2017). High Throughput Sequencing (HTS) is an alternative method, being a molecular-biological approach capable of revealing not only the cyanobacteria taxa but even the entire microbial community (Hugerth & Andersson, 2017).

1.6.1 16S rRNA gene

Since the recognition of the small subunit (SSU) of ribosomal RNA (rRNA) as suitable gene for phylogenetic relationships by Woese and colleagues in 1977, the technique of amplicon sequencing became established widely (Woese & Fox, 1977). For revealing the phylogeny of species, the 16S rRNA offers many advantages which is why it is now considered as the golden standard (Bukin et al., 2019):

- It is functionally constant (in all organisms it is part of the ribosome’s protein synthesis)
- It is present in all three domains of life
- It contains relatively large information content
- It possesses different degrees of sequence conservation
- (Relatively) minor Horizontal Gene Transfer (HGT) has been observed

In general, 16S rRNA is around 1540 base pairs long and includes nine hypervariable regions (V1-9) (Gray et al., 1984). For this master thesis, primers have been chosen

which amplify the V3 to V4 region of the 16S rRNA. According to Zhang et al. (2018) this region is preferred for differentiation of cyanobacterial taxa.

1.6.2 The principle of Illumina Sequencing

High Throughput Sequencing describes a variety of methods that allow parallel sequencing of thousands of DNA fragments in a single experiment. One of these methods is Illumina sequencing, named after the market-dominating company. It is based on the principle of sequencing-by-synthesis (Figure 14), as after each sequencing cycle a fluorescently tagged deoxynucleosid triphosphate (dNTP) is added to the DNA strand. This tag blocks the polymerase, whereby synthesis is terminated. In the meantime, the fluorescence signal is detected, whereby specific wavelengths refer to one of the four bases (A, C, T, G). An enzyme is removing the fluorescence label with the result that the polymerase can continue with the synthesis (Brown, 2018). This technique allows very accurate base-by-base sequencing. Amplicon sequencing is a target approach where specific genomic regions are analyzed.

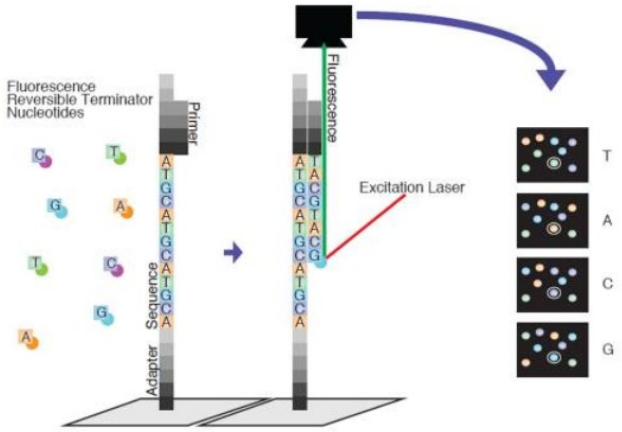

Fig. 14: Illumina sequencing workflow. **Modified** after Chaitankar et al. (2016).

1.6.3 Defining the optimal annealing temperature

Optimal annealing temperatures (T_a) for primer systems are crucial for revealing specific PCR products and thus, getting representative sequencing results. On the one hand, the temperature has to be high enough to obtain only specific bindings to the target DNA, while on the other hand, too high or low temperatures favour primer dimers and other unspecific bindings. Primer dimers describe a potential side-product of the PCR, when two primers hybridize to each other (Rychlik et al., 1990).

Before sequencing, PCRs need to be optimised by using a fluorescence dye such as EvaGreen™ and application of a range of annealing temperatures. The dye is incorporated into dsDNA during the hybridization process, which leads to an increase of a fluorescence signal during the PCR if more dsDNA is formed. The fluorescence signal, which is measured at 530 nm during elongation phase, is used to follow the PCR amplification process in real time. However, it is impossible to differentiate between specific products, non-specific products or primer dimers from the PCR amplification curve. This is the reason why subsequently melting curves need to be calculated. Since each dsDNA has its own melting temperature (T_M), mainly depending on the GC-content and the length of the product, the variability of the PCR products can be validated. In principal, the T_M describes the status, where 50% of the DNA is in double-stranded form, whereas the remaining 50% are already melted, thus single-stranded (Roche Manual).

In general, the T_M calculators are often based on the Wallace-formula (equation I), whereby A, T, G and C represent the frequency of the individual bases (Wallace et al., 1979):

Equation I: $$Melting\ Temperature\ [°C] = (A + T) * 2 + (G + C) * 4$$

1.7 In-situ Fluorescence measurements

Another approach for monitoring the algal community more directly is based on natural fluorescence. During photosynthesis, photons are absorbed by chlorophyll-molecules leading to the rise of electrons from the ground state to an excited state. A part of this energy is used for photochemistry, to build up biomass and maintain physiological processes, whereby the rest is lost via heat and fluorescence (Schimanski, 2002). Due to the fact that individual algal groups possess specific light-harvesting pigments, like the phycocyanin peripheral antenna of cyanobacteria, unique absorption and excitation spectra are linked to them. These so-called “Fingerprints” allow quantification and determination of the specific algal classes (Beutler et al., 2002). The advantage of such an in-situ measurement is its simple use and the fact that the results are obtained after 30 seconds. In Figure 15 the application of a fluorometer, which is specialized for bathing water monitoring, is shown.

Fig. 15: The bbe moldaenke AlgaeTorch is used for direct measurements of the chlorophyll content of microalgae and cyanobacteria by holding the torch 10-30 cm below the water surface until a discrete vibration of the device confirms a successful measurement. **Source:** Mag. Elisabeth Zwingraf

In general, the bbe moldaenke AlgaeTorch determines total chlorophyll and a cyanobacterial specific parameter, called cyanochlorophyll. The Torch`s construction is based on 2 x 3 LEDs with wavelengths of 470, 525 and 610 nm. These wavelengths are known to get absorbed by chlorophyll and phycocyanin, thus, algal and cyanobacterial biomass can be quantified. The results are also automatically corrected for turbidity, as an additional LED at 700 nm, which is not influencing the chlorophyll measurement, determines this parameter (bbe Moldaenke).

1.8 Aim of this Master Thesis

The aim of this master thesis has been to develop a monitoring system for cyanobacteria for the EU bathing waters via amplicon sequencing. Thus, amplicon sequencing of the 16S rRNA was performed to analyse the planktonic microbial community in the EU bathing waters, the Old Danube and other selected surface waters. For this purpose, general 16S bacterial primers and specific cyanobacterial primers were used for the amplification step.

Aside from planktonic samples, benthic mats were collected regularly from the Old Danube and the selected surface waters to reveal the role of benthic cyanobacteria as toxin-producers.

All in all, 100 planktonic samples and 19 benthic samples were collected over the bathing season 2020 (June-September). Moreover, a variety of abiotic factors was

documented and nutrient- and cyanotoxin concentrations were determined. Additionally, total chlorophyll and cyanochlorophyll contents were measured.

Finally, side-experiments were conducted to test different filtration techniques and extraction kits. Altogether, 160 extracts from five sampling dates were sequenced using two primer systems (universal bacterial and specific cyanobacterial primer pairs). Further data analysis was obtained by two different pipelines, mothur and DADA2, of which the former is based on traditional operational taxonomic unit (OTU) clustering and the latter on the calculation of so-called amplicon sequence variants (ASV).

The following hypotheses were tested:

- Either cyanotoxin measurements based on liquid chromatography mass spectrometry, or Illumina sequencing for revealing the cyanobacterial populations, both rather different approaches, were used to determine the risk of harmful cyanobacterial blooms. Both methods provide consistent results.
- Toxic cyanobacterial blooms occur under conditions of eutrophication, high temperatures (>20°C) and high level of human activity, since eutrophication is frequently a result of human activities.
- Measurements based on fluorescence are influenced by many factors, like presence of humic substances, shading and varying morphology of cells. This unpredictable variation in fluorescence spectra can lead to false statements about the dominance of the cyanobacterial community.
- When compared with cyanobacteria thriving at the surface, benthic cyanobacteria are an overlooked source of toxins due to the lower accessibility but should be included in monitoring in the future.

2 Materials and Methods

2.1 Sampling procedure

During the bathing season June – August 2020, 100 planktonic samples were collected, representing five sampling dates. Out of these, 85 samples were obtained from EU-bathing waters (corresponding to 17 samples per sampling date) and 15 samples were collected from the Old Danube (corresponding to three samples per sampling date). Furthermore, 19 benthic samples were collected.

Sampling started in early June (02.06.2020) and was completed by the end of August (20.08.2020), see Table 1. Sampling frequency was depending on the EU-bathing waters monitoring calendar, which has to be defined before the start of each bathing season. For establishment of the calendar the following requirements have to be fulfilled (2006/7/EC Annex IV):

1. One sample has to be taken before the start of each bathing season.
2. A minimum of four samples must be analyzed per bathing season.
3. The interval between sampling dates must not exceed one month.

Tab. 1: Summary of the sampling dates und number of samples obtained per zone and event.

Sampling date	Date	Planktonic samples	Benthic samples
1	2.6.2020 - 3.6.2020	20	6
2	15.6.2020 - 17.6.2020	20	3
3	6.7.2020 - 8.7.2020	20	1
4	27.7.2020 - 29.7.2020	20	3
5	17.8.2020 - 20.8.2020	20	6

The monitoring results of each EU-bathing water is summarized in its bathing water profiles. In Table 2 the level of cyanobacterial risk, based on chapter 4 of the corresponding bathing water profile, is given.

Tab. 2: Overview of the sample IDs for individual lakes and the associated assessment regarding the risk of mass proliferation of cyanobacteria, based on chapter 4 of the corresponding bathing water profiles. Each row represents one sampled lake.

Sample IDs	Level of cyanobacterial risk
1, 26, 49, 71, 92	high risk
2, 27, 50, 72, 93	high risk
3, 28, 51, 73, 94	high risk
4, 33, 58, 80, 101	moderate risk
5, 34, 59, 81, 102	moderate risk
6, 35, 52, 74, 95	moderate risk
7, 36, 53, 75, 96	moderate risk
8, 37, 54, 76, 97	moderate risk
9, 38, 55, 77, 98	moderate risk
10, 40, 56, 78, 99	no risk
11, 39, 47, 79, 100	high risk
12, 41, 62, 84, 105	high risk
13, 31, 60, 82, 103	moderate risk
14, 32, 61, 83, 104	moderate risk
15, 42, 63, 85, 106	moderate risk
16, 43, 64, 86, 107	no risk
17, 44, 65, 87, 108	no risk
18, 45, 66, 88, 109	high risk
19, 46, 67, 89, 110	moderate risk
20, 47, 68, 90, 111	high risk

2.1.1 Abiotic and biotic factors

For identification of parameters facilitating cyanobacterial blooms, the following abiotic factors were documented. Oxygen (O_2) was measured with a WTW FDO® 925-P

probe and pH with a WTW SensoLyt® 900-P probe, respectively, combined in a WTW MPP 930 IDS multiparametric shell. Temperature was calculated by the mean output of the two sensors.

Moreover, Secchi depth was measured from a boat whenever available or otherwise from shore.

In addition to physical measurements, in-situ fluorescence measurements were obtained for total chlorophyll and cyanochlorophyll. Therefore, the bbe moldaenke AlgaeTorch was used, by directly holding the Torch at 10 cm depth into the water (see Figure 15). For each sampling, the measurement was repeated three times and the average value was calculated.

For each sampling date weather conditions from the past and present, wind speed and direction, water level, choriotop distribution, as well as the presence of bryophytes, submerged and floating hydrophytes, and helophytes were documented.

2.1.2 Sampling of the planktonic zone

According to the bathing waters directive (2006/7/EC), sampling shall be carried out at those sites where the number of bathers is highest. Therefore, sampling point coordinates for the EU-bathing waters, which were published in the bathing water profiles, were taken, unless prevented by higher circumstances like i.e., high flood events. In most of the cases, the declared sampling point was reachable from the shore of the lake. For the three Old Danube samples, a boat for sampling was available. The sampling depth was equal to one arm length below surface (30-50 cm) in distinct distance from the sediment.

The planktonic samples for sequencing were collected by filling up a 0.5 L sterile plastic bottle from 30-50 cm depth. During the transport to the laboratory the samples were kept dark and cool using a cooling box or a transportable fridge (4°C). For almost each sampling site, nutrients and cyanotoxins were sampled in parallel by 1 L of water, each taken from the same depth. A schematic overview of the individual samples per site is given in Figure 16.

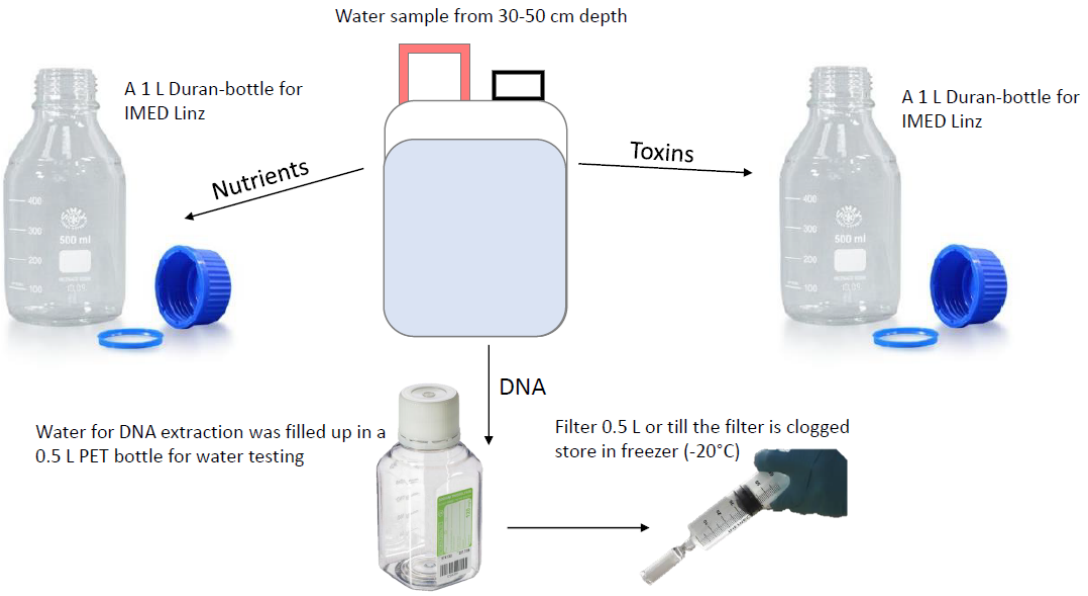

Fig. 16: Overview of planktonic water sampling at each sampling site for the three types of analysis.

2.1.3 Sampling of the benthic zone

For the benthic samples five representing stones were collected and stored in a labelled plastic bag within the cooling box till further processing in the laboratory. In general, by scratching from stones, an approximately 100 cm^2 representative area was collected in a 50 ml Falcon tube. Further samples were obtained from algae-covered walls, jetties, etc. and/or sediments by scuba-diving or from floating mats on the surface. The falcons were kept at 4°C till preparation.

2.2 Sample preparation

2.2.1 Filtration of planktonic samples with Sterivex™ filters

The planktonic samples were immediately filtered through a Sterivex™-GP 0.22 µm filter (Millipore, Billerica, Massachusetts, USA), by pressing water manually through the filter unit with a plastic syringe. The syringe was cleaned before with dH_2O and rinsed once with the sample itself. To estimate the filtered volume, a 1 L Duran bottle was used to capture the filtered water. The filtering was completed until the filter became clogged or when a total volume of water (max 0.6 L) was used.

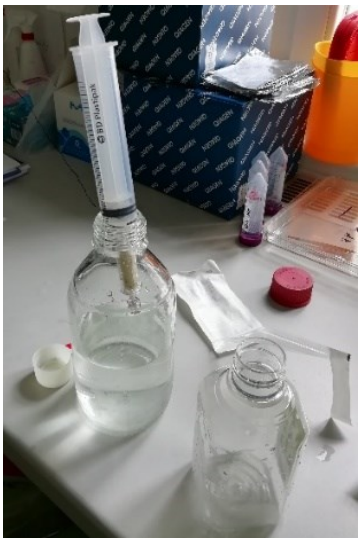

Fig. 17: Filtration of planktonic samples using pressure-driven filter units. A Sterivex™ filter was mounted on the syringe, which was initially filled up with sampling water. The water was then manually pushed through the filter unit and collected with a Duran bottle. Finally, the volume of filtered water, the colour of the filter and filtration time was recorded.

Fig. 18: Filtration of planktonic samples with membrane filters through vacuum pressure. Filtering with a vacuum pump offers the advantage that no manual positive pressure is required.

Finally, air was pushed through the filter unit several times to remove any remaining water. Filtration time, filter colour and volume of filtered water were recorded. Both ends of the Sterivex™ filter were then capped with an inlet and outlet cap, respectively, and were stored in the freezer at -20°C till DNA extraction. The filtration setup is shown in Figure 18.

2.2.2 Filtration of planktonic samples using membrane filters

Five samples were additionally selected to be filtered on a S-Pak® 0.22 µm membrane filter (Millipore, Billerica, Massachusetts, USA), with non-re-useable beakers. Therefore, these filter-covered beakers were filled up with 100 ml of water, whereby the filtration was supported by a vacuum-pump (Figure 18). Afterwards, the filters were cut into small pieces with a sterile scalpel and stored in a 5 ml Epi in the freezer at -20°C till DNA extraction. The filtration was repeated as these membrane filters were processed using two different extraction kits (DNeasy® PowerWater® Sterivex™ Kit and DNeasy® PowerWater® Kit).

2.2.3 Processing of benthic samples

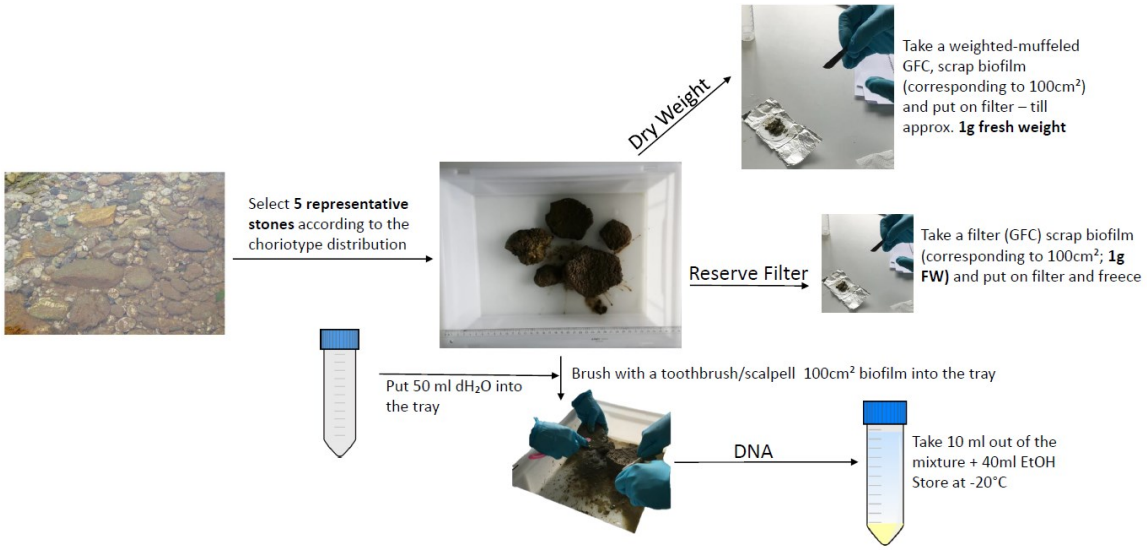

Fig. 19: Overview of benthic sampling and the three types of analysis.

In order to sample a representative community of the benthic biofilms, the collected number of five stones were put into a cleaned tray filled with 50 ml ddH_2O. With a scalpel and/or toothbrush a total area of 100 cm^2 was scratched off from all five stones. 10 ml were further transferred into a Falcon™ tube and filled up with 40 ml ethanol. The falcon was stored at -20°C till DNA extraction. This procedure is schematically drawn in Figure 19.

The dry weight of 100 cm^2 biofilm biomass was determined using a Whatman 1.2 µm GF/C filter, which was beforehand wrapped in aluminium foil and dried over night at 100°C in an incubator. Dry weight of the virgin filter was determined with a fine scale and noted. In the next step, the scratched off biomass was transferred onto the dried filter, folded, and covered with aluminium foil and again dried over night at 100°C afterwards. Finally, the dry weight of the biomass was determined by subtracting the weight between dried filter and biomass minus the weight of the dried virgin filter, based on equation II.

$$Equation\ II: Biomass\ dry\ Weight\ [g] = dried, stocked\ filter\ [g] - dried\ filter\ [g]$$

One extra filter per sample was stocked with 100 cm^2 biofilm as reserve and stored at -20°C.

2.3 Total phosphorus and cyanotoxin analysis

Total phosphorus (TP) was analyzed at AGES IMED Linz (Wieningerstraße 8, 4020 Linz). TP was determined by inductively coupled plasma mass spectrometry (ICP-MS) according to ÖNORM EN ISO 17294-1:2007 and ÖNORM EN ISO 17294-2:2017.

Moreover, the cyanotoxins (microcystin-LR, microcystin-RR, microcystin-YR, microcystin-AspDhbRR, anatoxin, nodularin, cylindrospermopsin) were analyzed at AGES IMED Linz with a QExactive Orbitrap Mass Spectrometer (Thermo Fisher Scientific, Waltham, Massachusetts, USA) which is based on chromatographic separation by high performance liquid chromatography followed by high resolution mass spectrometry (HPLC-HRMS).

2.4 DNA extraction (Isolation)

2.4.1 DNA extraction with DNeasy® PowerWater Sterivex™ Kit

From all Sterivex™ filtered samples and one part of the S-Pak® Membrane filtered samples the environmental genomic DNA was extracted using the DNeasy® PowerWater® Sterivex™ Kit (Qiagen, Hilden, Germany) following the manufacturer`s protocol. A few modifications were applied, since both the Vortex Adapter for Sterivex™ filters and the QIAVac 24 Plus Manifold vacuum device were not available. As an alternative to the Vortex adapter, packages of six filters were formed and vortexed on middle (1400 min^{-1}) or full (3000 min^{-1}) speed on an IKA® MS1 Minishaker, as recommended by the protocol. As alternative for spinning down the power bead tubes, a centrifuge with adaptors for 50 ml falcons was used. Each individual power bead tube was placed in a 50 ml falcon and centrifuged for 1 min at 4000 rpm.

As an alternative to the vacuum manifold, the supernatant and solution MR on the MB spin column were loaded repeatedly, i.e., 750 µl of the mixture were loaded seven times onto the MB spin columns. In between, a centrifugation step of 13,000 x g for 1 min was performed.

Furthermore, the solutions used for the washing steps (ethanol and solution PW) were reduced from 800 µl to 750 µl to avoid an additional centrifugation step. For elution of DNA from the spin column, two times 50 µl of DNA-free PCR-grade water were added on the centre of the spin column, pooled and finally stored at -20°C.

2.4.2 DNA extraction with DNeasy® PowerWater® Kit

In addition to the used DNeasy® PowerWater® Sterivex™ extraction kit, the aliquots of five S-Pak® Membrane filtered samples were extracted with the DNeasy® PowerWater® Kit (Qiagen, Hilden, Germany), following the manufacturer's protocol. Only minor modifications had to be done, as no vortex adapter was available. Thus, the power bead tubes were incubated on a shaker as described above. The environmental DNA was eluted from the spin column by adding two times 50 µl DNA-free PCR-grade water on the centre of the spin column. The extract was stored at -20°C.

2.4.3 DNA extraction with DNeasy® PowerBiofilm® Kit

For the extraction of the benthic samples the DNeasy® PowerBiofilm® Kit (Qiagen, Hilden, Germany) was used. For sample preparation, 2 ml of the ethanol + biofilm mixture was put into a 2 ml tube and centrifuged for 30 min at 4°C at 18000 x g. Afterwards, the supernatant was removed, and the pellet was re-suspended in 350 µl MBL buffer. The remaining steps were followed as described in the manufacturer`s protocol. Finally, 100 µl of DNA extract, obtained with DNA-free PCR-grade water, was stored at -20°C.

2.4.4 Blank control

Additionally, blank controls with 100 ml ddH_2O were prepared from all types of utilised filters and extraction kits. In Table 3 these filter types and extraction kits are summarized. Furthermore, the number of samples obtained for each filtration type and extraction kit is shown, which also includes the blank controls.

Tab. 3: Overview of planktonic samples filtration type and used extraction kit.

Type of filter	Type of extraction kit	Number of samples
Sterivex™ 0.22 µm filter	DNeasy® PowerWater® Sterivex™ Kit	100
S-Pak® 0.22 µm Membrane filter	DNeasy® PowerWater® Sterivex™ Kit	6
S-Pak® 0.22 µm Membrane filter	DNeasy® PowerBiofilm® Kit	6

2.5 Optimizing PCR conditions

To verify the success of DNA extraction and specification of PCR conditions for both primer pairs, several PCR reactions were set up with a LightCycler® 480 Instrument (Roche, Basel, Switzerland) using EvaGreen™ for producing a fluorescence signal. The primers used are listed in Table 4. On the one hand, primers amplifying the 16S rRNA region of the bacterial community (Bakt_341_F and Bakt_805_R) were used, while on the other hand also cyanobacterial primers 515F (forward), CYA781R(a) (reverse1) and CYA781R(b) (reverse2) were used for the specific amplification of the variable region V3 and V4 in the cyanobacterial 16S rRNA region.

Tab. 4: List of primers used for PCR and Illumina sequencing.

Primer names	Sequence (5`-3`)	Direction	Bp	Source
Bakt_341_F	CCTACGGGNGGCWGCAG	forward	17	Herlemann et al. (2011)
Bakt_805_R	GACTACHVGGGTATCTAATCC	reverse	21	Herlemann et al. (2011)
515F	GTGCCAGCMGCCGCGGTAA	forward	19	Turner et al. (1999)
CYA781R(a)	GACTACTGGGGTATCTAATCC CATT	reverse1	25	Nübel et al. (1997)
CYA781R(b)	GACTACAGGGGTATCTAATCC CTTT	reverse2	25	Nübel et al. (1997)

The components listed in Table 5 were used for the respective PCR reactions. First, a reaction mix was set up to facilitate correct pipetting. It consisted of KAPA HiFi HotStart ReadyMix (Roche, Basel, Switzerland), for the bacterial amplification. Moreover, it contained the forward and reverse primer, as well as EvaGreen™ fluorescence dye.

20 µl of the reaction mix were added into every slot of the LightCycler® 480 Multiwell Plate 96, followed by 5 µl of DNA. For the negative control (NTC), 5 µl of DNase free water was added.

Tab. 5: Used bacterial PCR components per sample.

	Component	Volume
1.	Roche KAPA HiFi HotStart ReadyMix	12.5 µl
2.	Forward Primer (conc. = 100 µM)	3.8 µl
3.	Reverse Primer (conc. = 100 µM)	3.8 µl
4.	Biotin EvaGreen™ Dye	0.4 µl
5.	DNA	5 µl
	Total volume per well	**25 µl**

For the cyanobacterial amplification, the HotStartTaq Master Mix (Qiagen, Hilden, Germany) was used (see Table 6). Due to the fact that two reverse primers were used, the final concentration had to become equal to that of the forward primer. Furthermore, experiments with different $MgCl_2$ concentrations revealed that establishing 1.5 µM $MgCl_2$ concentration produces the best output of the amplification curves.

Tab. 6: Used cyanobacterial PCR components per sample.

	Component	Volume
1.	Qiagen HotStartTaq Master Mix	12.5 µl
2.	Forward Primer (conc. = 100 µM)	0.1 µl
3.	Reverse Primer 1 (conc. = 100 µM)	0.05 µl
4.	Reverse Primer 2 (conc. = 100 µM)	0.05 µl
5.	Biotin EvaGreen™ Dye	0.5 µl
6.	$MgCl_2$	1.5 µl
7.	ddH_2O	5.8 µl
8.	DNA	5 µl
	Total volume per well	**25 µl**

The PCR plate was sealed with an appropriate sealing foil, centrifuged shortly and finally inserted into the LightCycler®. The conditions used are presented in Table 7 and 8, respectively. On the one hand, amplification curves of the PCR product were

documented, while on the other hand melting curves were determined to check whether the desired PCR-product has been amplified.

Tab. 7: Conditions for bacterial PCR.

	Step	**Temperature/Time**
1. Pre-denaturation	Pre-denaturation	95°C, 3 min
2.1. Amplification (45x)	Denaturation	95°C, 30 s
2.2.	Annealing	55°C, 30 s
2.3.	Elongation	72°C, 30 s
3. Final Extension	Final Extension	72°C, 5 min
4.1. Melting curve determination		95°C, 10 s
4.2.		45°C, 10 s
4.3.		95°C, continuous
5. Cool		45°C, 10 s

Tab. 8: Conditions for cyanobacterial PCR.

	Step	**Temperature/Time**
1. Pre-denaturation	Pre-denaturation	95°C, 15 min
2.1. Amplification (45x)	Denaturation	95°C, 30 s
2.2.	Annealing	65°C, 30 s
2.3.	Elongation	72°C, 30 s
3. Final Extension	Final Extension	72°C, 10 min
4.1. Melting curve determination		95°C, 10 s
4.2.		45°C, 10 s
4.3.		95°C, continuous
5. Cool		45°C, 10 s

Selected results of the bacterial and cyanobacterial PCR are presented both in the results chapter 3.4 and in the appendix chapter 8.2, respectively.

2.6 Amplicon sequencing with Illumina MiSeq

After optimizing the amplification conditions for both primer systems, the DNA extracts were measured with a Qubit™ 2.0 Fluorometer (Thermo Fisher Scientific, Waltham, Massachusetts, USA) using the dsDNA BR Assay Kit. Samples were diluted to a final concentration of 5 ng μl^{-1} to ensure equal probability of being sequenced.

The amplicon sequencing of general bacterial 16S rRNA and specific V3-V4 variable region of the 16S rRNA gene of cyanobacteria was performed by Dr. Stefanie Dobrovolny at AGES Spargelfeldstraße 91, 1220 Wien. Paired-end sequencing (2 x 300 bp) was carried out on a MiSeq platform (Illumina, San Diego, CA, USA). The components listed in Table 5 and 6 were used, as well as the conditions shown in Table 7 and 8, but without the melting curve determination steps. Monitoring of the PCR amplification curves using fluorescence indicated that 30 PCR cycles are sufficient using both cyanobacterial primers and bacterial primers.

2.7 Sequence analysis by bioinformatics procedures

2.7.1 Sequence analysis by mothur

Mothur was introduced by Schloss et al. (2009) to analyse the microbial community. Raw fastq files were processed following mothur`s SOP (Kozich et al., 2013) using version 1.44.0. First, the sequences and quality scores were extracted from the fastq files, followed by making the reverse complement of the reverse read to join forward and reverse read into contigs. To reduce sequencing and PCR errors, a filtering step was added which removed ambiguous bases and reads which were longer than expected. The quality filtered sequences were clustered into OTUs (≤ 3% dissimilarity) and the consensus taxonomy for every OTU was determined.

Chimera removal was performed with VSEARCH algorithm (Rognes et al., 2016) and classification by using the RDP`s Bayesian classifier (Wang et al., 2007). For taxonomic classification, the comprehensive SILVA SSU reference database (version 138; Quast et al., 2013) was used. Undesired lineages, like 18S rRNA fragments or 16S rRNA reads from Archaea, chloroplasts or mitochondria, which probably originated from non-specific amplification were excluded from further analysis.

To use the mothur generated data in further analysis, minor modifications had to be done. First, representative OTUs were extracted, headers simplified and distances between the representative OTU sequences were calculated. Finally, the acquired distance matrix was used to produce a TREE file, which contains a dendrogram with the distance relation between all OTUs.

2.7.2 Sequence analysis by DADA2

In parallel, the raw sequence data were processed in R (version 4.0.3; R Core Team, 2020) using the package Divisive Amplicon Denoising Algorithm 2 (DADA2), which was introduced by Callahan et al. (2016) (version 1.18.0). During quality trimming, truncation lengths were set to 250 bp and 220 bp for the bacterial forward and reverse reads. For the cyanobacterial forward and reverse reads the truncation lengths were set to 250 bp and 205 bp, respectively. Quality score was set to 2, which means that the read is shortened to the length corresponding to the first occurrence of a specific nucleotide reaching a quality score of 2 (implying 2 possibilities based on an expected error modelling).

Sequences were clustered into ASVs (no dissimilarity threshold) and assigned to the SILVA SSU reference database (version 138; Quast et al., 2013) for taxonomic classification. Similar to OTUs, the ASVs classified as chloroplast, mitochondria or archaea were excluded from further analysis.

2.7.3 Analyzation and visualization of the pipeline outputs with phyloseq

All further analysis were performed in R using the phyloseq package (version 1.34.0; McMurdie & Holmes, 2013). To ensure comparability, samples had to be randomized to the same number of reads (Cameron et al., 2020). By using the iNEXT package (version 2.0.20; Hsieh, Ma, & Chao, 2016) rarefaction curves for each sampling date, analysis pipeline and primer system were created to estimate loss of information by choosing the appropriate rarefying threshold. Rarefaction was performed by using vegan`s rrarefy command (version 2.5-7; Oksanen et al., 2020). In Table 9, the rarefying thresholds for each primer pair and analysis pipeline are summarized.

Due to the fact that sample ID 63 had only 824 or 341 reads based on the individual pipelines (using bacterial primers), samples from this location were removed for further analysis. In the case of cyanobacterial primers, sample ID 33 showed a rather low

number of reads (1990 and 1953, respectively) and was, therefore, also discarded. The rarefaction curves in the appendix (chapter 8.1) show that the determined thresholds of read numbers provide a representative estimation of taxa diversity.

Tab. 9: Summary of rarefaction threshold and ID which were removed due to low total read number.

Analysis and Primer	Rarefaction Threshold	Sample IDs removed
mothur, bacterial	16150	15, 42, 63, 85, 106
DADA2, bacterial	10130	15, 42, 63, 85, 106
mothur, cyanobacterial	2580	4, 33, 58, 80, 101
DADA2, cyanobacterial	2568	4, 33, 58, 80, 101

For visualization of the final data, the package ggplot2 (version 3.3.3; Wickham, 2016) was used. The Principal Component Analysis (PCA) was created using the ggplot2 extensions ggbiplot (version 0.55; Vu, 2011) and GGally (version 2.1.0; Schloerke et al., 2021) for the correlation matrices. The heat-trees were calculated using package metacoder (version 0.3.4; Foster, Sharpton, & Grünwald, 2017) and for the heatmap superheat (version 0.1.0; Barter & Yu, 2018) was used.

3 Results

3.1 Abiotic factors

3.1.1 Temperature

The temperature distribution over the sampling season is demonstrated in Figure 20. At the beginning, a continuous increase of the mean temperature over the first four sampling dates was observed (17.2°C to 21.0°C and 22.6°C), reaching a maximum at the 4th (23.7°C) sampling date. On the 5th and last sampling date, the temperature slightly decreased, according to the median, but on average remained high at 23.7°C. Especially during sampling dates 2 and 4, relatively low water temperatures were occasionally observed. This was due to the fact that one of the observed bathing waters is used as reservoir for a hydropower plant. Depending on raising or lowering the water level, abnormal low water temperatures were observed in addition to water level fluctuations in the meter range.

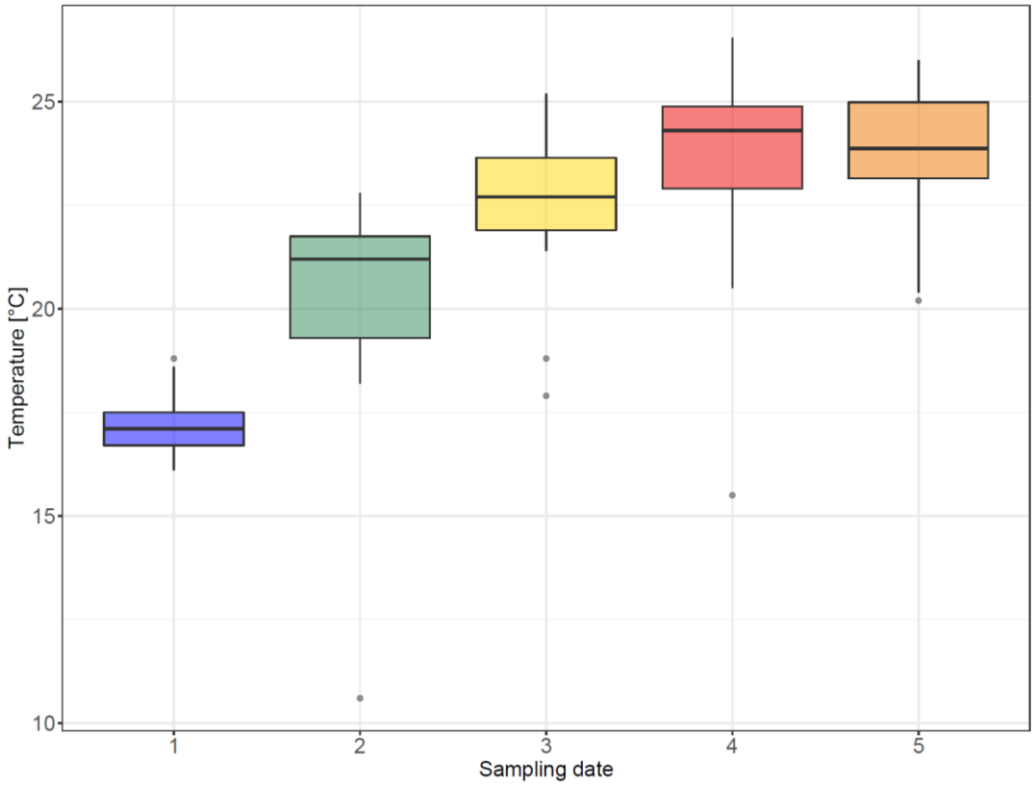

Fig. 20: Variation of the water temperature over the sampling season in °C. Depending on the median temperatures, colours were chosen to reflect the coldest (blue, sampling date 1) and warmest (red, sampling date 4) sampling event, respectively. Boxes show the 25% and 75% quantiles, while vertical lines represent those values that are 1.5 times lower and higher than the 25th and 75th percentiles, respectively. Individual data points represent extreme values which lie outside the 1.5 times interquartile range.

3.1.2 Oxygen

The concentration of dissolved oxygen over the season showed a similar trend as recorded for the water temperature (Figure 21). Starting from the 1st sampling event, a small increase in mean dissolved oxygen concentration could be observed until the 3rd sampling date. On average, oxygen increased from 111.8% (1st date) to 117.8%, on the 2nd sampling date, and reached a maximum on the 3rd sampling date (141.7%), indicating conditions of oversaturation resulting from algal photosynthetic activity. Extremely high oxygen levels (185%, 218% and two measurements 278%, respectively) were observed on the 3rd date, resulting in the highest mean oxygen concentration, although the boxplots indicated a further increase till the 4th sampling date (131.5%). Afterwards, the mean oxygen concentration decreased again, corresponding to on average value of 113.5%, which was similar to saturation conditions as observed on the 1st date.

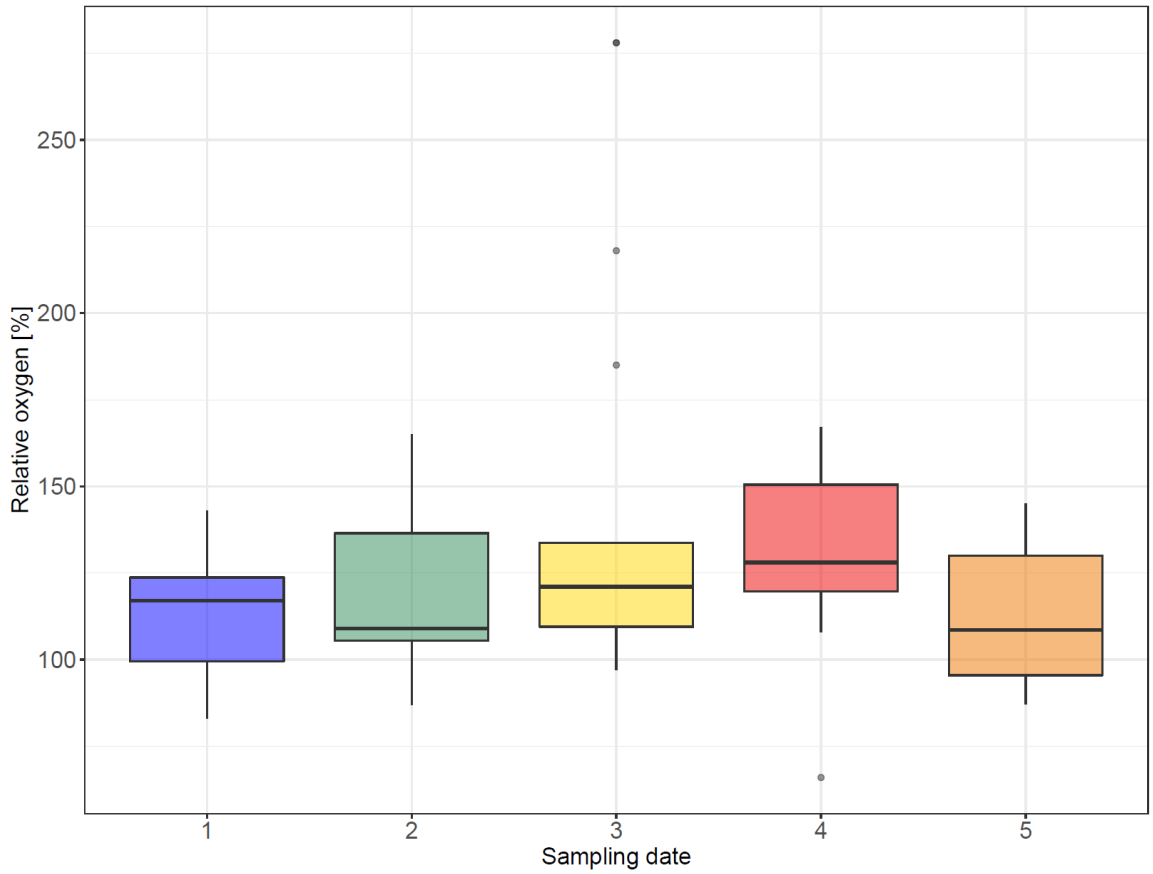

Fig. 21: Variation of dissolved oxygen concentration (in % saturation) over the sampling season. Boxes show the 25% and 75% quantiles, while vertical lines represent those values that are 1.5 times lower and higher than the 25th and 75th percentiles, respectively. Individual dots represent extreme values that lie outside the 1.5 times interquartile range.

3.1.3 pH

In contrast to oxygen saturation the pH showed rather little variation, ranging from 8.3 and 8.5 during the entire study period (Figure 22). In the beginning of the season, on average a pH of 8.4 was measured, which showed higher variability on the 2nd date but remained relatively stable for the rest of the study period.

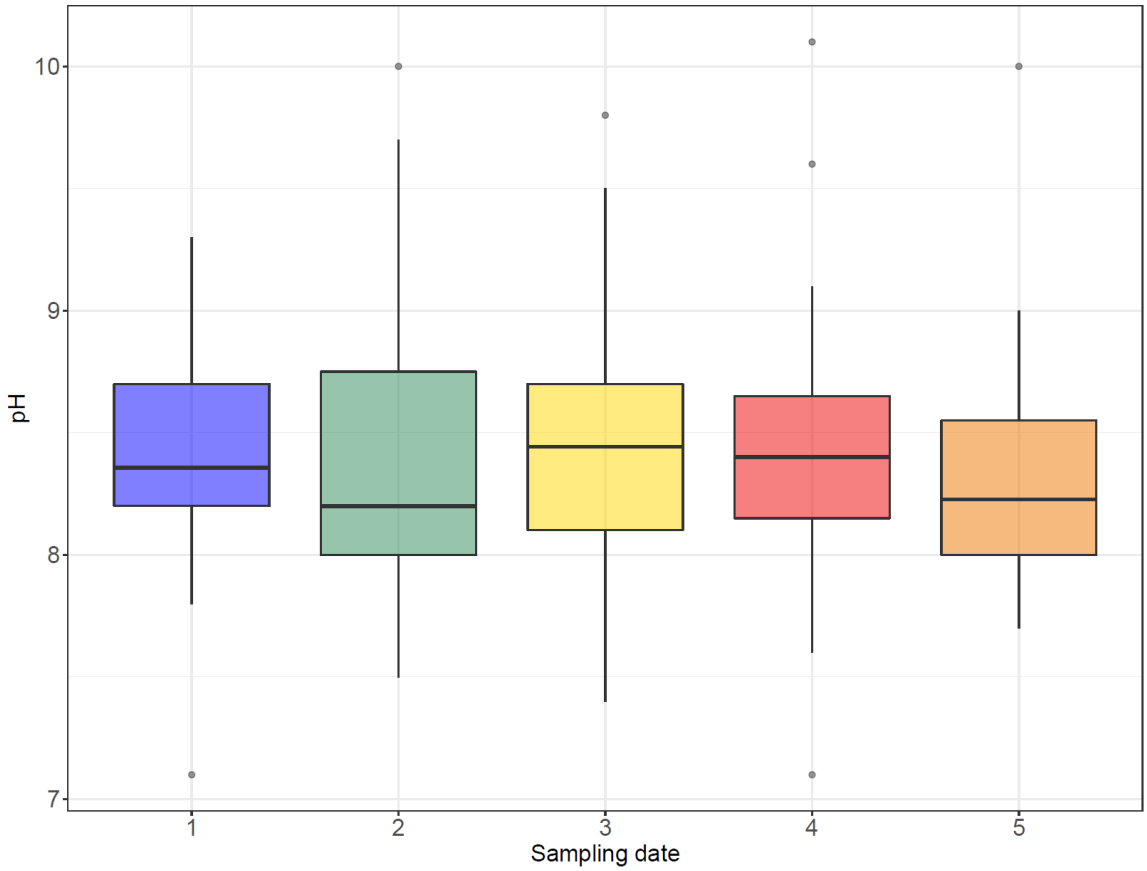

Fig. 22: Variation of the pH recorded over the sampling season. Boxes show the 25% and 75% quantiles, while vertical lines represent those values that are 1.5 times lower and higher than the 25th and 75th percentiles, respectively. Individual dots represent extreme values that lie outside the 1.5 times interquartile range.

3.1.4 Total Phosphorus

During the study period mean total phosphorus concentration varied between 14.6 µg L^{-1} (1st sampling date) and 28.3 µg L^{-1} (3rd sampling date) (Figure 23). From the beginning of the season, on average an increase of total phosphorus content was recognized, followed by a decline during the 4th and 5th sampling date. According to Vollenweider & Kerekes (1982), this range indicates mesotrophic to eutrophic conditions. A few extreme concentrations above 50 µg L^{-1} indicating hypereutrophic conditions were observed during dates 2-5.

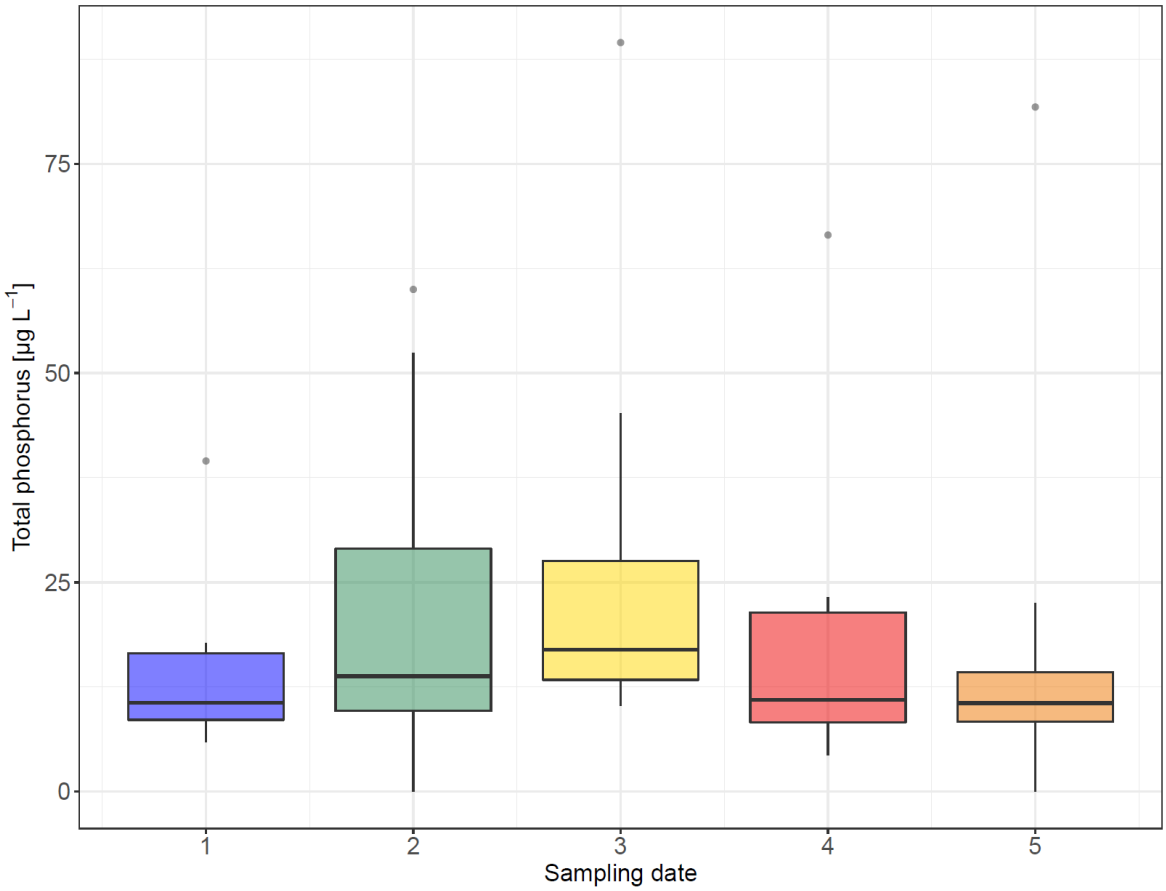

Fig. 23: Variation of total phosphorus concentration over the sampling season. Boxes show the 25% and 75% quantiles, while vertical lines represent those values that are 1.5 times lower and higher than the 25th and 75th percentiles, respectively. Individual dots represent extreme values that lie outside the 1.5 times interquartile range. (Total phosphorus concentrations were not obtained at all sampling sites, thus sample size was reduced to N = 8 during each sampling date).

3.2 Algae Torch Measurements

In Figure 24, the results obtained from the bbe moldaenke AlgaeTorch are visualized. In general, the mean concentration of total chlorophyll, representative for the algal community, increased over the sampling season. Nevertheless, the wide error bars indicate a considerable range of variation within the individual sampling dates. Accordingly, an increasing trend during the growing season was observed for the cyanochlorophyll. Overall, cyanochlorophyll increased from 5.3 µg Chl-a L^{-1} on the 1st date to 11.7 µg Chl-a L^{-1} on the last sampling date. Extreme concentrations of cyanochlorophyll were observed during the 4th and 5th sampling event (80.9, 101.5 and 70 µg Chl-a L^{-1}, respectively). A maximum of both mean fluorescence signals was measured during the 5th sampling event (36.6 µg Chl-a L^{-1} total chlorophyll and 11.7 µg Chl-a L^{-1} cyanochlorophyll).

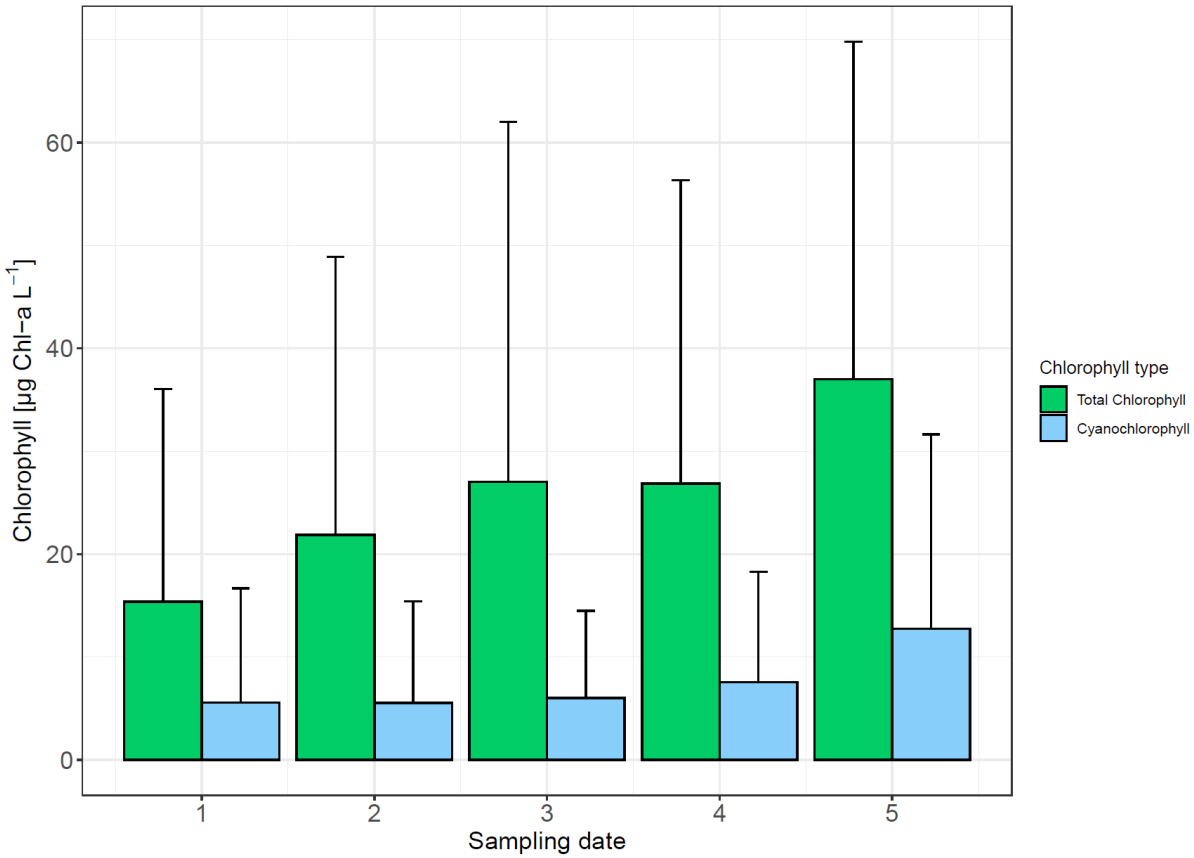

Fig. 24: Mean and standard deviation of total chlorophyll and cyanochlorophyll concentrations as recorded in vivo by using the fluoroprobe. Green barplots represent the total chlorophyll, which is calculated by an internal algorithm. It is based on the sum of all corresponding algal spectra, whereby cyanochlorophyll reveals values specific for the cyanobacterial community.

3.3 Experiments with different filters and extraction kits

Aside from the default DNA sampling and extraction procedure using the Sterivex™ filters and DNeasy® PowerWater® Sterivex™ Extraction Kit, other (more simple) membrane filters and DNA extraction procedures were tested. This comparison included (i) membrane filter and DNA extraction using the PowerWater Extraction Kit, (ii) membrane filter and DNA extraction using the Sterivex Extraction Kit and (iii) Sterivex filter and DNA extraction using the Sterivex Extraction Kit, which was the standard procedure applied in this study. The comparison used aliquots from five samples (ID 62, 84, 88, 105, 109) for which cyanotoxins were observed (Figure 25 and 26).

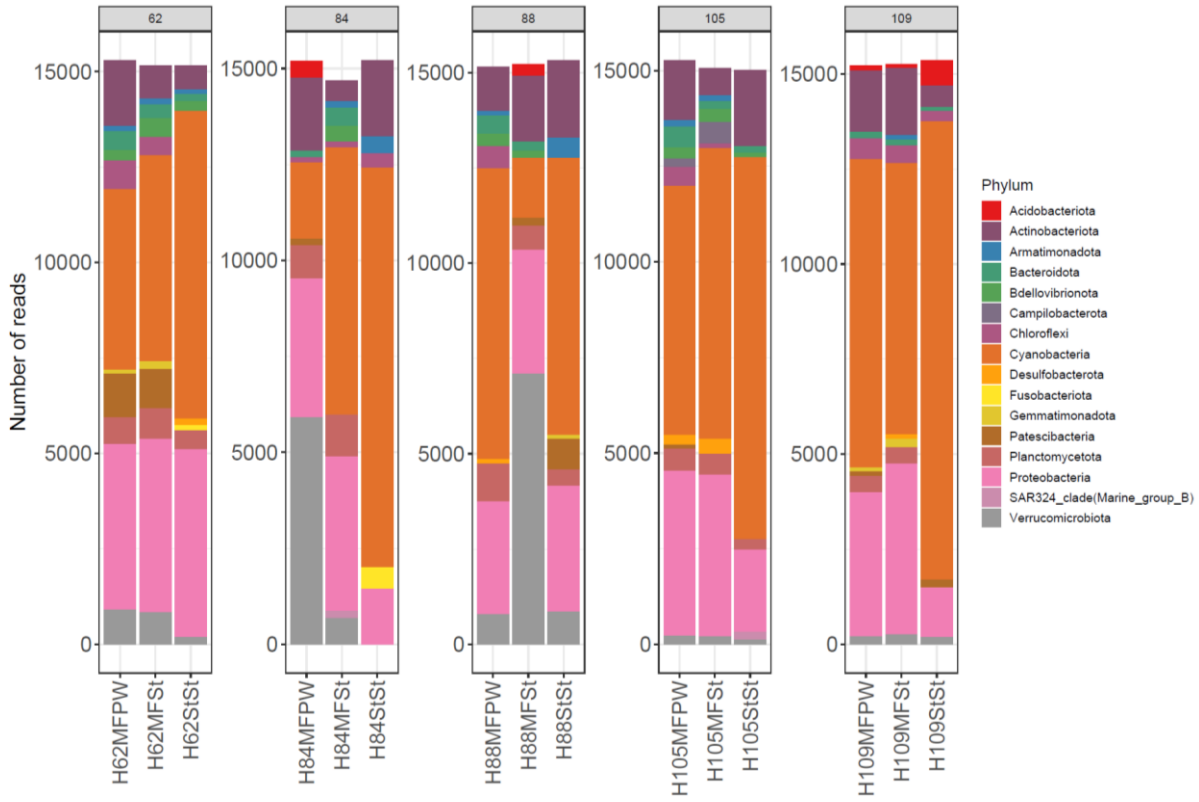

Fig. 25: Number of reads observed for each phylum using three different DNA sampling and extraction procedures. Rarefaction was performed at 15495 reads. Phyla showing less than 100 reads were discarded. Abbreviations: MFPW = Membrane Filter + PowerWater Extraction Kit, MFSt = Membrane Filter + Sterivex Extraction Kit, StSt = Sterivex Filter + Sterivex Extraction Kit (standard procedure applied in this study).

In Figure 25, the read numbers of the identified phyla based on the three different procedures is shown. When comparing the number of reads among the three different filtering methods and extraction kits, the maximum read number of cyanobacteria was observed using the standard procedure, i.e., Sterivex filtration and Sterivex extraction kit. For example, for sample IDs 84 and 88 a significant difference in cyanobacteria read numbers was observed. For sample ID 84, the S-Pak® Membrane filter/PowerWater® Kit combination revealed 1987 cyanobacterial reads, the S-Pak® Membrane filter/Sterivex™ Kit set revealed 6959 cyanobacterial reads and, finally, the Sterivex™ filter/Sterivex™ extraction Kit yielded 10413 reads. For sample ID 88, the standard procedure resulted in 7275 cyanobacterial reads, similar to the S-Pak® Membrane filter/PowerWater® Kit combination (7616 cyanobacterial reads). Lowest cyanobacterial read number was obtained by the combination of S-Pak® Membrane filter/Sterivex™ Kit (1565 reads). For the three other samples ID 62, 105 and 109, the numbers of cyanobacterial reads were found to be comparable.

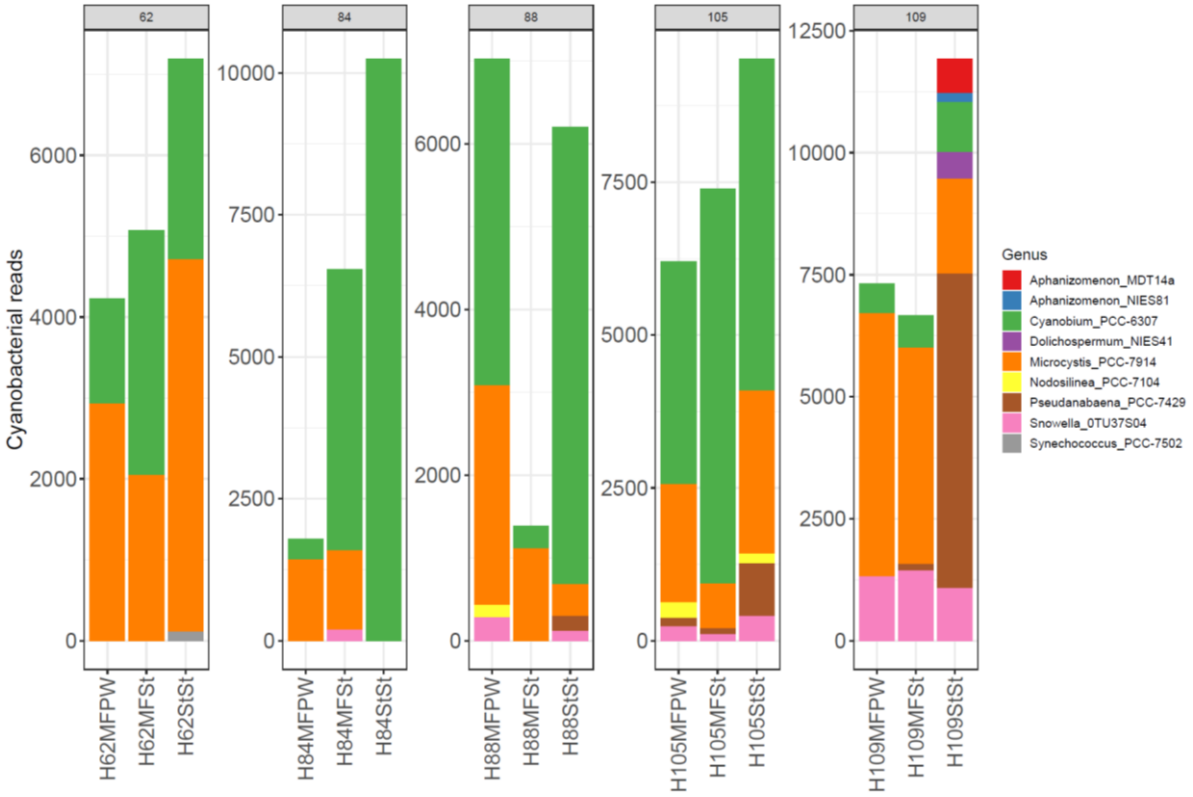

Fig. 26: Number of reads observed for each cyanobacterial genus using three different DNA sampling and extraction procedures. Rarefaction was performed at 15495 reads. Abbreviations: MFPW = Membrane Filter + PowerWater Extraction Kit, MFSt = Membrane Filter + Sterivex Extraction Kit, StSt = Sterivex Filter + Sterivex Extraction Kit (standard procedure applied in this study).

In Figure 26, the read numbers of the identified cyanobacterial genera determined by the three different procedures are shown. For sample ID 62, the results are consistent over the different treatments. In all three combinations, *Microcystis* (MFPW: 2932 reads, MFSt: 2046 reads, StSt: 4602 reads) and *Cyanobium* (MFPW: 1293 reads, MFSt: 3023 reads, StSt: 2478 reads) were detected. Additionally, 110 reads belonging to *Synechococcus* were determined using the combination of the Sterivex™ filters and Sterivex™ DNA extraction.

Contrarily, sample ID 84, 88, 105 and 109 resulted in different genus compositions. For sample ID 84, the combination of S-Pak® Membrane filter/PowerWater® Kit detected *Microcystis* (1426 reads) and furthermore 369 reads belonging to *Cyanobium*. In comparison, the Sterivex™ filter/Sterivex™ extraction Kit yielded 10246 reads, which were only assigned to *Cyanobium*. The S-Pak® Membrane filter/Sterivex™ Kit detected *Microcystis* (1390 reads), *Cyanobium* (4954 reads) and *Snowella* (196 reads).

Highest cyanobacterial read numbers were revealed for sample ID 88 using the combination of S-Pak® Membrane filter/PowerWater® Kit (3945 reads belonged to *Cyanobium*, 2653 reads to *Microcystis*, 284 reads to *Snowella* and 144 reads to *Nodosilinea*), followed by the Sterivex™ filter/Sterivex™ extraction Kit combination (5524 reads belonged to *Cyanobium*, 381 reads to *Microcystis*., 116 reads to *Snowella* and 181 reads to *Pseudanabaena*). Finally, with the combination of S-Pak® Membrane filter/Sterivex™ Kit, 1109 reads of *Microcystis* and 280 reads of *Cyanobium* were detected.

For sampling ID 105 the combination of Sterivex™ filter/Sterivex™ extraction Kit yielded the highest number of cyanobacterial reads (5428 reads belonging to *Cyanobium*, 2665 reads to *Microcystis*, 861 reads to *Pseudanabaena*, 397 reads to *Snowella*, 165 reads to *Nodosilinea*). Thereafter follows S-Pak® Membrane filter/Sterivex™ Kit (6458 reads belonging to *Cyanobium*, 734 reads to *Microcystis*, 101 reads to *Pseudanabaena* and 101 reads to *Snowella*) and S-Pak® Membrane filter/PowerWater® Kit (3646 reads belonging to *Cyanobium*, 1937 reads to *Microcystis*, 140 reads to *Pseudanabaena*, 229 reads to *Snowella*, 255 reads to *Nodosilinea*).

In sampling ID 109 agree the results of S-Pak® Membrane filter/PowerWater® Kit (5391 reads belonged to *Microcystis*, 1320 reads to *Snowella* and 611 reads to *Cyanobium*) and S-Pak® Membrane filter/Sterivex™ Kit (4433 reads belonged to *Microcystis*, 1430 reads to *Snowella*, 665 reads to *Cyanobium* and 143 reads to *Pseudanabaena*). In contrast to that, the results of the Sterivex™ filter/Sterivex™ extraction Kit, which yielded 6447 reads for *Pseudanabaena*, 1936 reads for *Microcystis*, 1076 for *Snowella*, 1035 for *Cyanobium*, 545 reads for *Dolichospermum*, 702 for *Aphanizomenon* (MDT14a) and 181 reads for *Aphanizomenon* (NIES81).

Considering the results for all five samples, the combination of the Sterivex™ filters and Sterivex™ DNA extraction Kit yielded the highest number of identified cyanobacterial reads and, furthermore, showed the highest diversity of cyanobacterial genera.

3.4 Optimisation of PCR Amplification

The PCR amplification curves of 46 plankton samples are shown in Figure 27-29. To determine the optimal conditions for the amplification during the sequencing process, different annealing temperatures and $MgCl_2$ concentrations were tested.

In Figure 27 the annealing temperature of 65°C was chosen since it was calculated by a T_m calculator. A negative control was used by adding ddH_2O instead of the DNA extract. No $MgCl_2$ was added. A fluorescence signal could be detected from all samples. Between 18 and 32 PCR cycles were necessary to receive an amplification curve from all environmental samples. The negative control did not show amplification till the 40th PCR cycle.

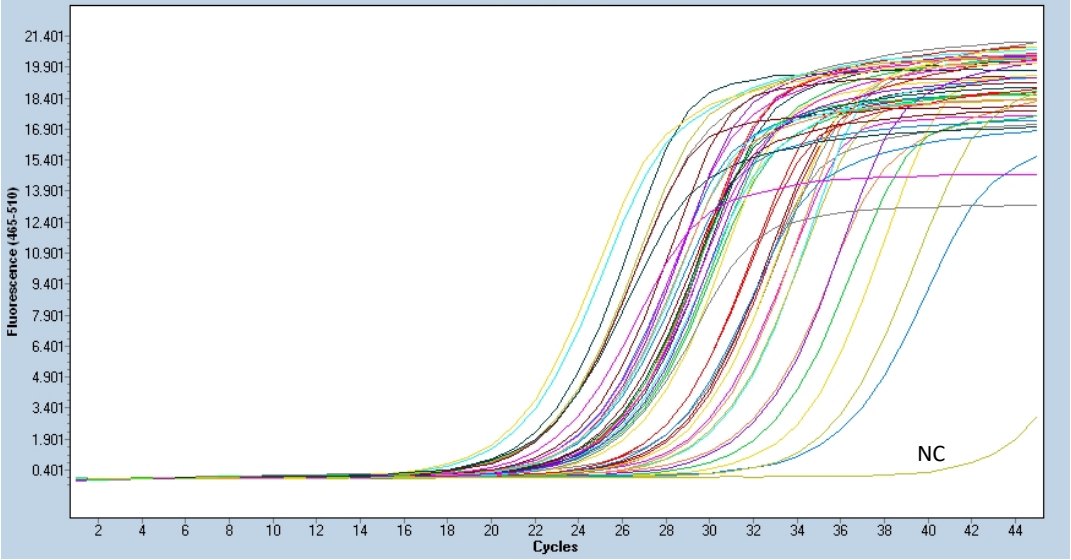

Fig. 27: Amplification curves for 46 plankton samples. For comparison the negative control (NC), which is coloured in yellow-green is included. Cyanobacterial primers with overhangs were used. Annealing temperature was 65°C. No $MgCl_2$ was added.

In the next step, $MgCl_2$ was added to the reaction mix which should enhance the activity of the DNA polymerase. Thus, a final concentration of 1.5 µM $MgCl_2$ was intended. Furthermore, a lower annealing temperature (62°C) was tested. In analogy to the former PCR experiments, a negative control (NC) was additionally amplified for comparison. This time, amplification already started after 16 PCR cycles. After 30 PCR cycles from all planktonic samples a fluorescence signal could be detected. The NC showed a signal only after 40 PCR cycles (Figure 28).

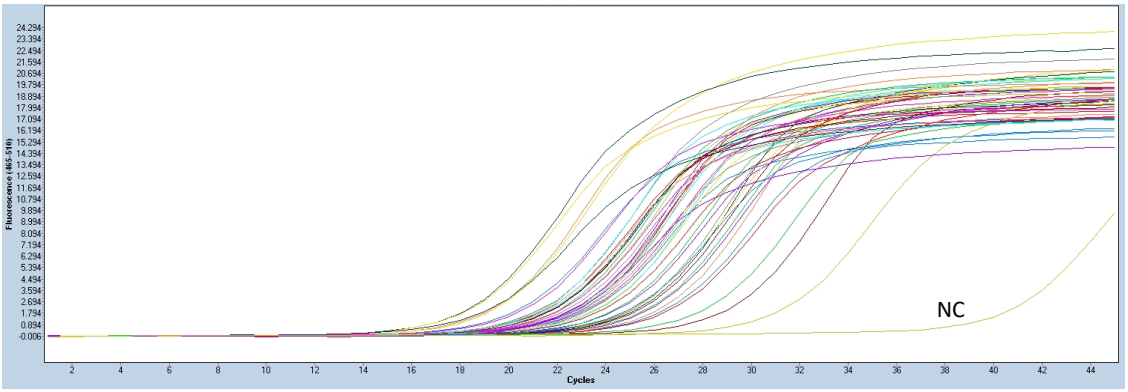

Fig. 28: Amplification curves for 46 plankton samples. The negative control (NC), which is coloured in yellow-green is included. Cyanobacterial primers with overhangs were used. Annealing temperature was 62°C and 1.5 µM $MgCl_2$ was added.

Finally, a PCR was set up with an annealing temperature of 65°C and 1.5 µM $MgCl_2$ end concentration in the reaction mix. Thereby, amplification of the samples already started after ten PCR cycles. After 30 PCR cycles, all environmental samples showed a fluorescence signal. The NC started to amplify after 35 PCR cycles (Figure 29).

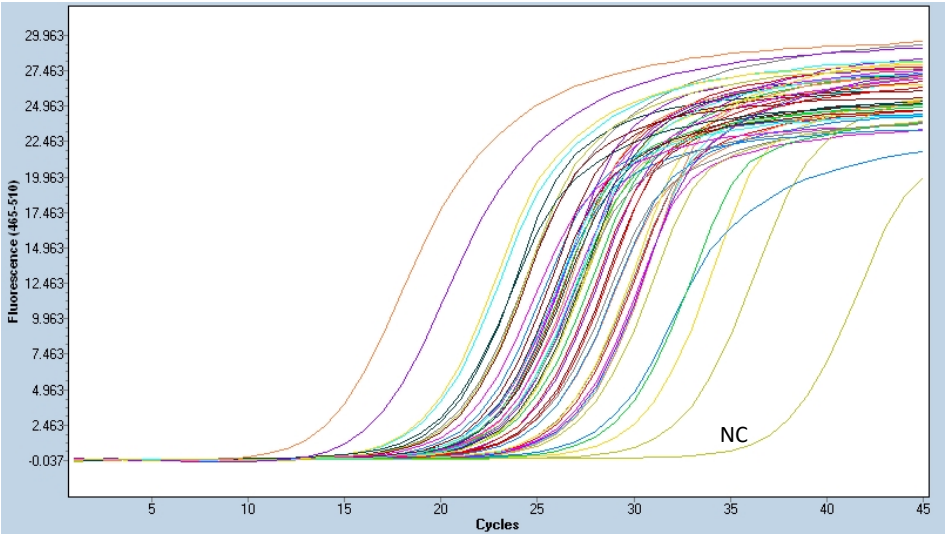

Fig. 29: Amplification curves for 46 plankton samples. The negative control (NC), which is coloured in yellow-green, is included. Cyanobacterial primers with overhangs were used. Annealing temperature was 65°C and 1.5 µM $MgCl_2$ was added.

These results indicate that optimal conditions for the amplification of 16S V3 to V4 region of cyanobacteria by using cyanobacterial primers after Nübel et al. (1997) and Turner et al. (1999) include a primer annealing temperature of 65°C, a concentration of 1.5 µM $MgCl_2$ and a PCR cycle limit of 30. These conditions, as summarized in Table 7, were used for sequencing.

3.5 Sequencing results

3.5.1 Community composition at the phylum level

All in all, 18 phyla above the minimum threshold of 50 reads were identified using mothur`s pipeline. In Figure 30, the 14 most relevant phyla are shown. On average, the phyla Bacteriodota, Actinobacteriota and Proteobacteria showed highest number of reads over the whole season with little seasonal variations. In contrast, the Campilobacteriota showed rather high sequence read numbers during sampling dates 1 to 3. However, on the 4th and 5th sampling date no Campilobacteriota were detected anymore. Furthermore, the Verrucomicrobiota show a rather decreasing trend in assigned number of reads from sampling date 1 to 3, but increased again during sampling dates 4 and 5. The most significant change in read numbers, however, was observed for the phylum of the cyanobacteria.

Other phyla, like Acidobacteriota, Armatimonadota, Bdellovibrionota, Chloroflexi, Desulfobacteriota, Gemmatimonadota, Patescibacteria, Planctomycetota occurred relatively stable and contributed relatively lower number of reads.

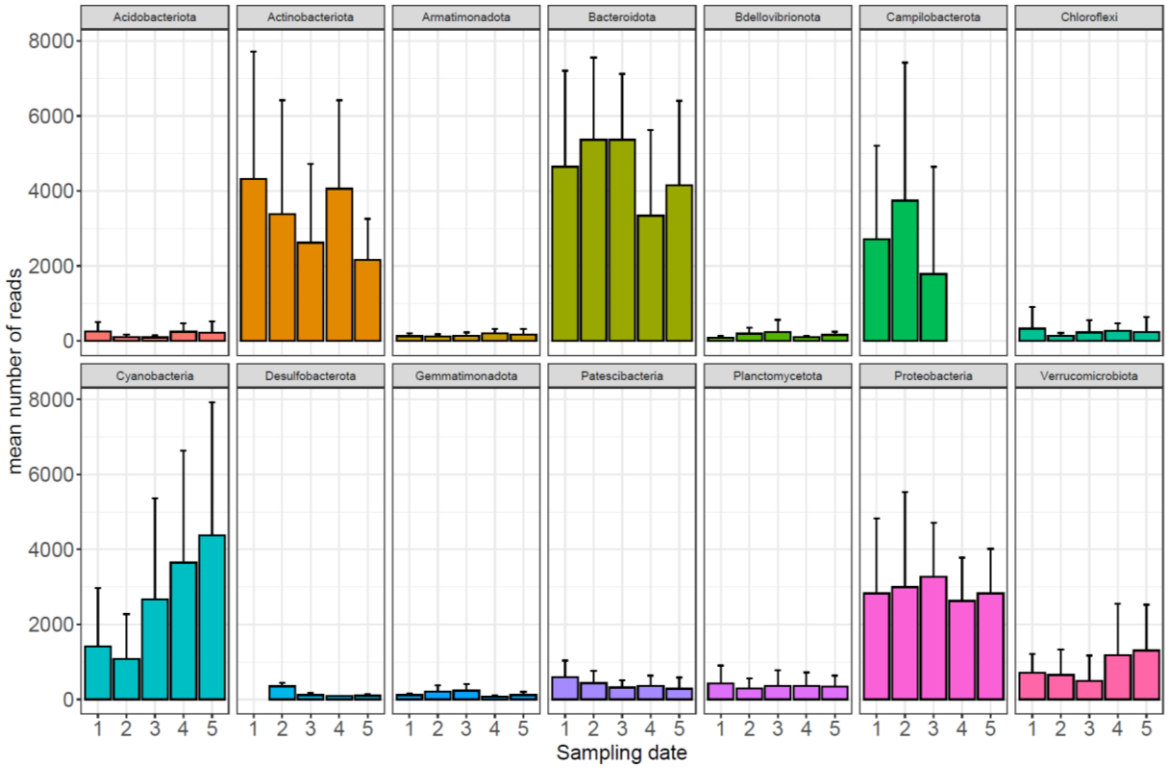

Fig. 30: Average read numbers and standard deviation for relevant bacterial phyla recorded during the five sampling dates over the season. The mothur sequence analysis pipeline was used. For each sampling date, 20 samples were analyzed. Additionally, low number of reads were identified for the phyla Firmicutes, Fusobacteriota, Myxococcota and Spirochaetota, but were excluded from the plot.

The phylum of Cyanobacteria showed the most extensive increase in read numbers over the season. In detail, these numbers of reads can also be observed later in Figure 32 for further comparison. In the beginning of the season, a slight decrease from an average of 1409 to 1081 reads was recorded. However, after the 2nd sampling date, an exponential increase from 2663 to 3646 reads was determined. Finally, in the 5th sampling date the mean read number reached the maximum of 4370 reads. Due to the fact, that for all samples rarefaction was performed at 16150 reads, the proportion of cyanobacterial reads increased from 9% to 27% in sampling date 1 to 5.

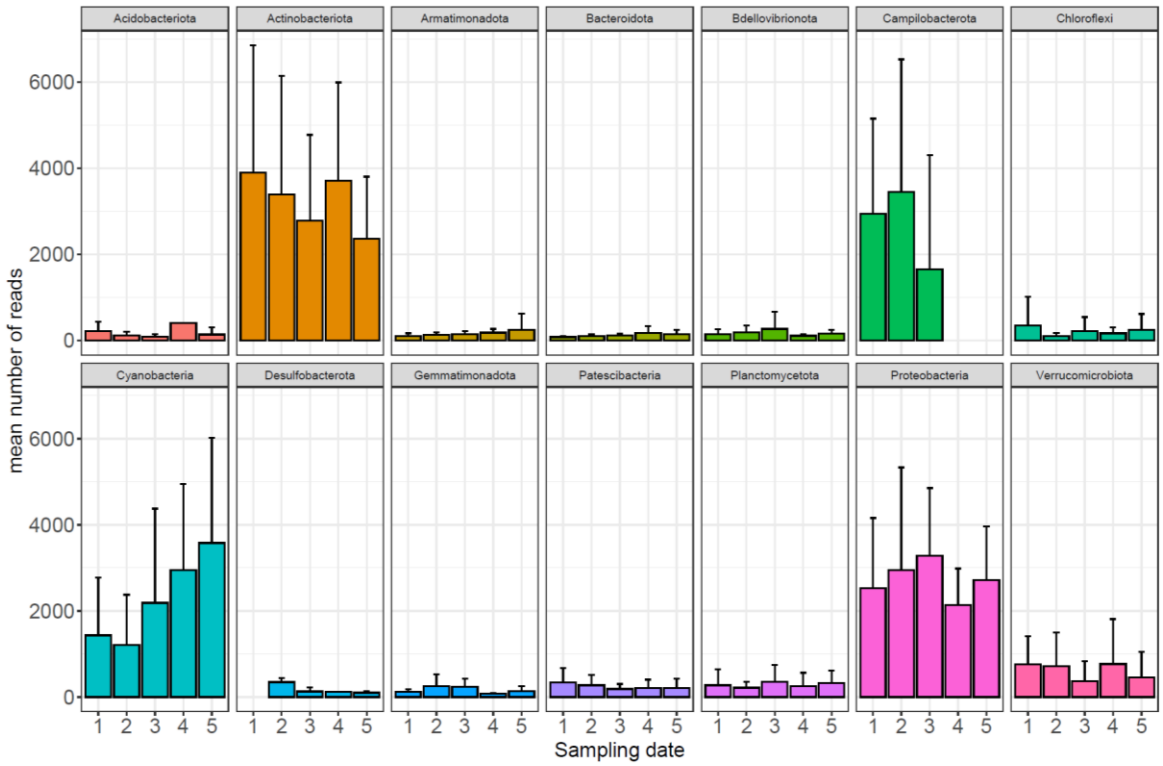

Fig. 31: Average read numbers and standard deviation for relevant bacterial phyla recorded during the five sampling dates over the season. The DADA2 sequence analysis pipeline was used. For each sampling date 20, samples were analyzed. Additionally, low number of reads were identified for the phyla Firmicutes, Fusobacteriota, Myxococcota, Nitrospirota and Spirochaetota, but were excluded from the plot.

Besides the mothur sequence analysis pipeline, a more recent developed sequence analysis pipeline called, DADA2 pipeline was used, and the results are shown in Figure 31. In general, a similar trend to mothur sequence analysis was observed: The Actinobacteriota and Proteobacteria showed relatively high number of reads over the entire sampling season. A contrasting observation can be found by consideration of

the low read numbers of Bacteriodota. According to DADA2 results, the Bacteriodota have a similar read number as the Armatimonadota, Bdellovibrionota, Chloroflexi, Gemmatimonadota, Patescibacteria, Planctomycetota and Verrucomicrobiota.

The read numbers for the cyanobacterial community were found comparable using both methods of sequence analysis, mothur and DADA2. Regarding the number of reads of cyanobacteria a pronounced increase was found between the 2nd – 5th sampling dates, starting from an average value of 600 reads and finally reaching an average maximum of 3577 reads on the 5th sampling date. The rarefaction-threshold was determined at 10130 reads (corresponding to the sample showing the lowest total read number), which resulted in a mean increase of cyanobacteria from 14% to 24% from sampling date 1 to 5.

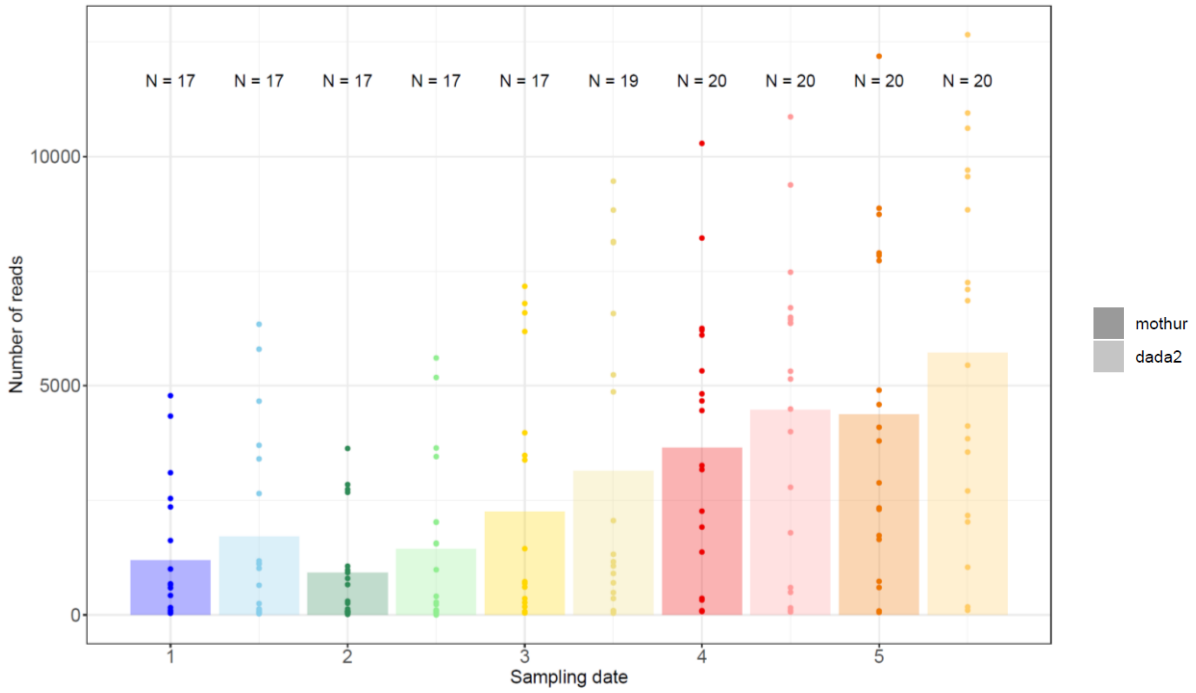

Fig. 32: Total cyanobacterial read numbers recorded during the sampling season by using two different sequence analysis pipelines (mothur, DADA2). The average is indicated by the barplots, whereby the individual number of reads per sampling site are indicated using dots. The N describes the number of shore lake samples found positive for cyanobacteria (>50 reads for the phylum). Due to different rarefaction thresholds, the DADA2 sequences were multiplied by 1.6 to facilitate comparing results.

In Figure 32, the cyanobacterial read numbers determined by mothur and DADA2 are compared. In particular, the number of samples where cyanobacterial reads were detected, is similar for mothur and DADA2.

During the 1st and 2nd sampling event, cyanobacterial reads were detected for 17 different stations, each. In contrast, mothur identified cyanobacteria only in 17 samples (out of 20 samples) during the 3rd sampling event, while DADA2 detected cyanobacteria in 19 sites. During the 4th and 5th sampling date, both pipelines obtained cyanobacteria in all 20 sampling stations. Correspondingly, a maximum of average cyanobacterial reads was obtained using mothur and DADA2 for the 5th sampling date.

It was shown that the variation in cyanobacterial read number between sampling stations was high, in particular during the 3rd, 4th and 5th sampling date. On the one hand, for several sites only low or no cyanobacteria were detected, such as the two shore lake samples with following IDs: 10, 40, 56, 78, 99 and 16, 43, 64, 86, 107, respectively. On the other hand, for numerous sites (e.g., ID 12, 41, 62, 84, 105 and 11, 39, 57, 79, 100, respectively) a high share of cyanobacteria reads occurred throughout the season.

3.5.2 Cyanobacterial genera composition

The distribution patterns of more frequent cyanobacterial genera are demonstrated in Figure 33 (for mothur) and 34 (for DADA2). According to mothur, eleven different cyanobacterial genera were detected with more than 50 reads. The most abundant cyanobacteria comprised the genus *Cyanobium*, showing a maximum at the 4th sampling date with an average value of 1006 reads. The second most abundant organism was *Microcystis*, corresponding to high read numbers in the beginning of the season (average of 320 reads), followed by a decreasing tendency until the 5th sampling date (average of 121 reads). In contrast, the read numbers assigned to the diazotrophic cyanobacterium *Dolichospermum* increased over the study period. While *Dolichospermum* was not detected during the 1st sampling date, it gradually increased till the end of the season and reached an average maximum of 56 reads. *Aphanizomenon* shows a similar phenological response, i.e., low read numbers in the beginning and an increase in read number towards the end, reaching a maximum in the 5th sampling date (maximum average read number: 103). Beside the former mentioned genera, also the frequent occurrence of *Planktothrix* is remarkable. *Planktothrix* occurred during the full range of sampling dates, with maximum read numbers obtained from the 3rd sampling event (maximum average read number: 115).

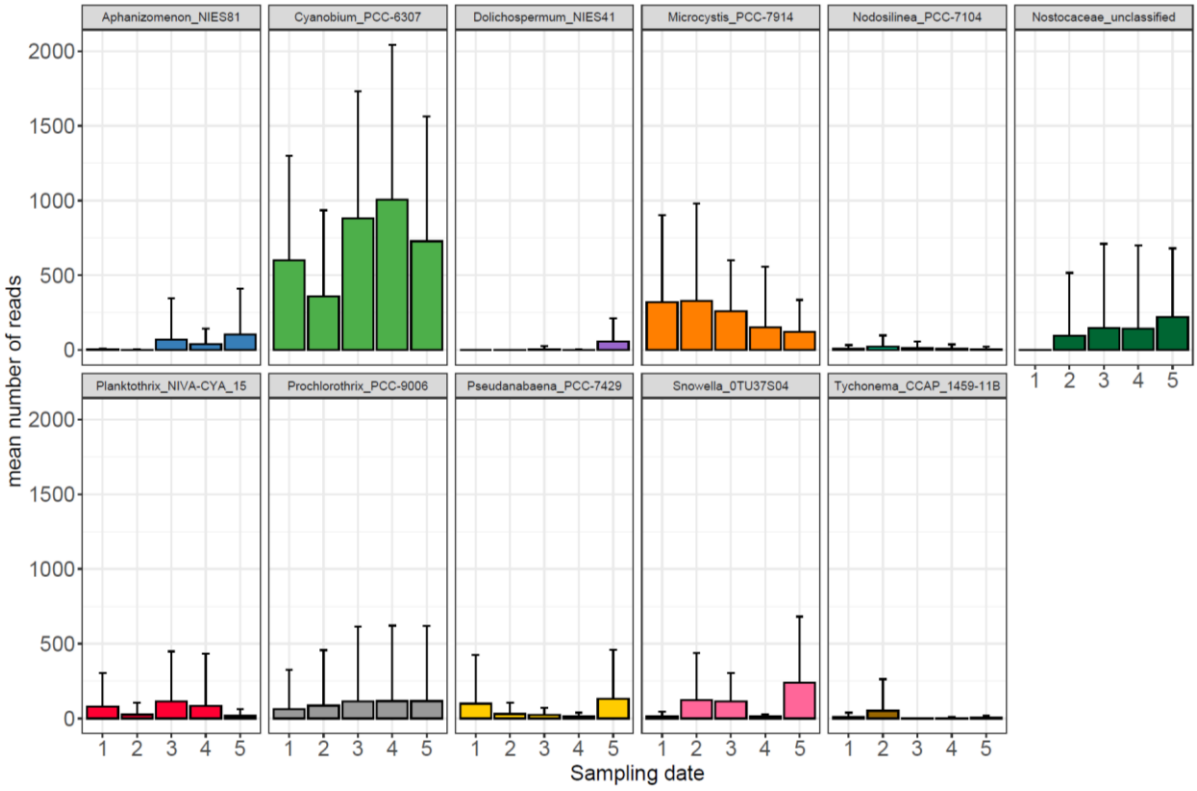

Fig. 33: Mean read numbers and standard deviation recorded for individual cyanobacteria genera during five sampling dates by using mothur for sequence analysis. Each bar represents the mean value of the number of reads from all sites for one sampling date.

Similar results as with mothur were obtained when using DADA2 in general. In example, the genus *Cyanobium* occurred most frequently, showing its maximum in the 4th sampling date (average number of reads: 3656). Furthermore, *Microcystis*, *Dolichospermum* and *Planktothrix did* show the same pattern in frequency of occurrence independent of the utilised pipeline. While the diazotrophic genera *Dolichospermum* and *Aphanizomenon* rather increased in read numbers, *Planktothrix* remained stable and *Microcystis* decreased in read number during the sampling season. Thus, the major difference between the two sequence analysis pipelines was found in the absolute number of reads. In other words, DADA2 deduced a higher read number for cyanobacteria (and other bacteria as well) and correspondingly also for each genera.

In addition to *Aphanizomenon* genotype strain NIES81, a second *Aphanizomenon* strain, namely MDT14a, was detected when using DADA2. While *Aphanizomenon* NIES81 showed about the same frequency of occurrence as MDT14a, the latter only

was detected after the 2nd sampling date. Notably, a few reads indicative of the brackish water genus *Nodularia* were identified using DADA2.

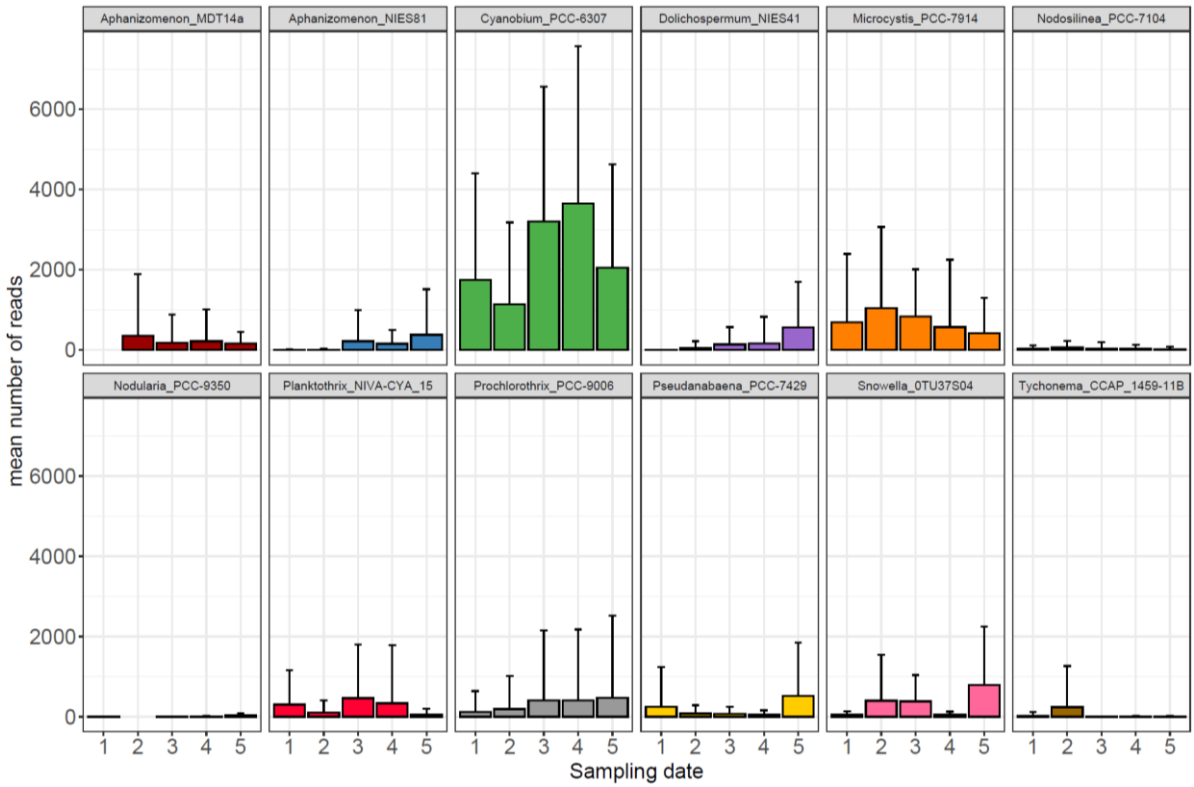

Fig. 34: Mean read numbers and standard deviation recorded for individual cyanobacteria genera during five sampling dates by using DADA2 for sequence analysis. Each bar represents the mean value of the number of reads from all sites for one sampling date.

3.5.3 Comparison of the two primer pairs used for PCR amplification

In addition to the comparison of sequence analysis pipelines, two primer pairs were compared regarding cyanobacteria genera detection, i.e., the general 16S bacterial primers and the more specific cyanobacterial primers which were used for the amplification. In Figure 35 and 36, the abundant genera were compared in read numbers based on the two different primer pairs as well as on the two sequence analysis pipelines, respectively. For this comparison 13 sampling stations were selected, which revealed the occurrence of cyanotoxins (see below). All in all, it was found that both primer systems revealed similar estimates of genus composition and distribution.

In most cases, the cyanobacterial-specific primers resulted in a similar cyanobacterial diversity (e.g., sample ID 79, 84 and 89) when compared with the general bacterial

primers. An exception was found for sample ID 77, which resulted in a small amount of *Cyanobium* reads based on usage of bacterial primers. For sample ID 62, using both primer systems, two genera assigned to *Cyanobium* and *Microcystis* were detected. Nevertheless, the amount of *Microcystis* in the cyanobacterial sequenced sample was relatively low when compared with the bacterial sequenced one.

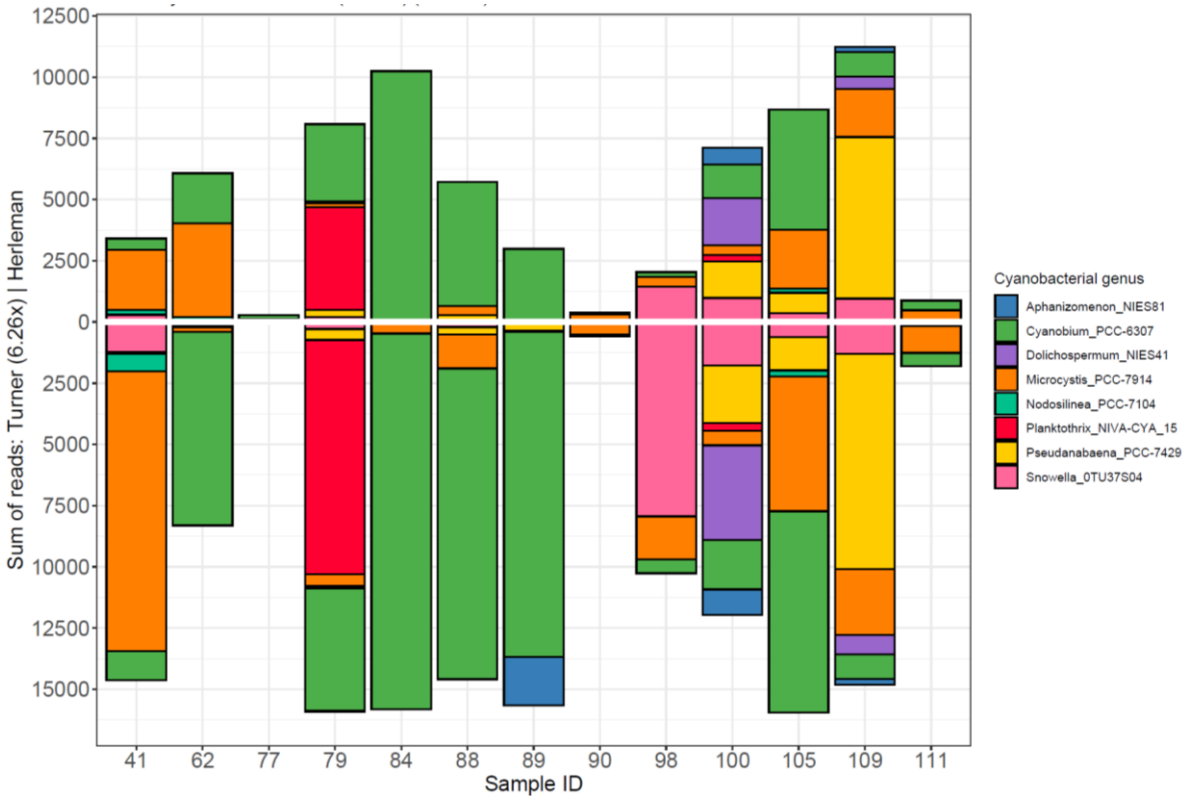

Fig. 35: Mean read numbers of cyanobacterial genera recorded for 13 selected sites (ID 41 belongs to the 2nd sampling date, ID 62 to the 3rd sampling date, IDs 77, 79, 84, 88, 89 to the 4th sampling date and IDs 90, 98, 100, 105, 109, 11 to the 5th sampling date) either resulting from general bacterial primers (upper half of the graph, positive scale) or from cyanobacteria specific primers (lower half of the graph, negative scale). For sequence analysis the pipeline mothur was used. Due to the different rarefaction thresholds applied for the two PCR based sequencing outputs, the cyanobacteria specific sequences were multiplied by 6.26 to facilitate comparing results.

Accordingly, using DADA2 analysis software rather comparable read numbers were obtained when comparing the bacterial and cyanobacterial primer system (see Figure 36). As mentioned above, the cyanobacterial primers resulted in one more genotype of *Aphanizomenon* (MDT14a) in samples ID 79, 84, 88, 89, 90, 100 and 111. In contrast, *Aphanizomenon* (strain MDT14a) was not detected in samples ID 88, 90, 100 and 111 using bacterial primers. As an exception, sample ID 62 did show a higher *Microcystis* read number when using the bacterial primers, in opposition to the

cyanobacterial primers. The same overestimate or underestimate was revealed using the mothur sequence analysis pipeline (see above).

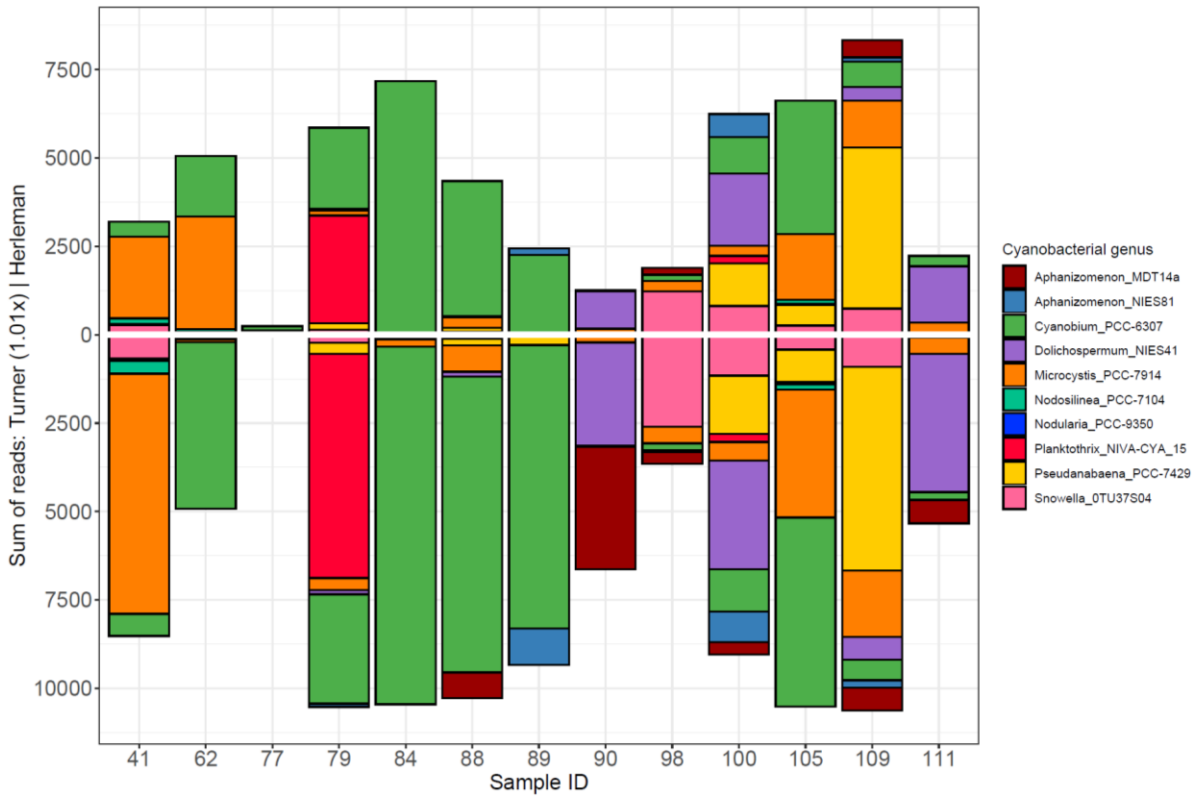

Fig. 36: Mean read numbers of cyanobacterial genera recorded for 13 selected sites (ID 41 belongs to the 2nd sampling date, ID 62 to the 3rd sampling date, IDs 77, 79, 84, 88, 89 to the 4th sampling date and IDs 90, 98, 100, 105, 109, 11 to the 5th sampling date) either resulting from general bacterial primers (upper half of the graph, positive scale) or from cyanobacteria specific primers (lower half of the graph, negative scale). For sequence analysis the pipeline DADA2 was used. Due to the different rarefaction thresholds applied for the two PCR based sequencing outputs, the cyanobacteria specific sequences were multiplied by 1.01 to facilitate comparing results.

3.5.4 Comparison of the two sequence analysis pipelines

In Figure 37, the read numbers for cyanobacterial genera were compared using the two different sequence analysis pipelines. In general, genus composition and numbers of reads were found similar, irrespective of the sequence analysis pipeline used. However, when looking more into detail, the *Aphanizomenon* (strain MDT14a) was detected in samples ID 88, 90, 98, 100, 109 and 111 using DADA2, while mothur did not reveal this specific genotype. The number of reads observed for *Dolichospermum* were also found to be lower when using mothur, since in samples ID 90 and 111 no single read was assigned to this genus. In contrast, 2891 and 3878 reads were

assigned to this genus via DADA2 for samples ID 90 and 111, respectively. However, both sequence analysis pipelines did not detect any cyanobacteria in sample ID 77.

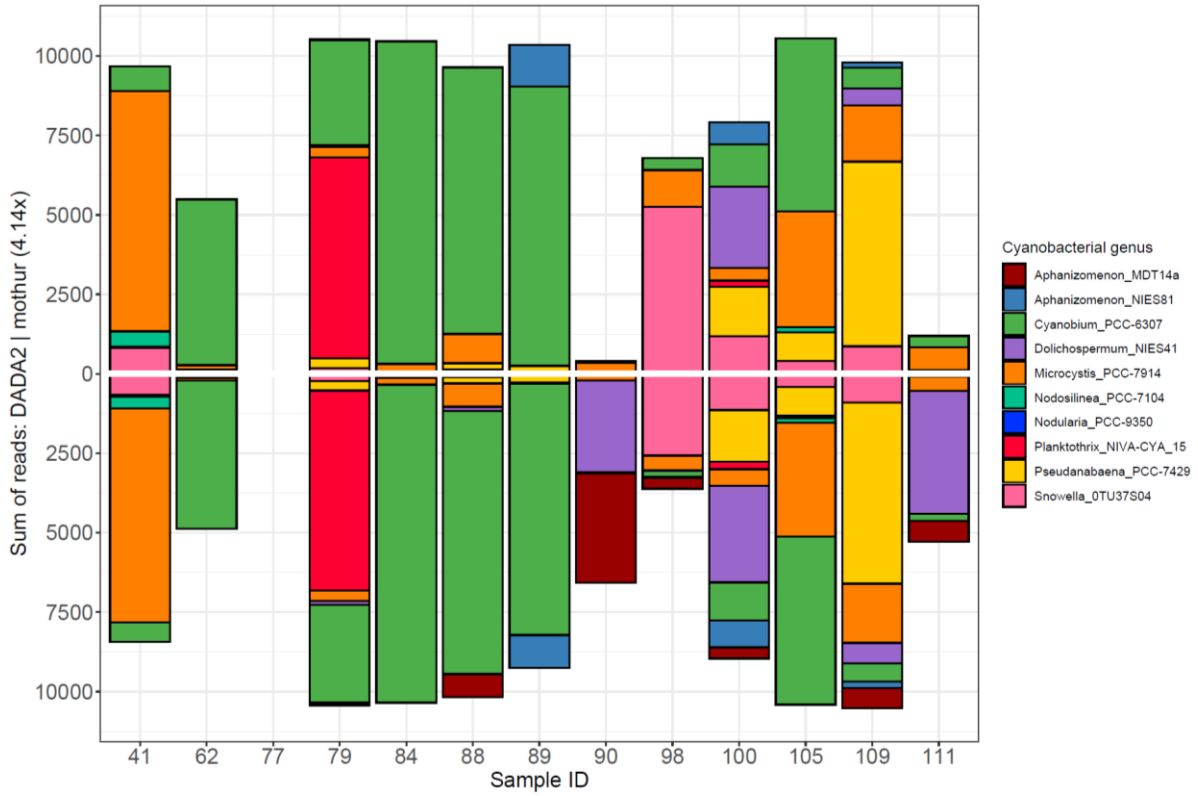

Fig. 37: Mean read numbers of cyanobacterial genera recorded for 13 selected sites (ID 41 belongs to the 2nd sampling date, ID 62 to the 3rd sampling date, IDs 77, 79, 84, 88, 89 to the 4th sampling date and IDs 90, 98, 100, 105, 109, 11 to the 5th sampling date) either resulting from mothur sequence analysis pipeline (upper half of the graph, positive scale) or from DADA2 sequence analysis pipeline (lower half of the graph, negative scale). For PCR amplification the specific cyanobacteria primers were used. Due to the different rarefaction thresholds applied for the two sequence analysis outputs the mothur read numbers were multiplied by 4.14 to facilitate comparing results.

Plotting the cyanobacterial read numbers from both sequence analysis pipelines against each other, a statistically highly significant positive linear relationship (r^2 = 0.959) was found, as shown in Figure 38. The scatter plot indicates, that the more cyanobacterial reads were detected by mothur, also higher amounts of reads assigned to cyanobacteria were observed by DADA2. The intercept (249) highlights that DADA2 assigned slightly more reads to cyanobacteria than mothur did. Notably, the higher read number estimates of DADA2 were evident only at the lower range of read numbers (0 - 5000 reads), while in the higher range above 5000 reads a contrary picture was drawn, where the DADA2 algorithm showed lower read numbers when compared with mothur.

In summary, a good agreement in results obtained by using specific cyanobacterial and general bacterial primer pairs as well as between both sequence analysis pipelines, mothur and DADA2, was observed. Nevertheless, in the majority of samples, DADA2 in combination with cyanobacterial-specific primers resulted in more sensitive detection of cyanobacterial genotypes. Since the aim of this thesis was to establish a workflow useful as early-warning system for toxic-cyanobacterial blooms in bathing waters, the analysis below is only shown using the cyanobacterial specific primers in combination with DADA2 algorithm.

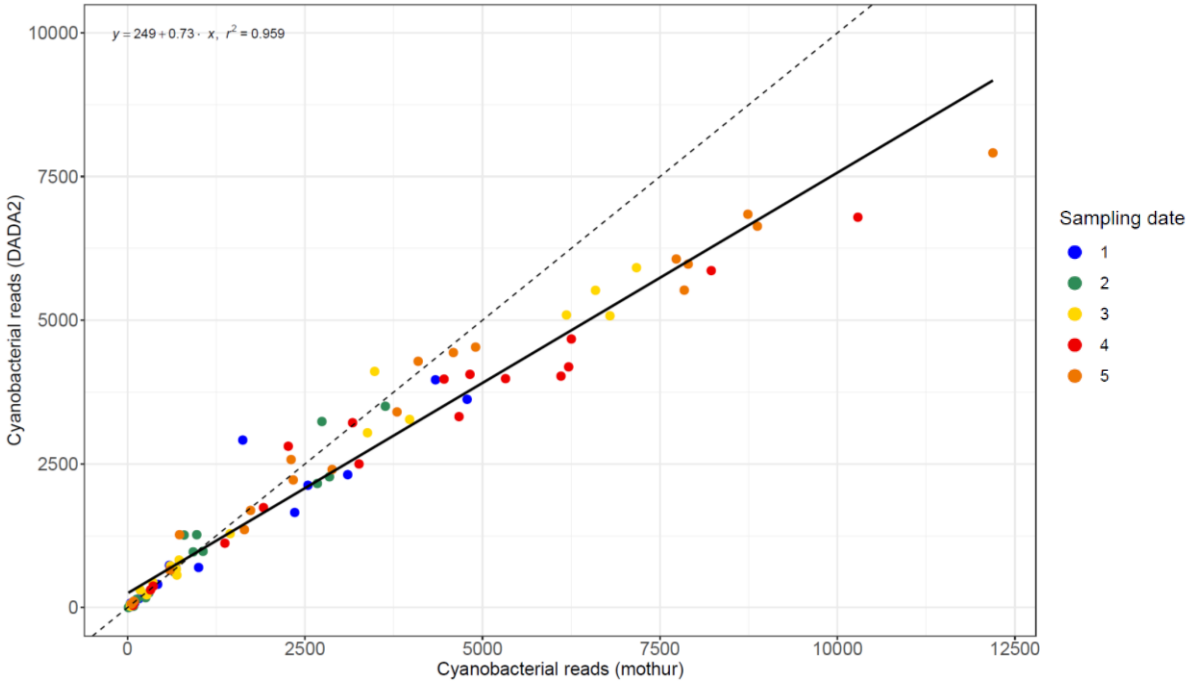

Fig. 38: Scatterplot of cyanobacteria read numbers calculated from either mothur sequence analysis pipeline (x-axis) or the DADA2 algorithm sequence pipeline (y-axis). The samples originating from the five different sampling dates are indicated by colour. The details of the linear regression curve were y = 249 + 0.73 x, were the regression coefficient (r^2) indicates a statistically significant relationship. The 1:1 relationship is indicated by a dotted line.

3.6 Cyanobacteria and their toxins

In general, microcystin and anatoxin-a were observed in numerous samples. Microcystins were composed of microcystin-LR (detected in 11 out of 103 samples, with the highest concentration measured in ID 62 at 2.01 µg L^{-1}), microcystin-RR (detected in 9 samples, with the highest concentration measured in ID 88 at 1.82 µg L^{-1}), microcystin-YR (detected in 5 samples, with the highest concentration measured in ID 62 at 2.89 µg L^{-1}) and microcystin AspDhbRR (detected in 3 samples, with the

highest concentration measured in ID 88 at 0.35 µg L^{-1}). A further abundant structural variant of microcystin, nodularin, was not detected. Another toxin, cylindrospermopsin, was undetectable throughout the season. In order to identify the the cyanobacteria possibly producing the observed toxins, all cyanobacterial genera which have been related to toxin production in the past were plotted against the detected toxins (see Figure 39-41). In particular, microcystin synthesis genes have been elucidated from *Microcystis* (Tillett et al., 2000), *Planktothrix* (Briand et al., 2005), *Anabaena* and *Nodularia* (Chorus & Bartram, 1999) previously. The anatoxin-a synthesis genes have been first described from *Oscillatoria* and later from *Anabaena* (Osswald et al., 2007). The genetic basis of toxin synthesis among so-called picocyanobacteria (e.g. *Cyanobium*) for producing microcystin or anatoxin-a is not well studied (Jakubowska & Szeląg-Wasielewska, 2015). Nevertheless, picocyanobacteria have been related to microcystin concentrations (Chorus & Welker, 2021).

In general, the concentration of detected toxins increased with the number of cyanobacterial reads (see Figure 39). In particular, at the beginning of the sampling season in early June, no toxins were detected. In total, 195715 reads were assigned to cyanobacteria. The most dominant genus was *Cyanobium*, to which 58% of the cyanobacterial sequences were assigned. The second most frequent genus was *Microcystis*, which occurred with a ratio of 23%. In addition, numerous read sequences could still be assigned to *Planktothrix* and *Pseudanabaena* with 10%, and 8%, respectively.

During the 2nd sampling date, a total microcystin concentration of 0.6 µg L^{-1} (composed of 0.25 µg L^{-1} microcystin-LR and 0.35 µg L^{-1} microcystin YR) was detected. For this sampling date, which took place in mid of June, 17113 reads were assigned in total to cyanobacteria. The vast majority of cyanobacterial reads were assigned to *Cyanobium* (38%) and *Microcystis* (35%). This time, cyanobacterial diversity increased, since furthermore 12% of the reads were assigned to *Aphanizomenon* (strain MDT14a) and *Tychonema* (8%). The proportion of *Planktothrix* und *Pseudanbaena*, however, decreased down to 3%, each.

At the beginning of July when the 3rd sampling date was performed, a strong increase in cyanotoxins could be observed. The total microcystin concentration was 5.4 µg L^{-1}

comprising microcystin-LR (2.11 µg L^{-1}), microcystin-RR (0.4 µg L^{-1}), and microcystin-YR (2.89 µg L^{-1}). The dominant genus again was *Cyanobium,* with a share of nearly 63% of the 37249 detected cyanobacterial reads. The number of *Microcystis* reads and *Aphanizomenon* (strain MDT14a) decreased to 16% and 3%, respectively. In addition, the genus *Planktothrix* (representing 9% of the total cyanobacterial reads) as well as *Dolichospermum* (3%) and *Aphanizomenon* strain NIES81 (4%) were frequently detected

During the 4th sampling event, which took place at the end of July, a maximum of toxins and cyanobacterial reads could be detected. In particular, a total microcystin concentration of 8 µg L^{-1} and 53152 cyanobacteria reads were detected. The largest proportion of microcystin was again made from microcystin-LR with 3.66 µg L^{-1}, followed by microcystin-RR with 2.63 µg L^{-1} and microcystin-YR with 1.23 µg L^{-1}. Furthermore, 0.48 µg L^{-1} of the microcystin variant AspDhbRR could be detected. Again, *Cyanobium* was the most dominant genus, resulting in a proportion of 70%. The second most frequent genus was *Microcystis* with 11% proportion. For other genera like *Planktothrix*, both *Aphanizomenon* strains and *Dolichospermum* decreased to 2-6% proportion.

Finally, declining mean cyanotoxin concentrations were observed during the last sampling date, which was held in mid-august. The total sum of toxins decreased to 5.81 µg L^{-1}, while the larger fraction was again assigned to microcystin-LR (2.49 µg L^{-1}), followed by microcystin-RR (1.97 µg L^{-1}), microcystin-YR (0.98 µg L^{-1}) and microcystin- AspDhbRR (0.26 µg L^{-1}). Only during this sampling date anatoxin-a was detected (0.11 µg L^{-1}). Furthermore, the number of detected reads assigned to cyanobacteria declined to 67961. Among these, *Cyanobium* contributed with a proportion of 49%. Nevertheless, the amount of *Aphanizomenon* (strain NIES81), *Dolichospermum* and *Pseudanabaena* increased in comparison to the 4th sampling date with a relative proportion of 9%, 13% and 12%, respectively. The proportion of *Microcystis* declined to 10%, and thus, *Dolichospermum* became the second most frequent genus.

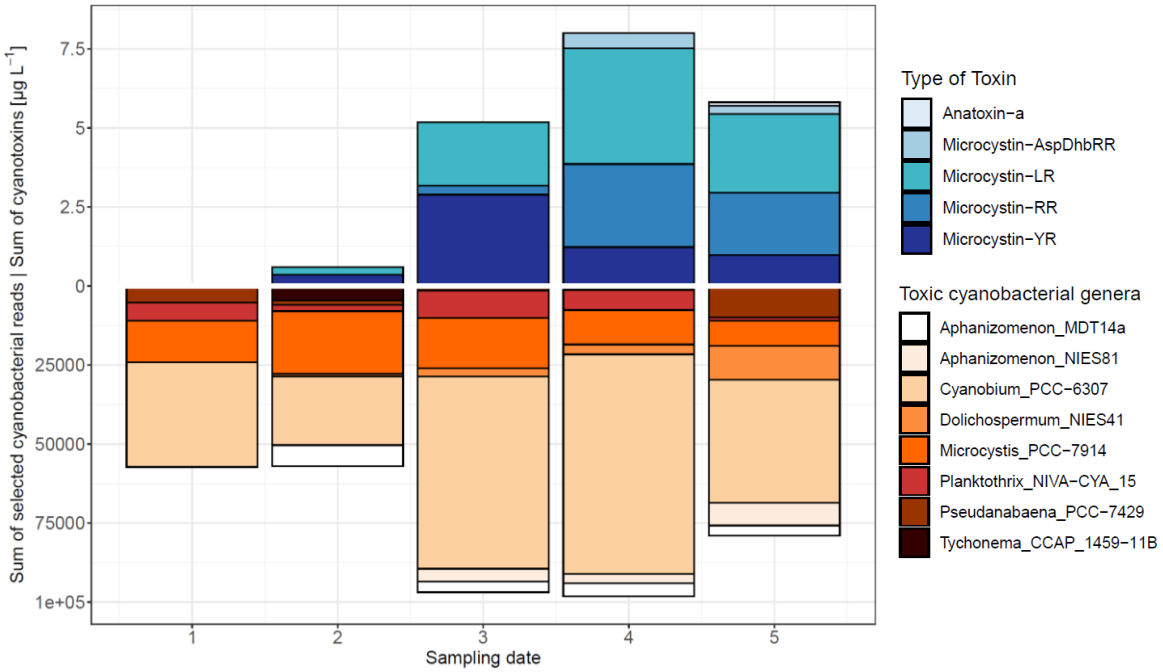

Fig. 39: Mean read numbers of cyanobacterial genera related to mean microcystins and anatoxin-a concentrations in µg L^{-1}. The microcystin and anatoxin-a concentrations (sum of free and cell-bounded) are indicated in the upper half of the graph (y-axis, positive scale), while the cyanobacterial reads observed for each genus are shown in the lower half of the graph (y-axis with negative scale). Except for *Cyanobium* (Christiansen et al., 2001) for all other cyanobacterial genera the respective genes of cyanotoxin synthesis have been described from isolated strains in the past (Rastogi et al., 2015). For PCR amplification the specific cyanobacteria primers and the subsequent DADA2 sequence analysis was used.

In Figure 40 and 41, the recorded cyanotoxin concentrations were plotted versus the read numbers for each sample. In both graphs, DADA2 was used for analysis of sequences, while sequence reads obtained from the two different primer pairs were analysed. In Figure 38 the read numbers of cyanobacterial genera originating from the cyanobacteria specific primer pair were compared with the cyanotoxin concentrations for each sample. Over the entire study period, cyanotoxins were detected at 13 sampling stations. One sample each was found cyanotoxin-positive during sampling date 2 (ID 41) and 3 (ID 62). On sampling date 4, the highest number of cyanotoxin positive samples (6) was observed (ID 77, 79, 84, 88, 89, 90). In the 5th sampling date, cyanotoxins were detected at five locations (ID 98, 100, 105, 109 and 111). The 13 cyanotoxin-positive samples originated from six different lake shore sites. All six shore lake sites found cyanotoxin positive on the 5th sampling date had measurable toxin-concentrations already on the 4th sampling event. Only at a single shore lake site (ID 41, 62, 84 and 105) toxins were detected during the entire season.

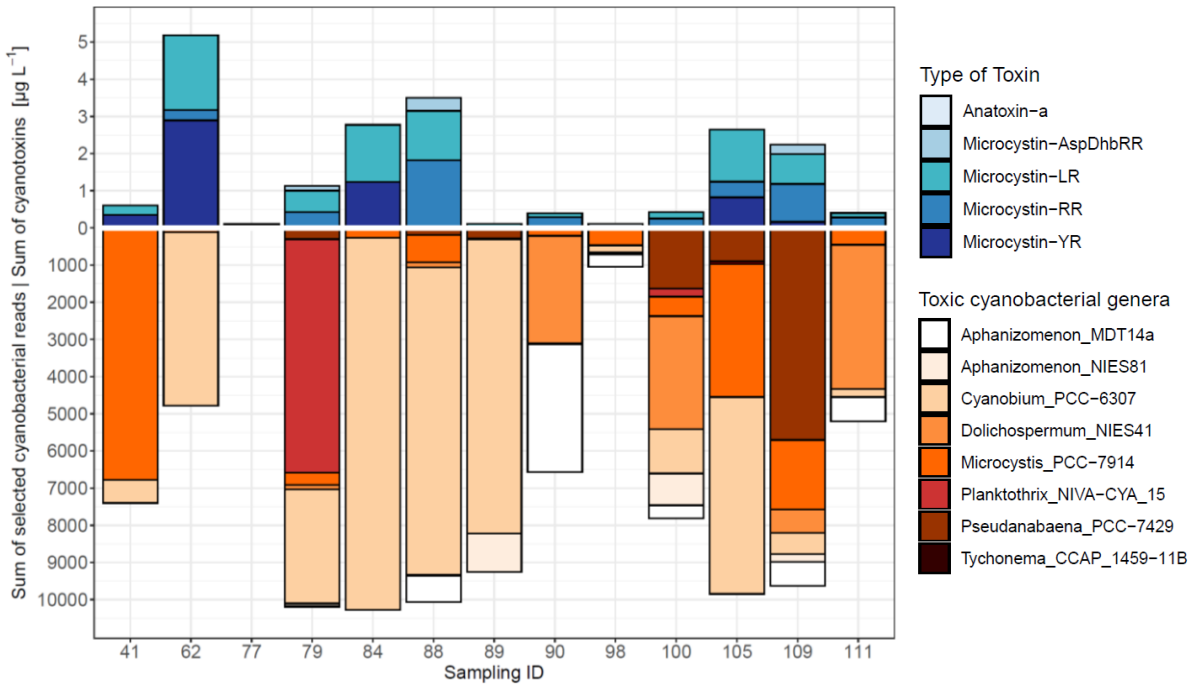

Fig. 40: Read numbers of cyanobacterial genera related to microcystins and anatoxin-a concentrations in µg L^{-1}. The microcystin and anatoxin-a concentrations (sum of free and cell-bounded) are indicated in the upper half of the graph (y-axis, positive scale), while the cyanobacterial reads observed for each genus are shown in the lower half of the graph (y-axis with negative scale). Except for *Cyanobium* (Christiansen et al., 2001) for all other cyanobacterial genera the respective genes of cyanotoxin synthesis have been described from isolated strains in the past (Rastogi et al., 2015). For PCR amplification the specific cyanobacteria primers and the subsequent DADA2 sequence analysis was used.

For sample ID 41, 0.25 and 0.35 µg L^{-1} of microcystin-LR and -RR were detected, and both primer pairs indicated the presence of *Microcystis* and *Cyanobium.* For sample ID 62 only *Cyanobium* was found when using the cyanobacterial primers. In contrast, bacterial primers indicated the co-occurrence of *Cyanobium* and *Microcystis* (Figure 39). For sample ID 77 only a trace of cyanotoxins, namely microcystin-RR (0.1 µg L^{-1}) was detected. Notably not a single read assigned to a cyanobacterial genus was detected using cyanobacterial specific primers. By using the bacterial primers, a small amount of *Cyanobium* could be detected. For sample ID 79 the dominant species was *Planktothrix,* followed by *Cyanobium* co-occurring with *Dolichospermum*, *Microcystis* and *Pseudanabaena*. For ID 84, 88 and 89 the dominant genus was *Cyanobium,* co-occurring with smaller read numbers of *Microcystis* in samples ID 84 and 88 and *Aphanizomenon* in samples ID 88 and 89. In the case of ID 90, only a small amount of microcystins was detected, but many reads were assigned to the genera *Dolichospermum* and *Aphanizomenon*. For ID 98 a low concentration of anatoxin-a

was recorded (0.11 µg L^{-1}), while in parallel *Microcystis*, *Aphanizomenon* and *Cyanobium* were found. For samples ID 100 and 109 a higher diversity of potentially toxic cyanobacterial genera co-occurring with *Pseudanabaena* was found. For the case of sample ID 100, a dominance of *Dolichospermum* with *Aphanizomenon*, *Cyanobium*, *Microcystis* and *Planktothrix* was observed. In addition, high read numbers of *Microcystis*, *Dolichospermum*, *Cyanobium* and *Aphanizomenon* were recorded for sample ID 109. Considering ID 105, the genera *Cyanobium*, *Microcystis* and *Pseudanabaena* were recorded. Finally, for sample ID 111 a high share of *Dolichospermum* and, additionally, *Microcystis* and *Cyanobium* were recorded by both primer systems.

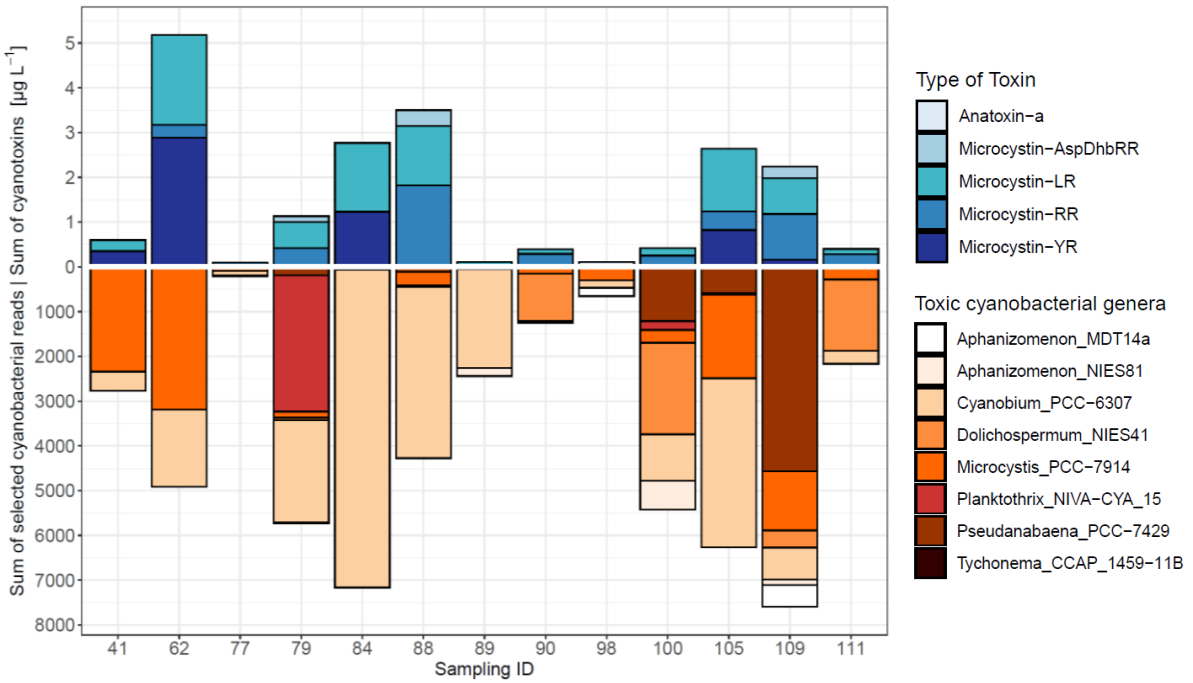

Fig. 41: Read numbers of cyanobacterial genera related to microcystins and anatoxin-a concentrations in µg L^{-1}. The microcystin and anatoxin-a concentrations (sum of free and cell-bounded) are indicated in the upper half of the graph (y-axis, positive scale), while the cyanobacterial reads observed for each genus are shown in the lower half of the graph (y-axis with negative scale). Except for *Cyanobium* (Christiansen et al., 2001) for all other cyanobacterial genera the respective genes of cyanotoxin synthesis have been described from isolated strains in the past (Rastogi et al., 2015). For PCR amplification the bacterial primers and the subsequent DADA2 sequence analysis was used.

In general, the results of both primer systems are consistent with each other, although individual samples show large differences (e.g. ID 62 and 90). Overall, not for all sites where cyanotoxins were measured, potential toxin-producing cyanobacteria could be

detected (e.g., ID 77, 84), though in most cases both methods, mass spectrometry and sequencing, agree well (e.g. ID 41, 62, 88, 105, 109).

3.7 Relationship of cyanobacteria (total) read numbers and physical parameters

To understand the influence of physical factors such as temperature, oxygen and pH on cyanobacterial read numbers, the following correlation matrix was constructed (Figure 42).

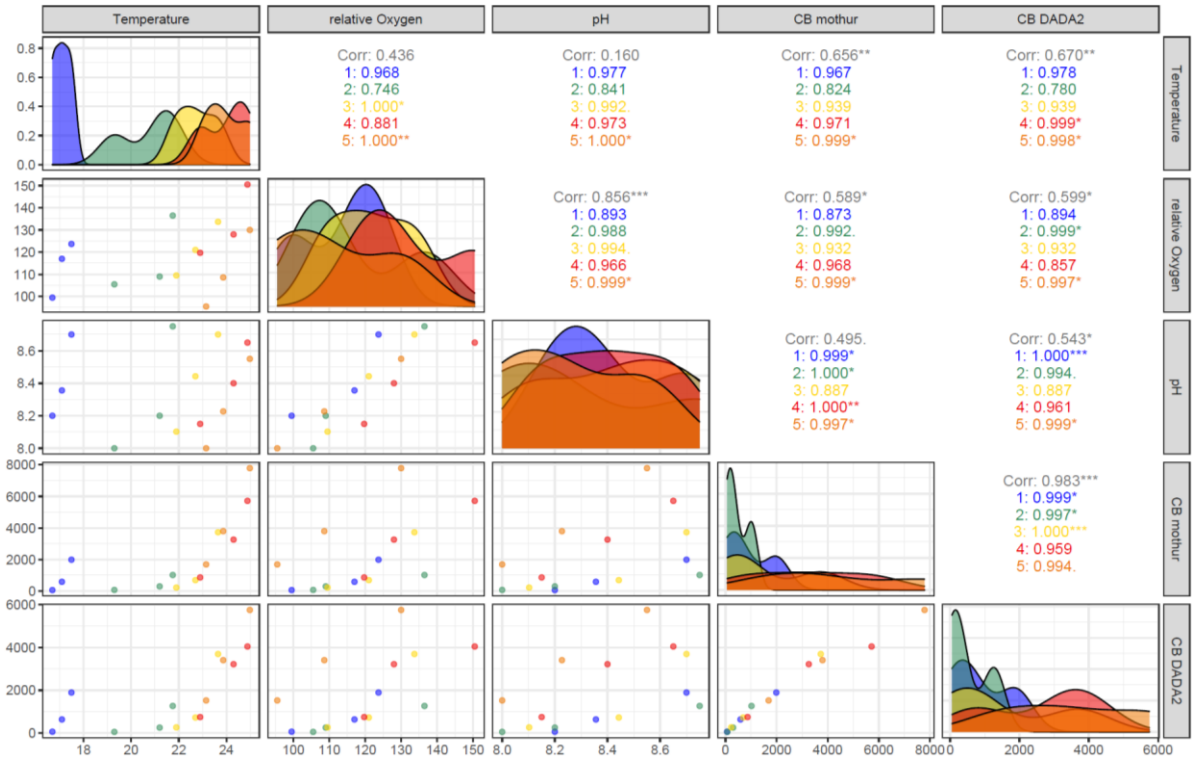

Fig. 42: Correlation matrix between abiotic factors (temperature, O_2 and pH) and HTS results (cyanobacterial reads analyzed by mothur and DADA2) recorded during the five sampling dates. As basis for the calculations for each variable the 25% quantile (q1), the median (=50% quantile, q2) and the 75% quantile (q3) were used. The distributions are indicated as density plots along the diagonal of the correlation matrix. The colours represent the sampling dates (1st = blue, 2nd = green, 3rd = yellow, 4th = red, 5th = orange). For each individual sampling date, the Pearson correlation coefficient was calculated. Significance levels: *** p < 0.001, ** p < 0.01, * p < 0.05, . p < 0.1

The density plots show the distribution of three statistical descriptors for each sampling date, namely the 25% quantile, the median, and the 75% quantile. The temperature profile shows distinct peaks for each sampling event with a gradual increase in temperature towards the 4th sampling date (see also Figure 20). On the contrary, oxygen and pH values were more homogenously distributed and overlapping among sampling dates. The HTS results for mothur and DADA2 showed specific peaks for the

first two sampling dates, due to a rather low number of cyanobacterial reads. From the 3rd sampling date onwards, higher (overlapping) read numbers were observed. Indeed, mothur and DADA2 read numbers showed high positive correlation (r = 0.983). This high correlation supports the observation from above (Fig. 38) that both sequence analysis pipelines result in highly comparable cyanobacterial read number estimates.

Furthermore, a highly significant correlation between oxygen and pH could be detected (r = 0.856). The positive linear relationship, which implies a higher pH value under higher oxygen concentrations.

Most importantly, a significant relationship between temperature and the cyanobacterial read numbers obtained by either mothur or DADA2 (r = 0.656 and 0.670), respectively was observed. When inspecting the scatterplot more closely, it could be seen that the linear regression model is not optimally chosen for this correlation, and rather an exponential model would fit.

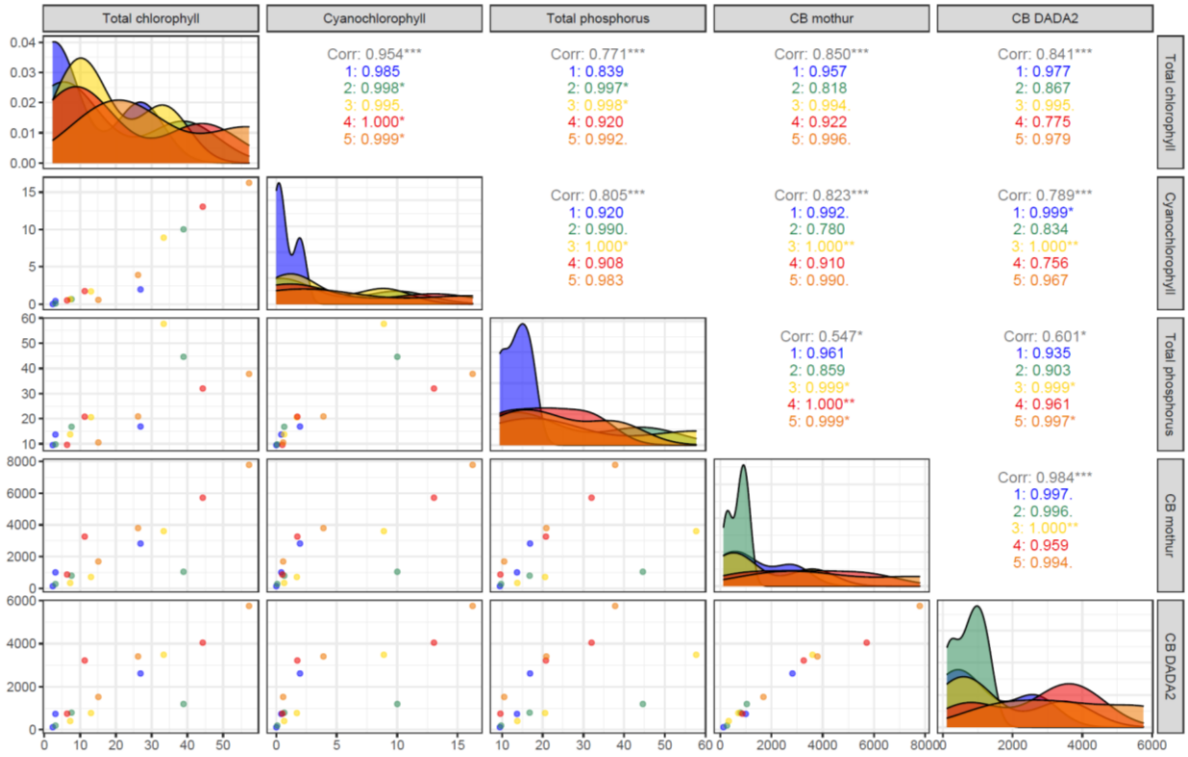

Fig. 43: Correlation matrix between fluorescence measurements, total phosphorus and HTS results (cyanobacterial reads analyzed by mothur and DADA2) recorded during the five sampling dates. As basis for the calculations for each variable the 25% quantile (q1), the median (=50% quantile, q2) and the 75% quantile (q3) were used. The distributions are indicated as density plots along the diagonal of the correlation matrix. The colours represent the sampling dates (1st = blue, 2nd = green, 3rd = yellow, 4th = red, 5th = orange). For each individual sampling date, the Pearson correlation coefficient was calculated. Significance levels: *** p < 0.001, ** p < 0.01, * p < 0.05, . p < 0.1.

Furthermore, the fluorescence measurements recorded *in situ* using the bbe AlgaeTorch were compared with cyanobacteria read numbers in Figure 43.

When inspecting the density plot for total chlorophyll (Figure 43), a general increasing trend during the study period was observed. Nevertheless, for each sampling date overlapping chlorophyll a concentrations were recorded. For cyanochlorophyll and total phosphorus a distinct peak of low cyanochlorophyll and total phosphorus was detected during the first sampling event. During sampling dates 2-5 the concentrations of cyanochlorophyll as well as TP were found highly overlapping. As can be inferred from the scatterplot shown in Figure 43, a highly significant correlation (r = 0.954) between total chlorophyll and cyanochlorophyll was observed. Total phosphorus showed significant correlation with total chlorophyll and cyanochlorophyll (r = 0.771 and 0.805, respectively), but relatively weak or no correlation with the sequencing results.

Moreover, cyanochlorophyll concentrations and the cyanobacterial read numbers analyzed by mothur showed a statistically significant correlation (r = 0.823). When inspecting the corresponding scatterplot in Figure 43 more in detail, it can be seen that fluorescence concentrations were underestimating the observed cyanobacteria read numbers. In order to test this relationship further, a scatterplot including the raw data from all samples was created (Figure 44). Indeed, a relationship between fluorescence and cyanobacterial read numbers was found. However, it is noteworthy that for a several samples low values of cyanochlorophyll were recorded which coincided with high numbers of cyanobacterial reads. In some extreme cases, such as for sample ID 76, 4189 cyanobacterial reads were identified while no cyanochlorophyll could be measured. The coefficient of determination (r^2 = 0.372) indicated a positive linear relationship, meaning that if higher cyanochlorophyll values are recorded by in-situ fluorescence measurement, more total cyanobacterial genera read sequences can be expected.

Summarizing up, temperature is the most important factor, for cyanobacterial read numbers, though by an exponential relationship. The two utilised analysis software, mothur and DADA2, correlated strongly, indicating that both pipelines are able to deliver plausible community compositions.

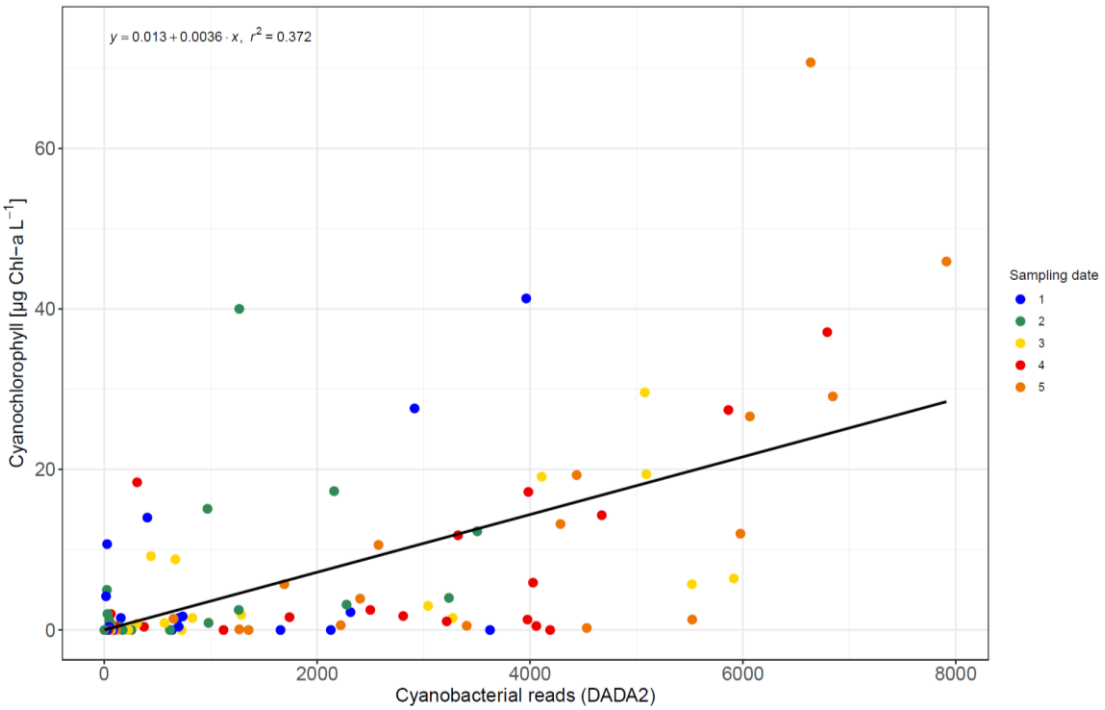

Fig. 44: Scatterplot showing the correlation of cyanobacterial read numbers obtained by HTS (bacterial Primers, mothur) and cyanochlorophyll determined by fluorescence *in situ* measurement (bbe AlgaeTorch). All data points were used for the correlation. The different colours indicate the five different sampling dates. The regression coefficient (r^2) does indicate a statistical significant correlation

3.8 Principal Component Analysis

In Figure 45, a Principal Component Analysis (PCA), based on the correlation matrix of the metadata and the cyanobacterial read numbers is shown. The first principal component (PC1) explained 46%, whereby PC2 explained 16% of the variation. In total, 62% of the variance could be explained. The first PC axis showed close correlation with cyanochlorophyll (-0.388) and secchi depth (0.386). On the other hand, the second PC axis was mainly related to the number of cyanobacterial reads through both analysis pipelines (mothur: 0.418; DADA2: 0.401), whereas on the negative scale, PC2 was related to total phosphorus (-0.301).

Although the individual circles, which correspond to the sampling dates, overlap strongly, a trend in associated variables can be identified. Samples from the 1st and 2nd sampling event were characterized by lower water temperatures, lower cyanochlorophyll concentrations, lower toxin concentrations and lower pH. The samples of the two first sampling events also tended to show higher secchi depth. The later the samples were collected during the study season (sampling date 3, 4 and 5),

the more likely they tended to be affected by higher water temperature and higher cyanochlorophyll concentration. Furthermore, the number of cyanobacterial reads, identified by mothur and DADA2, and also the toxin concentrations increased over the sampling season. Finally, the secchi depth measurements followed the same trend, indicating that samples from the later study period were characterized by lower secchi depths. Notably, samples characterized by high total phosphorus also showed high oxygen levels, but seemed not to be related to extraordinary cyanobacteria read numbers or toxin concentrations.

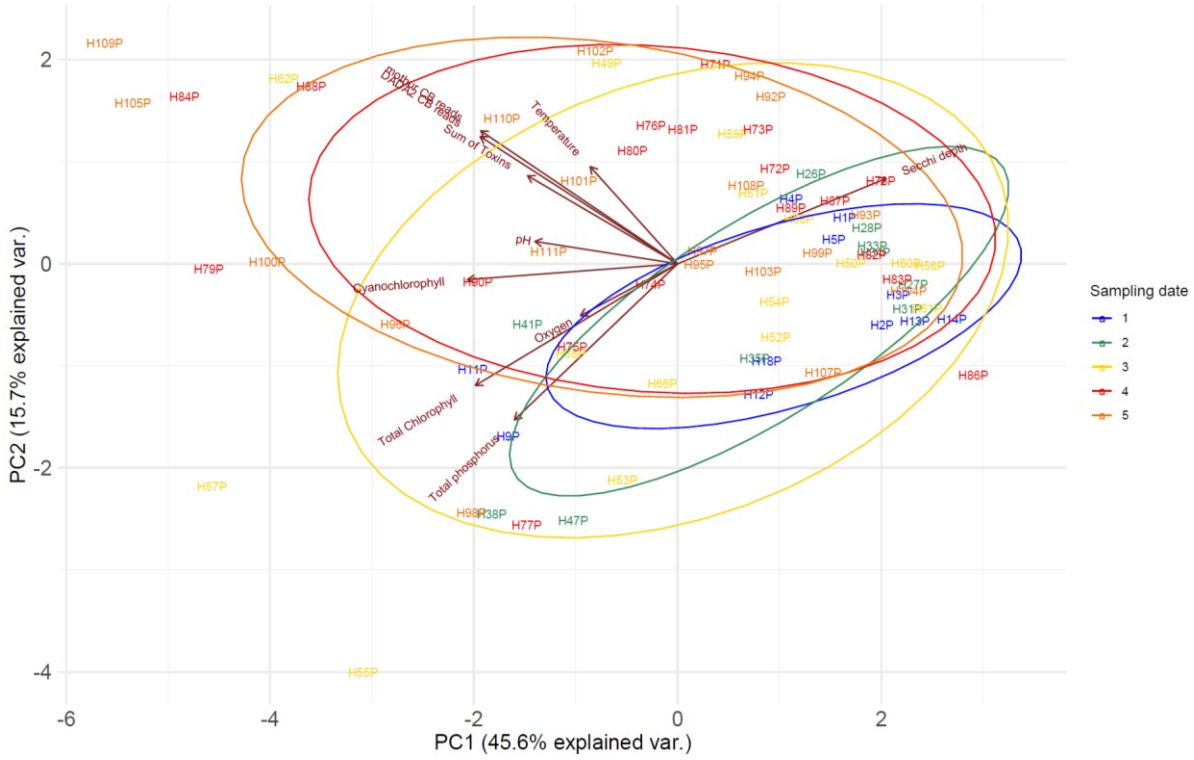

Fig. 45: Principal Component Analysis (PCA) of the metadata and HTS results. The measured variables are displayed as arrows, the individual samples are represented by their ID. The colours of the groups represent the sampling date. The data for the cyanobacterial read numbers were calculated from sequences using the bacterial more general primer pair.

3.9 Heatmap

The heatmap shown in Figure 46 can be used to compare the five sampling dates in respective to the recorded parameters. As indicated by the dendrogram, sampling date 1 and 2 were more closely related to each other. Both dates 1 and 2 were characterized by low toxin concentrations, low temperature and oxygen levels. Furthermore, the 1st and 2nd sampling date were characterized by lower concentrations of total chlorophyll, cyanochlorophyll as well as lower cyanobacterial read numbers.

According to the dendrogram, sampling dates 3 and 4 were also found most similar and were discriminated by higher toxin concentrations, especially in respect to microcystin-LR, -RR and -AspDhbRR. Moreover, the samples showed higher temperature and dissolved oxygen concentrations, while secchi depth was low. Fluorescence measurements indicated higher concentrations of total chlorophyll and cyanochlorophyll which was also supported by the HTS results and overall increasing from sampling date 1+2 to sampling date 3+4.

Finally, sampling date 5 was found more closely related to number 3 and 4 than to date 1 and 2. This last sampling date showed the highest cyanobacterial read numbers according to mothur and DADA2 as well as the highest fluorescence measurements. Nevertheless, total cyanotoxin concentrations were decreasing. Furthermore, temperature was decreasing as well and oxygen concentration was already relatively low. The lowest secchi depth readings were indicating high turbidity.

Furthermore, in Figure 46 the Pearson correlation coefficients between the total cyanotoxin concentrations and the recorded parameters were compared. Not surprisingly the total toxin concentration correlated most with variants microcystin-LR and microcystin-RR constituting the major share of total toxin concentration. On average, total microcystin was comprised of 42% microcystin-LR, 27.5% microcystin-YR, and 24.6% of microcystin-RR. Notably, for microcystin-YR the frequency of occurrence was irregular, i.e., more than half of microcystin-YR (2.89 µg L^{-1}, 53%) only was observed at site ID 62 during sampling date 3. Thus, the calculated Pearson correlation coefficient between total cyanotoxin concentration and microcystin-YR was found relatively low.

In general, temperature showed the highest correlation coefficient with total cyanotoxin concentration. This indicates a notable relationship with increase in water temperature. Moreover, both total cyanobacteria read number estimates showed a positive correlation with the total cyanotoxin concentration, suggesting that the more cyanobacterial reads were detected, the higher cyanotoxin concentrations were recorded.

Especially, the cyanochlorophyll concentration only showed a weak correlation in the case of fluorescence based measurements. Interestingly, secchi depth showed a

negative correlation, indicating that higher turbidity correlated positively with cyanotoxin concentration.

Overall, sampling dates 1 and 2 were characterized by low cyanobacterial read number, low toxin concentrations and high secchi depths. In contrast to that, sampling dates 3, 4 and 5, where the temperature was much higher, were defined by high cyanobacterial read numbers, high cyanotoxin concentrations, high oxygen concentration and low secchi depth.

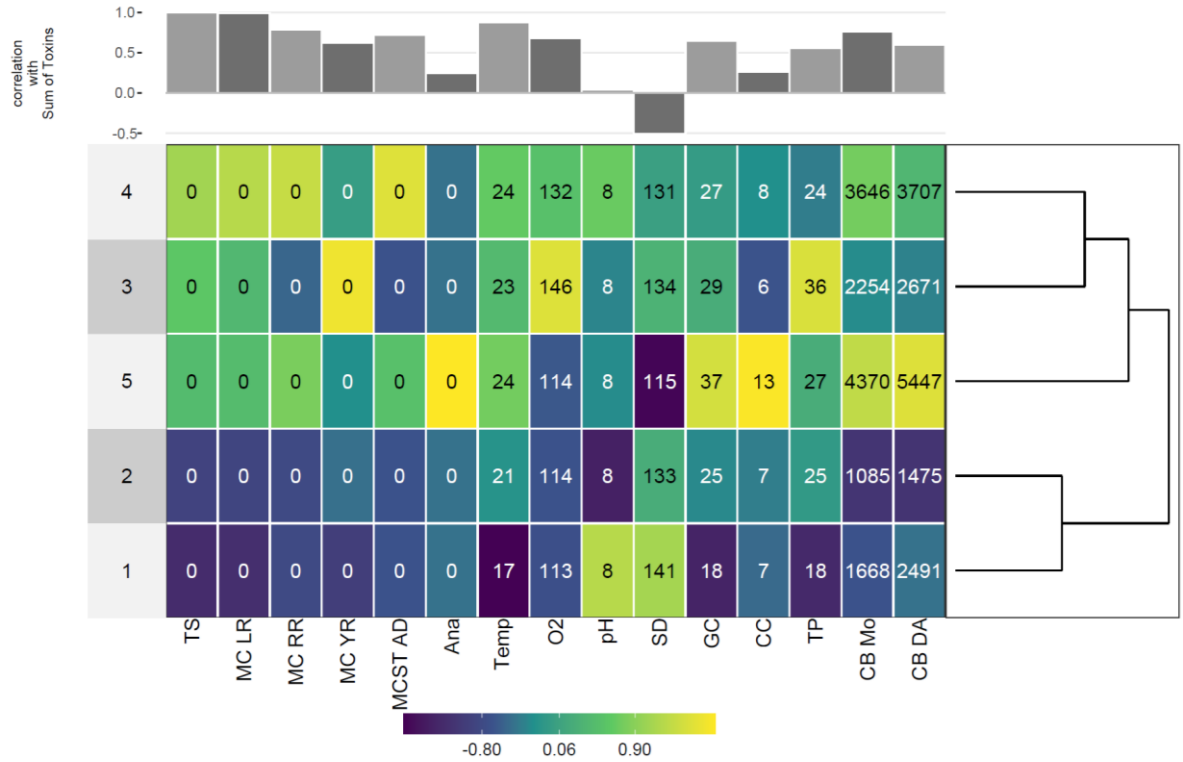

Fig. 46: Heat map of the various parameters characterizing the sampling dates. (A) On the horizontal axis the Pearson correlation (r) between the total cyanotoxin concentration and the various parameters is shown. +1 indicate a perfect positive linear relationship, -1 a perfect negative correlation. (B) On the vertical axis a dendrogram is shown, describing the relationship between the sampling dates. The colours of the grid represent the range from the minimum (dark-blue) to the maximum (yellow). The numbers in the box represent the mean values of the parameters per sampling dates. As only integers could be illustrated, only zeros are printed for toxin types. Abbreviations: TS = Sum of toxins [µg L^{-1}], MC LR = microcystin LR [µg L^{-1}], MC RR = microcystin RR [µg L^{-1}], MC YR = microcystin YR [µg L^{-1}], MCST AD = microcystin AspDhbRR [µg L^{-1}], Ana = anatoxin-a [µg L^{-1}], Temp = Temperature [°C], O2 = Oxygen [%], SD = Secchi depth [cm], GC = Total chlorophyll [µg Chl-a L^{-1}], CC = Cyanochlorophyll [µg Chl-a L^{-1}], TP = Total phosphorus [µg L^{-1}], CB Mo = Nr of cyanobacterial reads using mothur, CB Da = Nr of cyanobacterial reads using DADA2.

3.10 Benthos

Figure 47 show the cyanobacterial genera composition of the benthos samples. Only at two stations, where benthos sample were collected, cyanotoxins were detected. For sampling site H118B, no cyanobacterial reads were identified, though 0.11 µg L^{-1} microcystin-LR was detected. Contrarily, on sampling site H112B, where 0.13 µg L^{-1} Microcystin-RR was detected, 2454 reads assigned to *Tychonema* were found.

Interestingly, sampling site H30B, H69B and H120B, which derived from the same lake sediment, showed that over the complete season the cyanobacterial community is constantly dominated by *Phormidium* (1st sampling date: 1977 reads, 3rd sampling date: 1715 reads, 5th sampling date: 2943 reads).

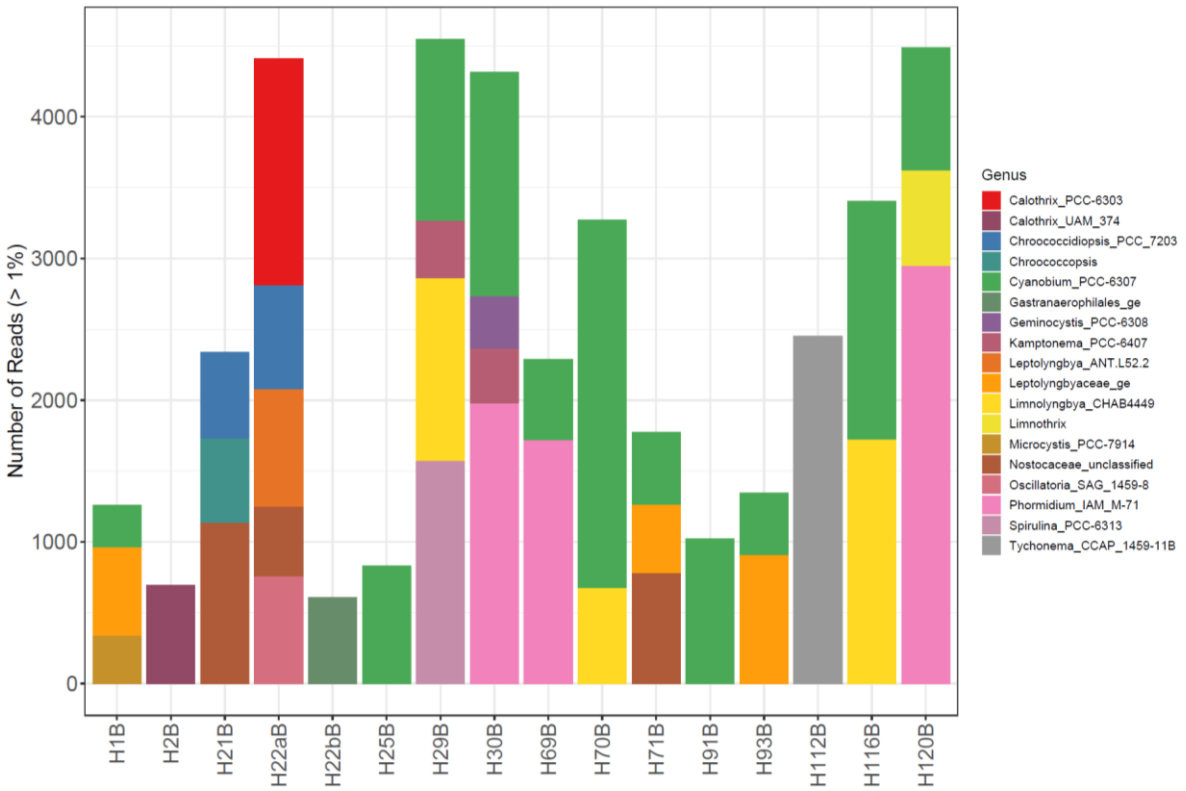

Fig. 47: Number of reads observed for each cyanobacterial genus from benthos samples. Rarefaction was performed at 29764 reads. Genera showing less than 300 reads (< 1%) were discarded. For sequence analysis mothur was used. For sample H22B, one sample (H22aB) was scratched off from a stone, while sample H22bB was collected from a surface-floating consortium of filamentous algae.

4 Discussion

4.1 The lumpers versus splitters debate - OTU versus ASV

The algorithms of mothur and DADA2 significantly differ in the way of filtering and clustering sequence reads. In the traditional approach used by mothur, the reads are clustered into Operational Taxonomic Units (OTUs) based on a fixed threshold of variation. This threshold, normally set at 3% dissimilarity, hence 97% similarity, was introduced by Stackebrandt & Goebel (1994).

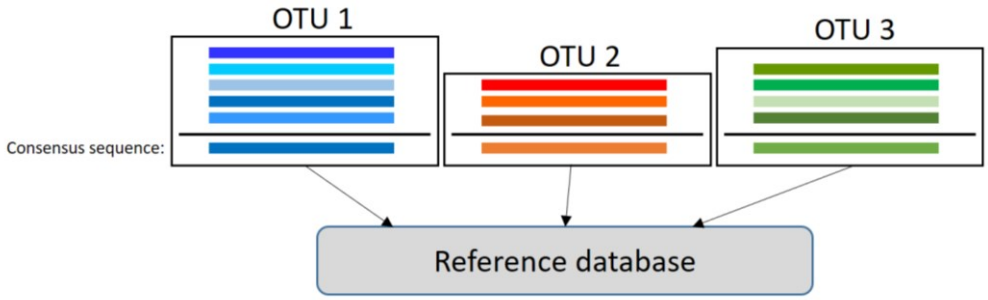

	Kingdom	Phylum	Class	Order	Family	Genus
OTU 1	Bacteria	Cyanobacteria	Cyanobacteriia	Cyanobacteriales	Microcystaceae	Microcystis_PCC-7914
OTU 2	Bacteria	Cyanobacteria	Cyanobacteriia	Cyanobacteriales	Nostocaceae	Aphanizomenon_NIES81
OTU 3	Bacteria	Cyanobacteria	Cyanobacteriia	Cyanobacteriales	Phormidiaceae	Planktothrix_NIVA-CYA_15

Fig. 48: Schematic overview of OTU clustering. A consensus, out of all 97% similar sequences, is constructed and compared to the reference database to reveal taxonomic information.

As alternative to OTUs, the approach of using Amplicon Sequence Variants (ASVs) is getting more and more attention and is implemented in DADA2 and illustrated in Figure 49. ASVs, sometimes also called exact sequence variants (ESV) or zero-radius OTUs (ZOTUs) (Edgar, 2018), are clusters of sequences with a 100% similarity threshold.

Advantages of using ASVs instead of OTUs are improvements in taxonomic resolution and consistency when it comes to comparison of datasets (Callahan et al., 2017). When following the OTU approach, a consensus sequence is representative for a group of similar sequences, which is aligned to a reference database to reveal taxonomic classification (Figure 48). In the case of ASVs, all sequences of one ASV are identical to each other, making it easier to match new sequences to already existing ASVs. Regarding the improvement of taxonomic resolution, ASVs can represent different microbiological strains assigned to one species, rather than grouped into one OTU if they still share more than 97% similarity (Fierer et al., 2017).

However, using ASVs can artificially increase diversity, as a high degree of sequence variation of the same species would end up in various different ASVs. Furthermore, considering the fact that PCR and the sequencing process itself produce errors, the major challenge is to delimit those from the real biological entities. In pipelines like DADA2, denoising steps should initially remove those errors to prevent construction of artificial ASVs.

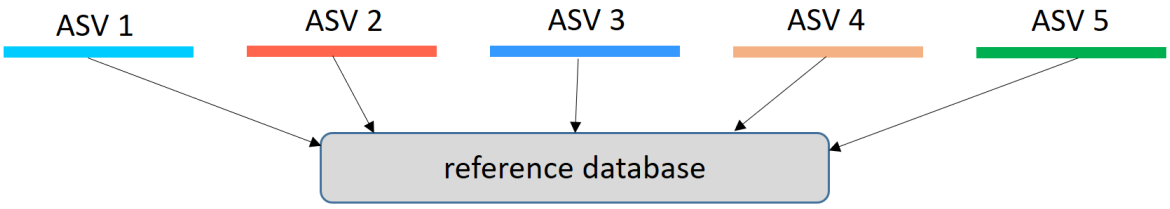

	Kingdom	Phylum	Class	Order	Family	Genus
ASV 1	Bacteria	Cyanobacteria	Cyanobacteriia	Cyanobacteriales	Microcystaceae	Microcystis_PCC-7914
ASV 2	Bacteria	Cyanobacteria	Cyanobacteriia	Cyanobacteriales	Nostocaceae	Aphanizomenon_MDT14a
ASV 3	Bacteria	Cyanobacteria	Cyanobacteriia	Cyanobacteriales	Microcystaceae	Microcystis_PCC-7914
ASV 4	Bacteria	Cyanobacteria	Cyanobacteriia	Cyanobacteriales	Nostocaceae	Aphanizomenon_NIES81
ASV 5	Bacteria	Cyanobacteria	Cyanobacteriia	Cyanobacteriales	Phormidiaceae	Planktothrix_NIVA-CYA_15

Fig. 49: Schematic overview of ASV processing. In contrast to individual OTU clustering based on similarity individual ASVs are maintained and taxonomically assigned.

Indicated by the results, the two approaches overall resulted in similar species composition and distribution. In detail, certain genotypes such as *Aphanizomenon* MDT14a were only identified by the ASV approach in DADA2. Nevertheless, a higher number of reads was not found for *Aphanizomenon* NIES81 in mothur`s OTU approach. The sequences of both reads possess a total length of 405 bases of which they differ in nine nucleotides. This accounts for a relative difference in sequence order between *Aphanizomenon* MDT14a and *Aphanizomenon* NIES81 of 2.2%, which is lower than the 3% dissimilarity threshold in mothur`s OTU clustering. Thus, the reads are grouped within one OTU from which the reference sequence is identified as *Aphanizomenon* NIES81.

Overall, DADA2 revealed higher number of cyanobacterial reads, since in almost all (except one) sampling locations cyanobacterial reads were obtained. Compared with mothur, only in 75 out of 100 samples cyanobacterial reads were recorded. This difference likely was caused by the mothur`s 97% similarity clustering approach. Moreover, these results indicate that estimated diversity was not artificially increased by sequencing errors. This conclusion is supported by experimental testing such as

performed by Callahan et al. (2017) and Edgar (2018). Both studies recommended that the ASVs should replace OTU clustering in metabarcoding. According to Edgar (2018), lumping and clustering is happening at every chosen threshold, but OTUs tend to be more affected by lumping species together as are ASVs by splitting.

4.2 The environmental context of cyanobacterial presence

4.2.1 Temperature

The most significant correlation of an abiotic factor with cyanobacterial dominance and cyanotoxin presence was found with temperature. The higher the water temperature, the more likely high numbers of cyanobacterial reads were recorded. This correlation has been reported frequently by others, like Paerl & Huisman (2008), which state that dominance of cyanobacteria in the phytoplankton community can be expected under conditions of higher temperatures (>25°C). Others like Harke et al. (2016) conclude on the basis of comprehensive literature review that *Microcystis* blooms already occur when temperature exceeds 15°C. Furthermore, physical stratification (the process were the water column is separated into layers of distinct temperatures due to the difference in density) is also advantageous for bloom-forming cyanobacteria (Davis et al., 2009). Furthermore, stratification can even prolong higher surface temperatures as vertical mixing is prevented, while otherwise cold, nutrient-rich water would be transferred to the surface (Dodds et al., 2009).

In this master thesis, an exponential increase of cyanobacterial reads and toxins was discovered between the 2nd and 3rd sampling date. Regarding to the corresponding temperature, an increase of an average temperature from 21.0°C to 22.6°C was observed. Furthermore, the warmest sampling locations even exceeded 25°C of water temperature. At all locations where toxins were detected, water temperature was higher than 22.8°C, indicating that more attention should be paid on risky bathing waters where temperatures exceed 22°C.

According to the summer balance by ZAMG (2020), the summer of 2020 was characterized by changeable weather and absence of long heat waves. Nevertheless, this summer has been classified as an on average warm summer, similarly occurring during the last decade. In low-land regions of Austria, the summer of 2020 was ranked the 14th warmest summer since 1767. However, it was the coldest since 2016 when compared to the last few years. Moreover, when averaged over the whole country,

25% more precipitation was recorded than in an average summer, which made it the rainiest summer since 2016.

In general, these interchanging environmental conditions are less optimal for the development of toxic algal blooms. In contrast, heat waves are often correlated with its development. Thus in general, the risk of CHABs occurrence is rising, as heat waves which are recently getting more and more typical also during Austrian summer, offer better conditions for their growth (Jöhnk et al., 2008; O'Neil et al., 2012). Cyanobacteria have several features in common, which allow them to dominate over other phytoplankton species under intense light conditions. First, they are able to perform vertical migration with the help of proteinaceous vacuoles, meaning specialized intracellular gas vesicles, which favour cell aggregation on the surface. This ability gives cyanobacteria a competitive advantage, as they can harvest the light at the surface efficiently, whereby causing shading for phototrophic species below (Porat, 2001).

Moreover, the fact that cyanobacteria are equipped with the accessory pigment, phycocyanin, allows them to perform positive net-photosynthesis even at a water depth were 1% of surface light defines the extent of the euphotic zone (Tilzer, 1987). This is crucial in respect of competitive ability and bathing waters monitoring routine. On the one hand, some specialized cyanobacteria can build up the major part of their total biomass at this depth, while on the other hand, such formation of metalimnetic layers is impossible to monitor using the framework of the EU-bathing water control system. In order to fulfil this gap, a massive increase of the sampling effort would be needed, which is currently not feasible for a two and three-weekly routine established so far.

4.2.2 Dissolved Oxygen

Oxygen in freshwater systems is mostly derived from exchange with the atmosphere, a physical process depending mostly on temperature, atmospheric pressure, mixing of the water column and other factors. The oxygen saturation concentration is higher the colder the water is and the higher the atmospheric pressure is (e.g., along a gradient in altitude). In the freshwater system itself, it is produced through photosynthesis and consumed by respiration and decomposition of organic substances.

In general, it can be stated that low oxygen concentrations in lakes are caused by high respiration rate of heterotrophic organisms and serve as an alarm signal for water quality conditions. However, high photosynthetic productivity, of macrophytes and/or phytoplankton, can lead to high oxygenation concentrations at the surface which is readily observed under hypereutrophic conditions (Schwoerbel & Brendelberger, 2013).

O_2 is mainly consumed by heterotrophic organisms through oxidation of carbon-sources, as O_2 is used as primary e-Donor (equation III). Whereby, CH_2O is the general stoichiometric representation of the formula for sugar. In equation IV the process of oxygenic photosynthesis is described, where solar energy is used for the fixation of CO_2, which results in production of sugar and O_2.

Equation III: $$CH_2O + O_2 \rightarrow CO_2 + H_2O + chemical\ Energy$$

Equation IV: $$6CO_2 + 6H_2O + \text{solar Energy} \rightarrow C_6H_{12}O_6 + 6O_2$$

In the case of excessive algal blooms, the high rate of decomposition of dying cells can lead to oxygen depletion in deeper zones (hypoxic zones) causing death of fish, invertebrates and macrophytes (Diaz & Solow, 1999). The results in this thesis are also showing the same trend. An increase in cyanobacterial read numbers was accompanied by an increase in dissolved oxygen concentrations.

To prevent oxygen depleted zones in endangered lakes, an aeration system for the water column is often installed. In Austrias such an aeration system was installed intermittently during the years 1995-1996 in the Old Danube (Vienna), suffering from cyanobacterial blooms, before the soluble reactive phosphorus precipitation measures were started (Dokulil, Hamm, & Kohl, 2001; Trimbee & Prepas, 1988).

4.2.3 pH

The pH varies in freshwater systems between 6.5 to 9.0. It is also increased by primary productivity, such as during algal bloom formation. Due to the general prevailing conditions of CO_2 limitation, HCO_3^- is often used as primary C-source which leads to an increase in OH^- ions, resulting in an increase of pH. According to the classical equation of calcium dissolution versus CO_2 concentration in water, the increase in pH must lead to biogenic decalcification (Wetzel, 2001). Cyanobacterial dominance frequently has been correlated with an alkaline environment, which might be related to

a more efficient use of HCO_3^- when compared with eukaryotic algae (Benayache et al., 2019).

According to this study, again a correlation between pH and cyanobacterial read numbers was observed. The higher the number of cyanobacterial reads, the higher the pH. Interestingly, the correlation matrix in Figure 42 indicates a rather high positive correlation between dissolved oxygen and pH (r = 0.856), suggesting that oxygen concentration and pH can indeed be linked to higher cyanobacterial read numbers and cyanotoxin occurrence.

4.2.4 Nutrients

Most importantly, in freshwater systems the reduction of phosphorus (P) has caused significant prevention of cyanobacterial blooms (Trimbee & Prepas, 1988; Watson et al., 1997), as nitrogen demand can be fulfilled by nitrogen-fixing cyanobacteria, like *Dolichospermum, Aphanizomenon, Cylindrospermopsis, Nodularia* and *Nostoc* (Schindler et al., 2008).

Though, cyanobacterial harmful blooms are also caused by non-N_2-fixing cyanobacteria like *Planktothrix* and *Microcystis*, which also depend on nitrate and ammonium concentrations in water (Kim et al., 2020). Furthermore, Vézie et al. (2002) reported that high levels of both, nitrogen and phosphorus, favour the growth of toxic *Microcystis* strains over non-toxic ones. Contrarily, Sevilla et al. (2010) states that the presence of nutrients are not a good predictor for harmful algal blooms, as no direct influence is linked to the production of toxins. Regarding to nitrogen, ammonium is the preferred N-source over nitrate and nitrite for cyanobacteria (Herrero et al., 2004).

In this thesis, no direct correlation between overall cyanobacterial read numbers and total phosphorus content could be observed. Nevertheless, a correlation between total phosphorus content and *Planktothrix* read numbers was observed, which agrees with the findings reported in Briand et al. (2008).

4.3 Who is responsible for cyanotoxin production?

In total, cyanotoxins were found in 13 out of 111 samples. In most cases *Microcystis* was identified as the most likely producer of cyanotoxins, like in sample IDs 41, 62, 84, 88, 98, 105 and 109. Furthermore, *Dolichospermum* was found as the most likely producer of cyanotoxins in ID 90, 100 and 111. In ID 79, the genus *Planktothrix* is

related to the production of the microcystin variants, whereby in ID 89 *Aphanizomenon* is considered as the potential producer.

Interestingly, as the sampling season progresses, the origin of the toxins is less often attributed to *Microcystis*. As can be also seen from Figure 31 and 32, read numbers of *Microcystis* decline over the season. According to Peng et al. (2018), *Microcystis* blooms may produce more microcystin in the beginning of the season. During the season, a succession of the toxigenic cyanobacteria can be observed, i.e., from a community dominated by *Microcystis* to a co-occurrence of the genera *Aphanizomenon*, *Microcystis* and *Dolichospermum*.

In Figure 50, a heat-tree is constructed, showing the number of ASVs counted for each cyanobacterial genus. It also indicates the genera, for which cyanotoxin production has been described previously. The most prominent and abundant genus *Microcystis* is a unicellular organism, which forms buoyant (surface floating) colonies (see Figure 3 and 8).

Interestingly, Chia et al. (2018) could reveal nutrient-dependent reciprocal growth stimulation between non-N_2-fixing *Microcystis* and N_2-fixing *Dolichospermum*. Under high nutrient conditions of both, nitrogen (N) and phosphorus (P), *Dolichospermum* is more sensitive to the allelopathic substances of *Microcystis* and growth is suppressed. When conditions change (especially under N-limitation), dominance of *Dolichospermum* over *Microcystis* will occur (Tromas et al., 2017). Moreover, Chia et al. (2018) could demonstrate that non-fixing *Microcystis* can suppress N_2-fixing *Dolichospermum* under nutrient rich conditions. To make things more complex, Li & Li (2012) could show that microcystin production is increased by *Microcystis* in response to presence of *Dolichospermum.* Chia et al. (2018) and Chen et al. (2016) could observe a downregulation of microcystin synthesis gene transcription by *Microcystis* when co-cultured with *Aphanizomenon flos-aquae*. In summary, interspecific co-occurrence and nutrient availability might affect cyanotoxin biosynthesis.

The data in this thesis show dominance of *Microcystis* under lower total phosphorus concentrations in the beginning of the season as well as low read numbers of *Dolichospermum*. However, the maximum concentration of total phosphorus was observed during the 3rd sampling date, followed by a steady decrease till the 5th

sampling event. Nevertheless, dominance of *Dolichospermum* was continuously increasing, whereby *Microcystis* read numbers rather declined.

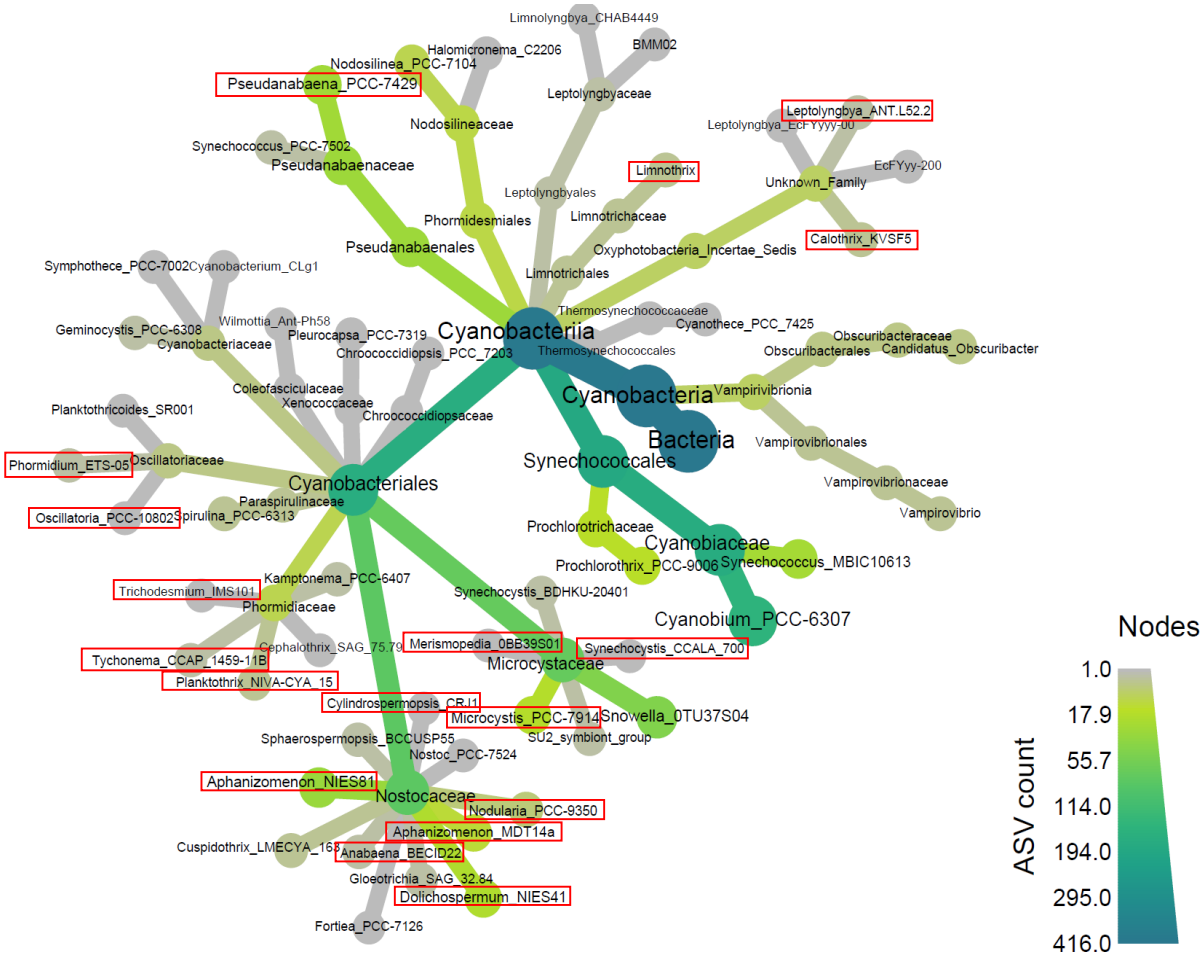

Fig. 50: A heat-tree showing the phylogenetic relationship of detected cyanobacteria. The colour represents the number of ASV found during the 5th sampling date by using bacterial primers and processing the sequence reads through the DADA2 pipeline. The red boxes indicate those genera, for which cyanotoxin production has been described.

Other prominent toxic-bloom forming genera, such as *Planktothrix* and *Aphanizomenon*, for example caused toxic algal blooms in Ammersee (Germany) and Mondsee (Austria) during the late 20th or early 21st century (Dokulil et al., 2001). According to Briand et al. (2008) toxic *Planktothrix* blooms are mainly driven by elevated nutrient concentrations, especially phosphorus. This coincides with the findings in this thesis, where the number of *Planktothrix* reads had its maximum during the 3rd sampling event, and afterwards consistently decreased.

Cylindrospermopsis, which caused the algal bloom in the late 20th century in the Old Danube (Vienna, Austria) (Dokulil, Donabaum, & Teubner, 2018), was not prominent at all. Moreover, the cyanotoxin cylindrospermopsin was not detected.

4.4 Fluorescence measurements for a quick local insight

Measurements of chlorophyll *a* have long been used to get a proxy for total algal biomass, as it is the major photosynthetic pigment of prokaryotic and eukaryotic algae (Bertone, Burford, & Hamilton, 2018). Moreover, the prevalence of phycobilins in cyanobacteria offers an opportunity to estimate total cyanobacterial biomass. Various studies could show that real biomass of both, algal and cyanobacteria, correlate well with the recorded in-vivo fluorescence. Thus, this tool is often recommended for real-time applications like bathing-water monitoring and water management (Brient et al., 2008).

However, one of the limitation of fluorescence measurements is the fact that algae in general change their fluorescence response depending on environmental conditions (Beutler et al., 2003). The classical investigations led to the understanding of chromatic adaptation (Tandeau De Marsac, 1977). In particular, the ratio between chlorophyll *a* and phycocyanin can be influenced by light regime, nutrient availability, physiological status (like stage of growth) and strain dominance (Beutler et al., 2002; Seppälä et al., 2007). It is generally understood that phycobilins are used in part for nitrogen storage and degraded under N-limiting conditions (Kromkamp, 1987).

While Chang et al. (2012) states that phycocyanin pigments dominate in the exponential growth phase, Ziegmann et al. (2010) showed that highest phycocyanin content is measured during later stages of growth. Furthermore, fluorescence measurements are influenced by the current light regime, as cells tend to produce less phycocyanin under high light conditions (Beutler et al., 2003).

The variable results in the course of this thesis indicate that even the daytime of measurements can have an effect on the results of the fluorescence measurement. Bertone, Burford, & Hamilton (2018) state that under conditions with low cyanobacterial biomass, values determined by fluorescence are often underestimated. These findings coincide with the results shown in this work. As demonstrated in Figure 44, cyanobacterial biomass was underestimated, when compared with read numbers,

especially in cases of low cyanobacterial occurrence. One bias of using the bbe moldaenke AlgaeTorch is the fact that the measurement is obtained in 10 cm depth. McBride & Rose (2018) highlight that surface cyanobacteria produce less phycocyanin, leading to underestimations of the fluorescence measurement. They suggest nighttime measurements which is, unfortunately, inapplicable for the purpose of the bathing-water monitoring.

Nevertheless, the in-situ fluorescence approach offers a quick insight into the phytoplankton community composition, which facilitates the decision to manage further activities concerning a certain bathing water site (McQuaid et al., 2011). The direct evidence is obtained from the correlation matrix (Figure 43), where a correlation between the AlgaeTorch measurements and the number of cyanobacterial reads could be observed.

4.5 Filter- and DNA extraction comparison

The experimental comparison using S-Pak® membrane filters versus Sterivex™ filter and DNeasy® PowerWater® Kit versus DNeasy® PowerWater® Sterivex™ Kit resulted in differences of results on cyanobacterial read numbers and genera composition.

In this study, using the standard DNA extraction procedure consisting of Sterivex™ filters and DNeasy® PowerWater® Sterivex™ Kit, a relatively high effort of personnel is required. For example, the water sample has to be filtered manually through the filter unit. However, a vacuum pump in combination with known filtered volume could be applied in the future. In contrast, the open S-Pak® membrane filters would offer a more comfortable way of being filtered by vacuum. The membrane filtration mode workflow would also fit better into currently established procedures for (open) sample filtrations in many laboratories.

The two tested DNA extraction procedures also showed differences in feasibility and time investment. Using the DNeasy® PowerWater® Kit, twelve samples were processed in parallel during 2 ½ hours. In contrast, using the DNeasy® PowerWater® Sterivex™ Kit, the same amount of twelve samples were processed during 4 hours. In general, a duration of 20 minutes of vortexing at maximum speed (as in the DNeasy® PowerWater® Sterivex™ Kit), compared to only five minutes of vortexing (as in the

DNeasy® PowerWater® Kit), might result in a higher yield of DNA through detaching cell from the filter membrane into the cell lysis buffer more efficiently. The results of this study might support this influence, though it has to be stated that a subsample of five was not enough to get statistically significant results.

4.6 Benthos

Traditionally, planktonic cyanobacteria species are associated with the production of cyanotoxins (Chorus & Bartram, 1999). Consequently, the role of benthic cyanobacterial species in toxin production is frequently not considered. Especially in lakes, where water flow is constantly low, benthic mats with a thickness of several millimetres can establish pretty well. In Figure 52 an example of such a massive benthic mat in a bathing water, consisting nearly exclusively out of *Phormidium*, is shown.

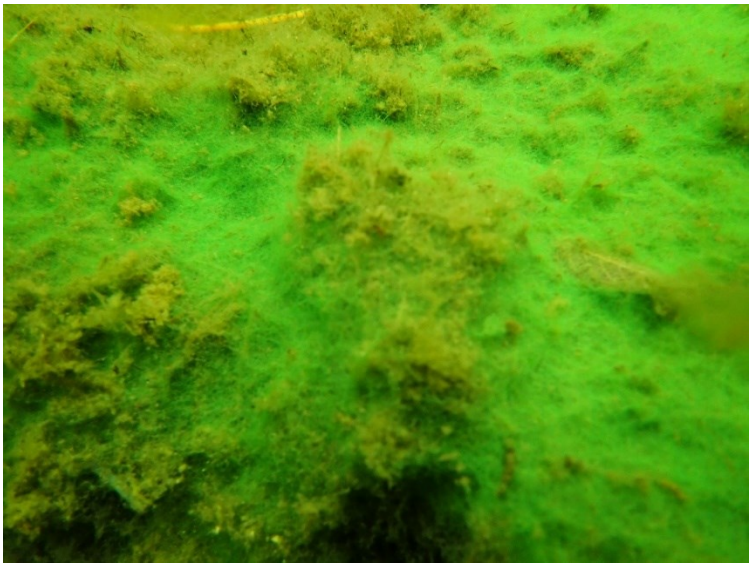

Fig. 52: Mat community formed by *Phormidium* on the sediment in the littoral.

According to Wood et al. (2007) benthic cyanobacterial mats mostly consist out of filamentous Oscillatoriales, whereby genera like *Oscillatoria* and *Phormidium* are the most prominent ones. Interestingly, its composition has been found relatively constant over the season when the community is once established. In contrast, planktonic genera show a succession over the season, for example a peak in *Dolichospermum* occurrence towards the end of the season, whereby *Microcystis* was found more prominent at the beginning (see Figure 34).

Referring to Figure 47, ID H30B, H69B and H120B belong to the same lake and benthic samples were obtained in June, July and September. Throughout the season, the only one genus found was *Phormidium*, later on benthic *Limnothrix* was also detected. Although, such massive algal mats with potentially-toxic species were observed, no cyanotoxins could be detected.

Examples of toxic-benthic cyanobacteria include *Tychonema*, *Trichodesmium*, *Leptolyngbya*, and *Calothrix* (see Figure 51) (Meriluoto et al., 2017; Rastogi et al., 2015). Thus, the toxigenic potential of benthic mats is considered underestimated and needs further research. Nevertheless, a trade-off between workload and the risk of overlooking cyanotoxins is required in the sense of routine bathing-waters monitoring, where personnel resources are generally limited. According to the results of this study, the majority of the observed cyanotoxins could be linked to planktonic genera, while benthic samples were rarely detected positive for cyanotoxins.

5 Conclusion

To monitor the presence of toxin producers, amplicon sequencing, as applied in this study, is considered as an appropriate method. Using general bacterial and specific cyanobacterial primers, it was possible to show that both resulted in similar distributions and proportions. Both analysis pipelines revealed similar results, though DADA2 and its implemented ASV approach revealed higher number of cyanobacterial reads and could also distinguish between different strains within one cyanobacterial species.

In total, in 13 out of 100 samples cyanotoxins were detected. It should be noted that summers with heatwaves such as during 2018 coupled to longer lasting stable good weather conditions are expected to favour bloom-forming cyanobacteria and cyanotoxin occurrence. The results indicate that the structural variants microcystin-LR and RR are in general the most frequently encountered cyanotoxins. In addition to the hepatotoxic microcystins, the neurotoxin anatoxin-a was detected. Cylindrospermopsin and nodularin were not identified during the entire study period. In early June, microcystin most likely was produced by *Microcystis*, while later during the summer additional potential microcystin producers increased in proportion, such as *Dolichospermum* and *Planktothrix*.

Overall, the results between amplicon sequencing and chemical-analytical results were consistent, both regarding quantitative estimates for cyanobacterial read numbers as well as for cyanotoxin occurrence and concentrations. Thus, the combination of both methods can offer a useful monitoring system to predict and define cyanobacterial harmful blooms in bathing waters.

Temperature was revealed as the most influential factor increasing cyanobacterial read numbers. Due to climate change, the role of temperature in favouring cyanobacteria mass development might therefore increase even further.

The advantage of in-situ fluorescence measurements is to receive information about phytoplankton community composition within seconds. Though the results of this study suggest that correlation with cyanobacterial read numbers is not high, a positive relationship could be observed. Thus, the fluorescence probe measurement is considered useful as a guiding proxy for cyanobacteria development in the field.

6 References

Adams, D. G., & Duggan, P. S. (2008). Cyanobacteria-bryophyte symbioses. *Journal of Experimental Botany*, *59*(5), 1047–1058. https://doi.org/10.1093/jxb/ern005

Alexova, R., Haynes, P. A., Ferrari, B. C., & Neilan, B. A. (2011). Comparative protein expression in different strains of the bloom-forming cyanobacterium Microcystis aeruginosa. *Molecular and Cellular Proteomics*, *10*(9), 1–16. https://doi.org/10.1074/mcp.M110.003749

Barter, R. L., & Yu, B. (2018). Superheat: An R Package for Creating Beautiful and Extendable Heatmaps for Visualizing Complex Data. *Journal of Computational and Graphical Statistics*, *27*(4), 910–922. https://doi.org/10.1080/10618600.2018.1473780

bbe Moldaenke *AlgaeTorch - Das handliche Messinstrument für den sofortigen Einsatz*. www.bbe-moldaenke.de

Benayache, N.-Y., Nguyen-Quang, T., Hushchyna, K., McLellan, K., Afri-Mehennaoui, F.-Z., & Bouaicha, N. (2019). An Overview of Cyanobacteria Harmful Algal Bloom (CyanoHAB) Issues in Freshwater Ecosystems. *IntechOpen*. https://doi.org/http://dx.doi.org/10.5772/57353

Berman-Frank, I., Lundgren, P., & Falkowski, P. (2003). Nitrogen fixation and photosynthetic oxygen evolution in cyanobacteria. *Research in Microbiology*, *154*, 157–164. https://doi.org/10.1016/S0923-2508(03)00029-9

Berry, J. P. (2008). Cyanobacterial Toxins as Allelochemicals with Potential Applications as Algaecides, Herbicides and Insecticides. *Marine Drugs*, *6*(2), 117–146. https://doi.org/10.3390/md20080007

Bertone, E., Burford, M. A., & Hamilton, D. P. (2018). Fluorescence probes for real-time remote cyanobacteria monitoring: A review of challenges and opportunities. *Water Research*, *141*, 152–162. https://doi.org/10.1016/j.watres.2018.05.001

Beutler, M., Wiltshire, K. H., Arp, M., Kruse, J., Reineke, C., Moldaenke, C., & Hansen, U. P. (2003). A reduced model of the fluorescence from the cyanobacterial photosynthetic apparatus designed for the in situ detection of cyanobacteria.

Biochimica et Biophysica Acta - Bioenergetics, *1604*, 33–46. https://doi.org/10.1016/S0005-2728(03)00022-7

Beutler, M., Wiltshire, K. H., Meyer, B., Moldaenke, C., Lüring, C., Meyerhöfer, M., Hansen, U. P., & Dau, H. (2002). A fluorometric method for the differentiation of algal populations in vivo and in situ. *Photosynthesis Research*, *72*(1), 39–53. https://doi.org/10.1023/A:1016026607048

BIO-RAD. (2020). *Miniaturized method (Most Probable Number) for the enumeration of enterococci in surface and waste waters*.

Bourke, A. T. C., Hawes, R. B., Neilson, A., & Stallman, N. D. (1983). An outbreak of Hepato-Enteritis (the palm island mystery disease) possibly caused by algal intoxication. *Toxicon*, *3*, 45–48.

Briand, E., Gugger, M., François, J. C., Bernard, C., Humbert, J. F., & Quiblier, C. (2008). Temporal variations in the dynamics of potentially microcystin-producing strains in a bloom-forming Planktothrix agardhii (Cyanobacterium) population. *Applied and Environmental Microbiology*, *74*(12), 3839–3848. https://doi.org/10.1128/AEM.02343-07

Briand, J. F., Jacquet, S., Flinois, C., Avois-Jacquet, C., Maisonnette, C., Leberre, B., & Humbert, J. F. (2005). Variations in the microcystin production of Planktothrix rubescens (Cyanobacteria) assessed from a four-year survey of Lac du Bourget (France) and from laboratory experiments. *Microbial Ecology*, *50*(3), 418–428. https://doi.org/10.1007/s00248-005-0186-z

Brient, L., Lengronne, M., Bertrand, E., Rolland, D., Sipel, A., Steinmann, D., Baudin, I., Legeas, M., Le Rouzic, B., & Bormans, M. (2008). A phycocyanin probe as a tool for monitoring cyanobacteria in freshwater bodies. *Journal of Environmental Monitoring*, *10*(2), 248–255. https://doi.org/10.1039/b714238b

Brown, T. A. (2018). *Genomes 4*. Garland Science.

Bukin, Y. S., Galachyants, Y. P., Morozov, I. V., Bukin, S. V., Zakharenko, A. S., & Zemskaya, T. I. (2019). The effect of 16s rRNA region choice on bacterial community metabarcoding results. *Scientific Data*, *6*, 1–14. https://doi.org/10.1038/sdata.2019.7

Callahan, B. J., McMurdie, P. J., & Holmes, S. P. (2017). Exact sequence variants should replace operational taxonomic units in marker-gene data analysis. *ISME Journal*, *11*(12), 2639–2643. https://doi.org/10.1038/ismej.2017.119

Callahan, B. J., McMurdie, P. J., Rosen, M. J., Han, A. W., Johnson, A. J. A., & Holmes, S. P. (2016). DADA2: High-resolution sample inference from Illumina amplicon data. *Nature Methods*, *13*(7), 581–583. https://doi.org/10.1038/nmeth.3869

Cameron, E. S., Schmidt, P. J., Tremblay, B. J. M., Emelko, M. B., & Müller, K. M. (2020). To rarefy or not to rarefy: Enhancing microbial community analysis through next-generation sequencing. *BioRxiv*. https://doi.org/10.1101/2020.09.09.290049

Carmichael, W. W., Azevedo, S. M. F. O., An, J. S., Molica, R. J. R., Jochimsen, E. M., Lau, S., Rinehart, K. L., Shaw, G. R., & Eaglesham, G. K. (2001). Human fatalities form cyanobacteria: Chemical and biological evidence for cyanotoxins. *Environmental Health Perspectives*, *109*(7), 663–668. https://doi.org/10.1289/ehp.01109663

Carmichael, W. W., Beasly, V., Brunner, D., Eloff, J., Falconer, I., & Gorham, P. (1988). Naming of Cyclic Heptapeptide Toxins of Cyanobacteria (Blue-Green Algae). *Toxicon*, *26*(11), 971–973.

Carmichael, W. W., Biggs, D. F., & Gorham, P. R. (1975). Toxicology and pharmacological action of anabaena flos-aquae toxin. *Science*, *187*(4176), 542–544. https://doi.org/10.1126/science.803708

Catherine, Q., Susanna, W., Isidora, E. S., Mark, H., Aurélie, V., & Jean-François, H. (2013). A review of current knowledge on toxic benthic freshwater cyanobacteria - Ecology, toxin production and risk management. *Water Research*, *47*(15), 5464–5479. https://doi.org/10.1016/j.watres.2013.06.042

Chaitankar, V., Karakülah, G., Ratnapriya, R., Giuste, F., Brooks, M. J., & Swaroop, A. (2016). Next Generation Sequencing Technology and Genomewide Data Analysis: Perspectives for Retinal Research. *Prog Retin Eye Res.*, *55*, 1–31. https://doi.org/10.1016/j.preteyeres.2016.06.001.Next

Chang, D. W., Hobson, P., Burch, M., & Lin, T. F. (2012). Measurement of cyanobacteria using in-vivo fluoroscopy - Effect of cyanobacterial species,

pigments, and colonies. *Water Research*, *46*(16), 5037–5048. https://doi.org/10.1016/j.watres.2012.06.050

Chen, R., Li, F., Liu, J., Zheng, H., Shen, F., Xue, Y., & Liu, C. (2016). The combined effects of Dolichospermum flos-aquae , light, and temperature on microcystin production by Microcystis aeruginosa. *Chinese Journal of Oceanology and Limnology*, *34*(6), 1173–1182.

Chia, M. A., Jankowiak, J. G., Kramer, B. J., Goleski, J. A., Huang, I. S., Zimba, P. V., do Carmo Bittencourt-Oliveira, M., & Gobler, C. J. (2018). Succession and toxicity of Microcystis and Anabaena (Dolichospermum) blooms are controlled by nutrient-dependent allelopathic interactions. *Harmful Algae*, *74*, 67–77. https://doi.org/10.1016/j.hal.2018.03.002

Chorus, I., & Bartram, J. (1999). Toxic Cyanobacteria in Water: A guide to their public health consequences, monitoring and management. In *WHO*. F & FN Spon. https://doi.org/10.1046/j.1365-2427.2003.01107.x

Chorus, I., Falconer, I. R., Salas, H. J., & Bartram, J. (2000). Health risks caused by freshwater cyanobacteria in recreational waters. *Journal of Toxicology and Environmental Health - Part B: Critical Reviews*, *3*(4), 323–347. https://doi.org/10.1080/109374000436364

Chorus, I., & Welker, M. (2021). *Toxic Cyanobacteria in Water. A Guide to Their Public Health Consequences, Monitoring and Management* (Second Edi). Taylor & Francis.

Christiansen, G., Dittmann, E., Via Ordorika, L., Rippka, R., Herdman, M., & Börner, T. (2001). Nonribosomal peptide synthetase genes occur in most cyanobacterial genera as evidenced by their distribution in axenic strains of the PCC. *Archives of Microbiology*, *176*(6), 452–458. https://doi.org/10.1007/s002030100349

Codd, G. A., Morrison, L. F., & Metcalf, J. S. (2005). Cyanobacterial toxins: Risk management for health protection. *Toxicology and Applied Pharmacology*, *203*, 264–272. https://doi.org/10.1016/j.taap.2004.02.016

Cusick, K. D., & Sayler, G. S. (2013). An overview on the marine neurotoxin, saxitoxin: Genetics, moleculartargets, methods of detection and ecological functions. *Marine*

Drugs, *11*(4), 991–1018. https://doi.org/10.3390/md11040991

Davis, T. W., Berry, D. L., Boyer, G. L., & Gobler, C. J. (2009). The effects of temperature and nutrients on the growth and dynamics of toxic and non-toxic strains of Microcystis during cyanobacteria blooms. *Harmful Algae*, *8*(5), 715–725. https://doi.org/10.1016/j.hal.2009.02.004

Devlin, J. ., Edwards, O. E., Gorham, P. R., Hunter, N. R., Pike, R. K., & Stavric, B. (1977). Anatoxin-a, a toxic alkaloid from. *Canadian Journal of Chemistry*, *55*, 1367–1371.

Diaz, R. J., & Solow, A. (1999). Ecological and Economic Consequences of Hypoxia in the Gulf of Mexico. *NOAA Coastal Ocean Program Decision Analysis Series No. 16*.

Dittmann, E., Fewer, D. P., & Neilan, B. A. (2013). Cyanobacterial toxins: Biosynthetic routes and evolutionary roots. *FEMS Microbiology Reviews*, *37*(1), 23–43. https://doi.org/10.1111/j.1574-6976.2012.12000.x

Dodds, W. K., Bouska, W. W., Eitzmann, J. L., Pilger, T. J., Pitts, K. L., Riley, A. J., Schloesser, J. T., & Thornbrugh, D. J. (2009). Eutrophication of U. S. freshwaters: Analysis of potential economic damages. *Environmental Science and Technology*, *43*(1), 12–19. https://doi.org/10.1021/es801217q

Dodds, W. K., & Whiles, M. R. (2010). *Freshwater Ecology. Concepts & Environmental applications of limnology* (Second Edi). Elsevier Inc.

Dokulil, M., Hamm, A., & Kohl, J.-G. (2001). *Ökologie und Schutz von Seen* (1. Auflage). Facultas.

Dokulil, M. T., & Teubner, K. (2000). Cyanobacterial dominance in lakes. *Hydrobiologia*, *438*, 1–12. https://doi.org/10.1023/A:1004155810302

Dokulil, Martin T., Donabaum, K., & Teubner, K. (2018). *The Alte Donau: Successful Restoration and Sustainable Management. An Ecosystem Case Study of a Shallow Urban Lake.* Sp.

Edgar, R. C. (2018). Updating the 97% identity threshold for 16S ribosomal RNA OTUs. *Bioinformatics*, *34*(14), 2371–2375. https://doi.org/10.1093/bioinformatics/bty113

Ehrenberg, C. G. (1830). Neue Beobachtungen über blutartige Erscheinungen in Ägypten, Arabien und Sibirien, nebst einer Übersicht und Kritik der früher bekannten. *Ann. Phys. Chem.*, *18*, 477–514.

Elliott, J. A. (2012). Is the future blue-green? A review of the current model predictions of how climate change could affect pelagic freshwater cyanobacteria. *Water Research*, *46*(5), 1364–1371. https://doi.org/10.1016/j.watres.2011.12.018

Fierer, N., Brewer, T., & Choudoir, M. (2017). *Lumping versus splitting - is it time for microbial ecologists to abandon OTUs ?* http://fiererlab.org/2017/05/02/lumping-versus-splitting-is-it-time-for-microbial-ecologists-to-abandon-otus/

Foster, Z. S. L., Sharpton, T. J., & Grünwald, N. J. (2017). Metacoder: An R package for visualization and manipulation of community taxonomic diversity data. *PLoS Computational Biology*, *13*(2), 1–15. https://doi.org/10.1371/journal.pcbi.1005404

Francis, G. (1878). Poisonous Australian lake. *Nature*, *18*, 11–12. https://doi.org/10.1038/018011d0

Frias-Lopez, J., Bonheyo, G. T., Jin, Q., & Fouke, B. W. (2003). Cyanobacteria associated with coral black band disease in Caribbean and Indo-Pacific reefs. *Applied and Environmental Microbiology*, *69*(4), 2409–2413. https://doi.org/10.1128/AEM.69.4.2409-2413.2003

Gray, M. W., Sankoff, D., & Cedergren, R. J. (1984). On the evolutionary descent of organisms and organelles: a global phylogeny based on a highly conserved structural core in small subunit ribosomal RNA. *Nucleic Acids Research*, *12*(14), 5837–5852.

Grigoryeva, N. (2019). Self-Fluorescence of Photosynthetic System: A Powerful Tool for Investigation of Microalgal Biological Diversity, Microalgae - From Physiology to Application. *IntechOpen*, 1–23. https://doi.org/10.5772/intechopen.88785

Harke, M. J., Steffen, M. M., Gobler, C. J., Otten, T. G., Wilhelm, S. W., Wood, S. A., & Paerl, H. W. (2016). A review of the global ecology, genomics, and biogeography of the toxic cyanobacterium, Microcystis spp. *Harmful Algae*, *54*, 4–20. https://doi.org/10.1016/j.hal.2015.12.007

Herlemann, D. P. R., Labrenz, M., Jürgens, K., Bertilsson, S., Waniek, J. J., &

Andersson, A. F. (2011). Transitions in bacterial communities along the 2000 km salinity gradient of the Baltic Sea. *ISME Journal*, *5*(10), 1571–1579. https://doi.org/10.1038/ismej.2011.41

Herrero, A., Muro-Pastor, A. M., & Flores, E. (2001). Nitrogen Control in Cyanobacteria. *Journal of Bacteriology*, *183*(2), 411–425. https://doi.org/10.1128/JB.183.2.411-425.2001

Herrero, Antonia, Muro-Pastor, A. M., Valladares, A., & Flores, E. (2004). Cellular differentiation and the NtcA transcription factor in filamentous cyanobacteria. *FEMS Microbiology Reviews*, *28*(4), 469–487. https://doi.org/10.1016/j.femsre.2004.04.003

Holland, A., & Kinnear, S. (2013). Interpreting the Possible Ecological Role(s) of Cyanotoxins: Compounds for Competitive Advantage and/or Physiological Aide? *Marine Drugs*, *11*(7), 2239–2258. https://doi.org/10.3390/md11072239

Hsieh, T. C., Ma, K. H., & Chao, A. (2016). iNEXT: an R package for rarefaction and extrapolation of species diversity (Hill numbers). *Methods in Ecology and Evolution*, *7*(12), 1451–1456. https://doi.org/10.1111/2041-210X.12613

Huber, C. S. (1972). The Crystal Structure and Absolute Configuration of 2,9-Diacetyl-9-azabicyclo[4,2,1]non-2,3-ene*. *Acta Cryst.*, *B28*(2577).

Hudnell, H. K. (2008). Cyanobacterial harmful algal blooms: State of the Science and Research Needs. In *Journal of Chemical Information and Modeling* (Vol. 53, Issue 9). Springer. https://doi.org/10.1017/CBO9781107415324.004

Hugerth, L. W., & Andersson, A. F. (2017). Analysing microbial community composition through amplicon sequencing: From sampling to hypothesis testing. *Frontiers in Microbiology*, *8*(SEP), 1–22. https://doi.org/10.3389/fmicb.2017.01561

Huisman, J., Codd, G. A., Paerl, H. W., Ibelings, B. W., Verspagen, J. M. H., & Visser, P. M. (2018). Cyanobacterial blooms. *Nature Reviews Microbiology*, *16*(8), 471–483. https://doi.org/10.1038/s41579-018-0040-1

Huisman, J., Matthijs, C. P., & Visser, P. M. (2005). Harmful Cyanobacteria. In *Aquatic ecology series* (Vol. 3). Springer. https://doi.org/10.1117/12.723170

Ikawa, M., Wegener, K., Foxall, T. L., & Sasner, J. J. (1982). Comparison of the toxins of the blue-green alga Aphanizomenon flos-aquae with the Gonyaulax toxins. *Toxicon*, *20*(4), 747–752. https://doi.org/10.1016/0041-0101(82)90122-2

Isichei, A. O. (1990). The role of algae and cyanobacteria in arid lands. A review. *Arid Soil Research and Rehabilitation*, *4*, 1–17. https://doi.org/10.1080/15324989009381227

Jackson, C., Clayden, S., & Reyes-Prieto, A. (2015). The Glaucophyta: The blue-green plants in a nutshell. *Acta Societatis Botanicorum Poloniae*, *84*(2), 149–165. https://doi.org/10.5586/asbp.2015.020

Jakubowska, N., & Szeląg-Wasielewska, E. (2015). Toxic picoplanktonic cyanobacteria - Review. *Marine Drugs*, *13*(3), 1497–1518. https://doi.org/10.3390/md13031497

Jang, M. H., Ha, K., Jung, J. M., Lee, Y. J., & Takamura, N. (2006). Increased microcystin production of Microcystis aeruginosa by indirect exposure of nontoxic cyanobacteria: Potential role in the development of Microcystis bloom. *Bulletin of Environmental Contamination and Toxicology*, *76*(6), 957–962. https://doi.org/10.1007/s00128-006-1011-1

John, N., Baker, L., Ansell, B. R. E., Newham, S., Crosbie, N. D., & Jex, A. R. (2019). First report of anatoxin-a producing cyanobacteria in Australia illustrates need to regularly up-date monitoring strategies in a shifting global distribution. *Scientific Reports*, *9*(1), 1–9. https://doi.org/10.1038/s41598-019-46945-8

Jöhnk, K. D., Huisman, J., Sharples, J., Sommeijer, B., Visser, P. M., & Stroom, J. M. (2008). Summer heatwaves promote blooms of harmful cyanobacteria. *Global Change Biology*, *14*(3), 495–512. https://doi.org/10.1111/j.1365-2486.2007.01510.x

Kaloudis, T., Triantis, T. M., & Hiskia, A. (2017). Taste and Odour Compounds Produced by Cyanobacteria. In *Handbook of Cyanobacterial Monitoring and Cyanotoxin Analysis* (pp. 196–201). https://doi.org/10.1002/9781119068761.ch20

Kim, K., Mun, H., Shin, H., Park, S., Yu, C., Lee, J., Yoon, Y., Chung, H., Yun, H., Lee, K., Jeong, G., Oh, J. A., Lee, I., Lee, H., Kang, T., Ryu, H. S., Park, J., Shin, Y., &

Rhew, D. (2020). Nitrogen Stimulates Microcystis-Dominated Blooms More than Phosphorus in River Conditions That Favor Non-Nitrogen-Fixing Genera. *Environmental Science and Technology*, *54*(12), 7185–7193. https://doi.org/10.1021/acs.est.9b07528

Kozich, J. J., Westcott, S. L., Baxter, N. T., Highlander, S. K., & Schloss, P. D. (2013). Development of a dual-index sequencing strategy and curation pipeline for analyzing amplicon sequence data on the miseq illumina sequencing platform. *Applied and Environmental Microbiology*, *79*(17), 5112–5120. https://doi.org/10.1128/AEM.01043-13

Kromkamp, J. (1987). Formation and functional significance of storage products in cyanobacteria. *New Zealand Journal of Marine and Freshwater Research*, *21*(3), 457–465. https://doi.org/10.1080/00288330.1987.9516241

Kurmayer, R., Sivonen, K., Wilmotte, A., & Salmaso, N. (2017). *Molecular Tools for the Detection and Quantification of Toxigenic Cyanobacteria*.

Lampert, W., & Sommer, U. (1997). *Limnoecology: The Ecology of Lakes and Streams*. Oxford University Press. https://doi.org/10.1093/plankt/fbn013

Lee, E. R. (2008). *Phycology*. Cambridge University Press.

Legrand, C., Rengefors, K., Fistarol, G. O., & Granéli, E. (2003). Allelopathy in phytoplankton - Biochemical, ecological and evolutionary aspects. *Phycologia*, *42*(4), 406–419. https://doi.org/10.2216/i0031-8884-42-4-406.1

Li, Y., & Li, D. (2012). Competition between toxic Microcystis aeruginosa and nontoxic Microcystis wesenbergii with Anabaena PCC7120. *Journal of Applied Phycology*, *24*, 69–78. https://doi.org/10.1007/s10811-010-9648-x

Lüttge, U. (1997). Cyanobacterial Tintenstrich communities and their ecology. *Naturwissenschaften*, *84*, 526–534. https://doi.org/10.1007/s001140050439

Mantzouki, E., Lürling, M., Fastner, J., de Senerpont Domis, L., Wilk-Woźniak, E., Koreivienė, J., Seelen, L., Teurlincx, S., Verstijnen, Y., Krztoń, W., Walusiak, E., Karosienė, J., Kasperoviienė, J., Savadova, K., Vitonytė, I., Cillero-Castro, C., Budzynska, A., Goldyn, R., Kozak, A., … Ibelings, B. W. (2018). Temperature effects explain continental scale distribution of cyanobacterial toxins. *Toxins*,

10(4), 1–24. https://doi.org/10.3390/toxins10040156

McBride, C. G., & Rose, K. C. (2018). Automated High-frequency Monitoring and Research. In *Lake Restoration Handbook* (pp. 419–461). Springer, Cham. https://doi.org/https://doi.org/10.1007/978-3-319-93043-5_13

McMurdie, P. J., & Holmes, S. (2013). Phyloseq: An R Package for Reproducible Interactive Analysis and Graphics of Microbiome Census Data. *PLoS ONE*, *8*(4). https://doi.org/10.1371/journal.pone.0061217

McQuaid, N., Zamyadi, A., Prévost, M., Bird, D. F., & Dorner, S. (2011). Use of in vivo phycocyanin fluorescence to monitor potential microcystin-producing cyanobacterial biovolume in a drinking water source. *Journal of Environmental Monitoring*, *13*, 455–463. https://doi.org/10.1039/c0em00163e

Mereschkowsky, C. (1905). Über Natur und Ursprung der Chromatophoren im Pflanzenreiche. *Biologischen Zentralblatt*, *25*, 593–604. https://doi.org/10.1080/09670269910001736342

Meriluoto, J., Spoof, L., & Codd, G. A. (2017). Handbook of Cyanobacterial Monitoring and Cyanotoxin Analysis. In *Advances in Oceanography and Limnology* (Vol. 8, Issue 2). John Wiley & Sons, Ltd. https://doi.org/10.4081/aiol.2017.7221

Molot, L. A., Watson, S. B., Creed, I. F., Trick, C. G., Mccabe, S. K., Verschoor, M. J., Sorichetti, R. J., Powe, C., Venkiteswaran, J. J., & Schiff, S. L. (2014). A novel model for cyanobacteria bloom formation: The critical role of anoxia and ferrous iron. *Freshwater Biology*, *59*, 1323–1340. https://doi.org/10.1111/fwb.12334

Moreira, C., Ramos, V., Azevedo, J., & Vasconcelos, V. (2014). Methods to detect cyanobacteria and their toxins in the environment. *Applied Microbiology and Biotechnology*, *98*(19), 8073–8082. https://doi.org/10.1007/s00253-014-5951-9

Muro-Pastor, A. M., & Hess, W. R. (2012). Heterocyst differentiation: From single mutants to global approaches. *Trends in Microbiology*, *20*(11), 548–557. https://doi.org/10.1016/j.tim.2012.07.005

Neilan, B. A., Pearson, L. A., Muenchhoff, J., Moffitt, M. C., & Dittmann, E. (2013). Environmental conditions that influence toxin biosynthesis in cyanobacteria. *Environmental Microbiology*, *15*(5), 1239–1253. https://doi.org/10.1111/j.1462-

2920.2012.02729.x

Nübel, U., Garcia-Pichel, F., & Muyzer, G. (1997). PCR primers to amplify 16S rRNA genes from cyanobacteria. *Applied and Environmental Microbiology*, *63*(8), 3327–3332. https://doi.org/10.1128/aem.63.8.3327-3332.1997

O'Neil, J. M., Davis, T. W., Burford, M. A., & Gobler, C. J. (2012). The rise of harmful cyanobacteria blooms: The potential roles of eutrophication and climate change. *Harmful Algae*, *14*, 313–334. https://doi.org/10.1016/j.hal.2011.10.027

Ohtani, I., Moore, R. E., & Runnegar, M. T. C. (1992). Cylindrospermopsin: A Potent Hepatotoxin from the Blue-Green Alga Cylindrospermopsis raciborskii. *Journal of the American Chemical Society*, *114*, 7941–7942. https://doi.org/10.1021/ja00046a067

Oksanen, A. J., Blanchet, F. G., Friendly, M., Kindt, R., Legendre, P., Mcglinn, D., Minchin, P. R., Hara, R. B. O., Simpson, G. L., Solymos, P., Stevens, M. H. H., & Szoecs, E. (2020). *Vegan: Community Ecology Package. R package*. *January*.

Oshima, Y. (1995). Postcolumn Derivatization Liquid Chromatographic Method for Paralytic Shellfish Toxins. *Journal of AOAC INTERNATIONAL*, *78*(2), 528–532. https://doi.org/10.1093/jaoac/78.2.528

Osswald, J., Rellán, S., Gago, A., & Vasconcelos, V. (2007). Toxicology and detection methods of the alkaloid neurotoxin produced by cyanobacteria, anatoxin-a. *Environment International*, *33*(8), 1070–1089. https://doi.org/10.1016/j.envint.2007.06.003

Paerl, H. W., & Huisman, J. (2008). Blooms like it hot. *Science*, *320*(5872), 57–58. https://doi.org/10.1126/science.1155398

Pearson, L., Mihali, T., Moffitt, M., Kellmann, R., & Neilan, B. (2010). On the chemistry, toxicology and genetics of the cyanobacterial toxins, microcystin, nodularin, saxitoxin and cylindrospermopsin. In *Marine Drugs* (Vol. 8, Issue 5). https://doi.org/10.3390/md8051650

Peng, G., Martin, R. M., Dearth, S. P., Sun, X., Boyer, G. L., Campagna, S. R., Lin, S., & Wilhelm, S. W. (2018). Seasonally Relevant Cool Temperatures Interact with N Chemistry to Increase Microcystins Produced in Lab Cultures of Microcystis

aeruginosa NIES-843. *Environmental Science and Technology*, *52*(7), 4127–4136. https://doi.org/10.1021/acs.est.7b06532

Porat, R. (2001). Diel Buoyancy Changes by the Cyanobacterium Aphanizomenon ovalisporum from a Shallow Reservoir. *Journal of Plankton Research*, *23*(7), 753–763. https://doi.org/10.1093/plankt/23.7.753

Puddick, J., Prinsep, M. R., Wood, S. A., Kaufononga, S. A. F., Cary, S. C., & Hamilton, D. P. (2014). High Levels of Structural Diversity Observed in Microcystins from Microcystis CAWBG11 and Characterization of Six New Microcystin Congeners. *Marine Drugs*, *12*, 5372–5395. https://doi.org/10.3390/md12115372

Quast, C., Pruesse, E., Yilmaz, P., Gerken, J., Schweer, T., Yarza, P., Peplies, J., & Glöckner, F. O. (2013). The SILVA ribosomal RNA gene database project: Improved data processing and web-based tools. *Nucleic Acids Research*, *41*, D590–D596. https://doi.org/10.1093/nar/gks1219

R Core Team. (2020). *R: a Language and Environment for Statistical Computing. R Foundation for Statistical Computing, Vienna, Austria https://www.R-project.*

Rai, A. N., Bergman, B., & Rasmussen, U. (2002). *Cyanobacteria in Symbiosis*. Kluwer Academic Publishers.

Rampelotto, P. H. (2013). Extremophiles and Extreme Environments. *Life*, *3*, 482–485. https://doi.org/10.3390/life3030482

Rantala, A., Fewer, D. P., Hisbergues, M., Rouhiainen, L., Vaitomaa, J., Börner, T., & Sivonen, K. (2004). Phylogenetic evidence for the early evolution of microcystin synthesis. *Proceedings of the National Academy of Sciences of the United States of America*, *101*(2), 568–573. https://doi.org/10.1073/pnas.0304489101

Rastogi, R. P., Madamwar, D., & Incharoensakdi, A. (2015). Bloom dynamics of cyanobacteria and their toxins: Environmental health impacts and mitigation strategies. *Frontiers in Microbiology*, *6*(NOV), 1–22. https://doi.org/10.3389/fmicb.2015.01254

Reynolds, C. S., & Walsby, A. E. (1975). Water blooms. *Biological Reviews of the Cambridge Philosophical Society*, *50*, 437–481. https://doi.org/10.1111/j.1469-185X.1975.tb01060.x

Roche. (n.d.). *Roche LightCycler 480 Instrument - Operator`s Manual*.

Rognes, T., Flouri, T., Nichols, B., Quince, C., & Mahé, F. (2016). VSEARCH: A versatile open source tool for metagenomics. *PeerJ*, *4*(e2584), 1–22. https://doi.org/10.7717/peerj.2584

Rychlik, W., Spencer, W. J., & Rhoads, R. E. (1990). Optimization of the annealing temperature for DNA amplification in vitro. *Nucleic Acids Research*, *18*(21), 6409–6412. https://doi.org/10.1093/nar/19.3.698-a

Sagan, L. (1967). On the origin of mitosing cells. *Journal of Theoretical Biology*, *14*, 225–274. https://doi.org/10.1016/0022-5193(67)90079-3

Schantz, E. J., Ghazarossian, V. E., Schnoes, H. K., Strong, F. M., Spinger, J. P., Pezzanite, J. O., & Clardy, J. (1975). The Structure of Saxitoxin. *Journal of the American Chemical Society*, *97*(5), 1238–1239. https://doi.org/10.1021/ja00838a045

Schimanski, J. (2002). Entwicklung und Erprobung eines Durchflußsensors zur Algenklassenbestimmung durch Chlorophyll-Fluoreszenz. *Diplomarbeit*.

Schindler, D. W., Hecky, R. E., Findlay, D. L., Stainton, M. P., Parker, B. R., Paterson, M. J., Beaty, K. G., Lyng, M., & Kasian, S. E. M. (2008). Eutrophication of lakes cannot be controlled by reducing nitrogen input: Results of a 37-year whole-ecosystem experiment. *Proceedings of the National Academy of Sciences of the United States of America*, *105*(32), 11254–11258. https://doi.org/10.1073/pnas.0805108105

Schirrmeister, B. E., Gugger, M., & Donoghue, P. C. J. (2015). Cyanobacteria and the Great Oxidation Event: Evidence from genes and fossils. *Palaeontology*, *58*(5), 769–785. https://doi.org/10.1111/pala.12178

Schloerke, B., Cook, D., Larmarange, J., Briatte, F., Marbach, M., Thoen, E., Elberg, A., Crowley, J., & Crowley. (2021). *GGally: Extension to "ggplot2". R package version 2.1.0.* https://cran.r-project.org/package=GGally

Schloss, P. D., Westcott, S. L., Ryabin, T., Hall, J. R., Hartmann, M., Hollister, E. B., Lesniewski, R. A., Oakley, B. B., Parks, D. H., Robinson, C. J., Sahl, J. W., Stres, B., Thallinger, G. G., Van Horn, D. J., & Weber, C. F. (2009). Introducing mothur:

Open-source, platform-independent, community-supported software for describing and comparing microbial communities. *Applied and Environmental Microbiology*, *75*(23), 7537–7541. https://doi.org/10.1128/AEM.01541-09

Schwoerbel, J., & Brendelberger, H. (2013). *Einführung in die Limnologie* (10th ed.). Springer Spektrum.

Seppälä, J., Ylöstalo, P., Kaitala, S., Hällfors, S., Raateoja, M., & Maunula, P. (2007). Ship-of-opportunity based phycocyanin fluorescence monitoring of the filamentous cyanobacteria bloom dynamics in the Baltic Sea. *Estuarine, Coastal and Shelf Science*, *73*(3–4), 489–500. https://doi.org/10.1016/j.ecss.2007.02.015

Sevilla, E., Martin-Luna, B., Vela, L., Teresa Bes, M., Luisa Peleato, M., & Fillat, M. F. (2010). Microcystin-LR synthesis as response to nitrogen: Transcriptional analysis of the mcyD gene in Microcystis aeruginosa PCC7806. *Ecotoxicology*, *19*, 1167–1173. https://doi.org/10.1007/s10646-010-0500-5

Singh, N. K., & Dhar, D. W. (2013). Cyanotoxins, related health hazards on animals and their management: A Review. *Indian Journal of Animal Sciences*, *83*(11), 1111–1127.

Stackebrandt, E., & Goebel, B. M. (1994). Taxonomic Note: A Place for DNA-DNA Reassociation and 16S rRNA Sequence Analysis in the Present Species Definition in Bacteriology. *The Lancet*, *44*(4), 846–849. https://doi.org/10.1016/S0140-6736(01)43317-4

Swails, B., & Rahim, Z. (2020). Toxins in water blamed for deaths of hundreds of elephants in Botswana. *CNN*. https://edition.cnn.com/2020/09/21/africa/botswana-elephant-deaths-intl/index.html. Date: 21.09.2020

Tandeau De Marsac, N. (1977). Occurrence and nature of chromatic adaptation in cyanobacteria. *Journal of Bacteriology*, *130*(1), 82–91. https://doi.org/10.1128/jb.130.1.82-91.1977

Taranu, Z. E., Gregory-Eaves, I., Leavitt, P. R., Bunting, L., Buchaca, T., Catalan, J., Domaizon, I., Guilizzoni, P., Lami, A., Mcgowan, S., Moorhouse, H., Morabito, G., Pick, F. R., Stevenson, M. A., Thompson, P. L., & Vinebrooke, R. D. (2015).

Acceleration of cyanobacterial dominance in north temperate-subarctic lakes during the Anthropocene. *Ecology Letters*, *18*, 375–384. https://doi.org/10.1111/ele.12420

Tillett, D., Dittmann, E., Erhard, M., Von Döhren, H., Börner, T., & Neilan, B. A. (2000). Structural organization of microcystin biosynthesis in Microcystis aeruginosa PCC7806: An integrated peptide-polyketide synthetase system. *Chemistry and Biology*, *7*(10), 753–764. https://doi.org/10.1016/S1074-5521(00)00021-1

Tilzer, M. M. (1987). Light-dependence of photosynthesis and growth in cyanobacteria: Implications for their dominance in eutrophic lakes. *New Zealand Journal of Marine and Freshwater Research*, *21*(3), 401–412. https://doi.org/10.1080/00288330.1987.9516236

Trimbee, A. M., & Prepas, E. E. (1988). The effect of oxygen depletion on the timing and magnitude of blue-green algal blooms. *Verh. Internat. Verein. Limnol.*, *23*, 220–226. https://doi.org/10.1080/03680770.1987.11897929

Tromas, N., Fortin, N., Bedrani, L., Terrat, Y., Cardoso, P., Bird, D., Greer, C. W., & Shapiro, B. J. (2017). Characterising and predicting cyanobacterial blooms in an 8-year amplicon sequencing time course. *ISME Journal*, *11*(8), 1746–1763. https://doi.org/10.1038/ismej.2017.58

Trout-Haney, J. V., Wood, Z. T., & Cottingham, K. L. (2016). Presence of the cyanotoxin microcystin in Arctic lakes of Southwestern Greenland. *Toxins*, *8*(9), 20–24. https://doi.org/10.3390/toxins8090256

Turner, S., Pryer, K. M., Miao, V. P. W., & Palmer, J. D. (1999). Investigating deep phylogenetic relationships among cyanobacteria and plastids by small subunit rRNA sequence analysis. *Journal of Eukaryotic Microbiology*, *46*(4), 327–338. https://doi.org/10.1111/j.1550-7408.1999.tb04612.x

Vezie, C., Brient, L., Sivonen, K., Bertru, G., Lefeuvre, J. C., & Salkinoja-Salonen, M. (1997). Occurrence of microcystin-containing cyanobacterial blooms in freshwaters of Brittany (France). *Archiv Fur Hydrobiologie*, *139*(3), 401–413. https://doi.org/10.1127/archiv-hydrobiol/139/1997/401

Vézie, C., Rapala, J., Vaitomaa, J., Seitsonen, J., & Sivonen, K. (2002). Effect of

nitrogen and phosphorus on growth of toxic and nontoxic Microcystis strains and on intracellular microcystin concentrations. *Microbial Ecology*, *43*(4), 443–454. https://doi.org/10.1007/s00248-001-0041-9

Visser, P. M., Verspagen, J. M. H., Sandrini, G., Stal, L. J., Matthijs, H. C. P., Davis, T. W., Paerl, H. W., & Huisman, J. (2016). How rising CO2 and global warming may stimulate harmful cyanobacterial blooms. *Harmful Algae*, *54*, 145–159. https://doi.org/10.1016/j.hal.2015.12.006

Vollenweider, R. A., & Kerekes, J. (1982). *Eutrophication of Waters, Monitoring, Assessment and Control*. OECD.

Vu, V. Q. (2011). *ggbiplot: A ggplot2 based biplot. R package version 0.55.* http://github.com/vqv/ggbiplot

Wallace, R. B., Shaffer, J., Murphy, R. F., Bonner, J., Hirose, T., & Itakura, K. (1979). Hybridization of synthetic oligodeoxyribonucleotides to φX 174 DNA: The effect of single base pair mismatch. *Nucleic Acids Research*, *6*(11), 3543–3558. https://doi.org/10.1093/nar/6.11.3543

Wang, Q., Garrity, G. M., Tiedje, J. M., & Cole, J. R. (2007). Naïve Bayesian classifier for rapid assignment of rRNA sequences into the new bacterial taxonomy. *Applied and Environmental Microbiology*, *73*(16), 5261–5267. https://doi.org/10.1128/AEM.00062-07

Wang, X., & Chen, X. (2019). Chapter 12 - Application of Novel Nanomaterials for Chemo- and Biosensing of Algal Toxins in Shellfish and Water. *In Micro and Nano Technologies, Novel Nanomaterials for Biomedical, Environmental and Energy Applications, Elsevier*, 353–414. https://doi.org/https://doi.org/10.1016/B978-0-12-814497-8.00012-6

Watson, S. B., McCauley, E., & Downing, J. A. (1997). Patterns in phytoplankton taxonomic composition across temperate lakes of differing nutrient status. *Limnology and Oceanography*, *42*(3), 487–495. https://doi.org/10.4319/lo.1997.42.3.0487

Watson, S. B., Ridal, J., & Boyer, G. L. (2008). Taste and odour and cyanobacterial toxins: impariment, prediction, and management in the Great Lakes. *Canadian*

Journal of Fisheries and Aquatic Sciences, *65*(8), 1779–1796.

Watzer, B., & Forchhammer, K. (2018). *Cyanophycin: A Nitrogen-Rich Reserve Polymer*. https://doi.org/10.5772/intechopen.77049

Wetzel, R. G. (2001). *Limnology - Lake and River Ecosystems* (third). Academic Press. https://www.elsevier.com/books/limnology/wetzel/978-0-08-057439-4

Wickham, H. (2016). *ggplot2: Elegant Graphics for Data Analysis.* (ISBN 978-3). Springer-Verlag New York.

Woese, C. R., & Fox, G. E. (1977). Phylogenetic structure of the prokaryotic domain: The primary kingdoms. *Proceedings of the National Academy of Sciences of the United States of America*, *74*(11), 5088–5090. https://doi.org/10.1073/pnas.74.11.5088

Wolk, C. P., Ernst, A., & Elhai, J. (1994). Heterocyst Metabolism and Development. *The Molecular Biology of Cyanobacteria*, 769–823. https://doi.org/10.1007/978-94-011-0227-8_27

Wood, S. A., Selwood, A. I., Rueckert, A., Holland, P. T., Milne, J. R., Smith, K. F., Smits, B., Watts, L. F., & Cary, C. S. (2007). First report of homoanatoxin-a and associated dog neurotoxicosis in New Zealand. *Toxicon*, *50*(2), 292–301. https://doi.org/10.1016/j.toxicon.2007.03.025

Xiao, M., Li, M., & Reynolds, C. S. (2018). Colony formation in the cyanobacterium Microcystis. *Biological Reviews*, *93*(3), 1399–1420. https://doi.org/10.1111/brv.12401

ZAMG. (2020). *Vorläufigen Sommerbilanz der ZAMG*. https://www.zamg.ac.at/cms/de/klima/news/sommer-2020-sehr-warm-und-relativ-feucht

Zhang, J., Ding, X., Guan, R., Zhu, C., Xu, C., Zhu, B., Zhang, H., Xiong, Z., Xue, Y., Tu, J., & Lu, Z. (2018). Evaluation of different 16S rRNA gene V regions for exploring bacterial diversity in a eutrophic freshwater lake. *Science of the Total Environment*, *618*, 1254–1267. https://doi.org/10.1016/j.scitotenv.2017.09.228

Ziegmann, M., Abert, M., Müller, M., & Frimmel, F. H. (2010). Use of fluorescence

fingerprints for the estimation of bloom formation and toxin production of Microcystis aeruginosa. *Water Research*, *44*(1), 195–204. https://doi.org/10.1016/j.watres.2009.09.035

Zilliges, Y., Kehr, J. C., Meissner, S., Ishida, K., Mikkat, S., Hagemann, M., Kaplan, A., Börner, T., & Dittmann, E. (2011). The cyanobacterial hepatotoxin microcystin binds to proteins and increases the fitness of Microcystis under oxidative stress conditions. *PLoS ONE*, *6*(3), 1–11. https://doi.org/10.1371/journal.pone.0017615

7 Zusammenfassung

Cyanobakterienblüten stellen ein großes Problem in Seen dar, da sie Auswirkungen auf das gesamte Ökosystem haben und Gesundheitsprobleme beim Menschen verursachen können. Dennoch sind Parameter, die die Entwicklung von toxischen Cyanobakterienblüten beeinflussen, unbekannt. Gemäß Artikel 8 der Badegewässerrichtlinie (2006/7/EG) soll ein Überwachungssystem mittels High Throughput Sequencing eingesetzt werden, welches die Zusammensetzung der Bakterienarten über die Saison betrachtet und als Frühwarnsystem fungiert.

Ziel dieser Masterarbeit war es, eine Arbeitsanleitung für das Monitoring von Cyanobakterien in österreichischen Badegewässern zu erarbeiten. Dazu wurden im Jahr 2020, regelmäßig über die Badesaison verteilt, an 20 Badestellen planktische und benthische Proben genommen und mit allgemeinen bakteriellen und spezifischen cyanobakteriellen 16S Primern analysiert. Daneben wurden Korrelationen mit der cyanobakteriellen Sequenzanzahl, der Toxinkonzentration und abiotischen und biotischen Faktoren durchgeführt, um Referenzpunkte bei in-situ Messungen zu bestimmen. Schließlich wurden benthische Matten gesammelt, um den Ursprung der Toxine aus benthischen, filamentösen Cyanobakterienkolonien abzuschätzen.

Die Ergebnisse zeigen, dass die cyanobakterielle Sequenzanzahl und die Cyanotoxinproduktion mit der Wasseroberflächentemperatur korrelieren. Darüber hinaus bietet die Technik der Amplikon-Sequenzierung einen großen Einblick in die bakterielle Gemeinschaft und ermöglicht die Überwachung und Vorhersage von cyanobakteriellen toxischen Algenblüten in Badegewässern. Die Analyse der Sequenzdaten ergab höhere Cyanobakterienhäufigkeiten, wenn sie in Amplicon Sequence Variants geclustert wurden, verglichen mit Operational Taxonomic Units. Mit Hilfe von in-situ-Fluoreszenzmessungen wurde eine grobe quantitative Abschätzung der cyanobakteriellen Gemeinschaft gewonnen. Die gesammelten benthischen Biofilme wurden oftmals von potenziell toxischen Cyanobakterien dominiert, dennoch konnte die Toxinproduktion nicht mit ihnen in Verbindung gebracht werden.

8 Appendix

8.1 Rarefaction Curves (RFC)

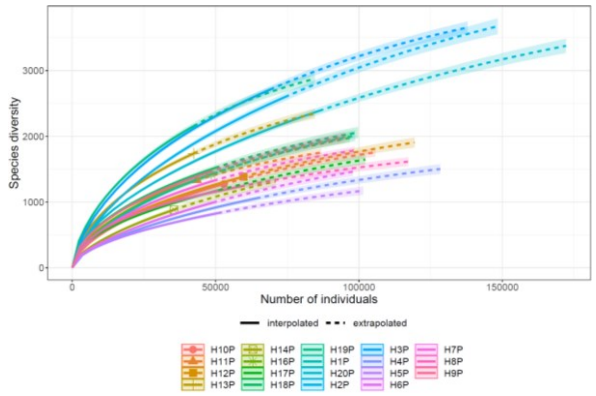

mothur Herleman C1

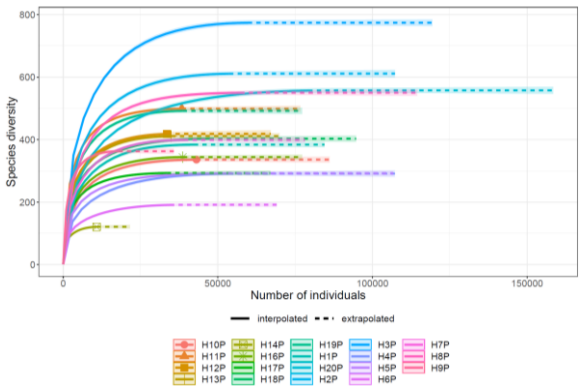

DADA2 Herleman C1

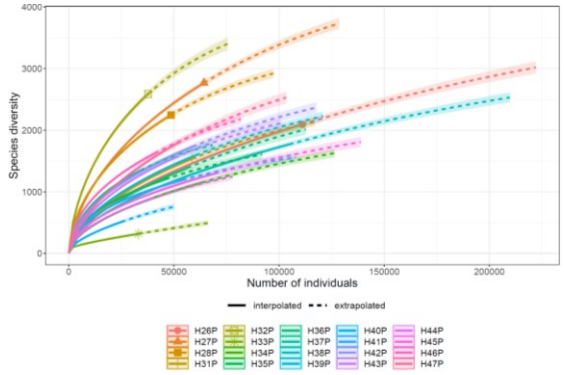

mothur Herleman C2

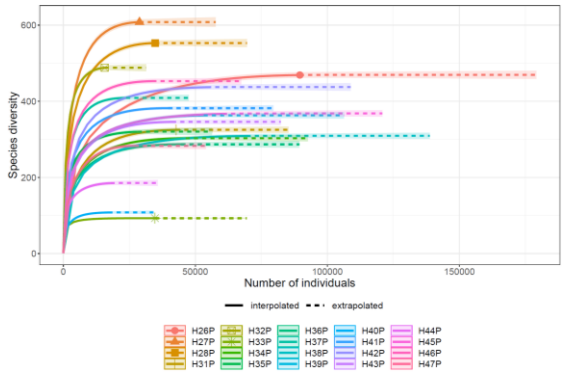

DADA2 Herleman C2

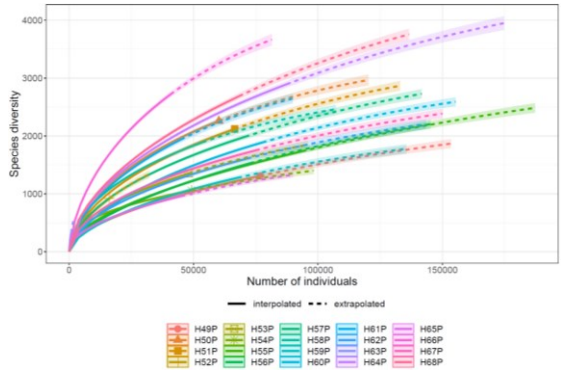

mothur Herleman C3

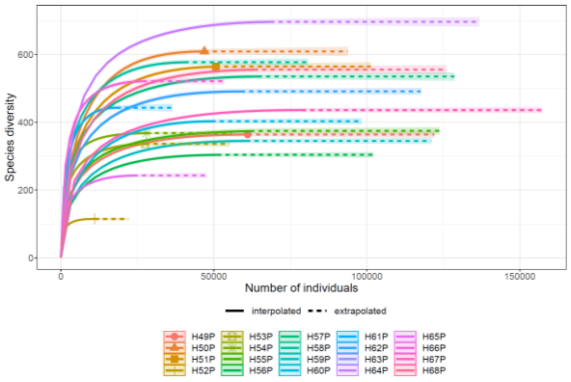

DADA2 Herleman C3

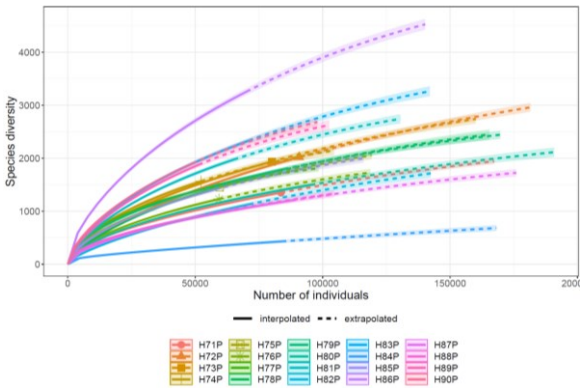

mothur Herleman C4

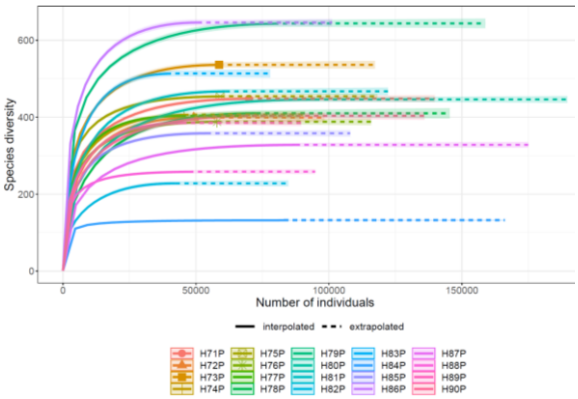

DADA2 Herleman C4

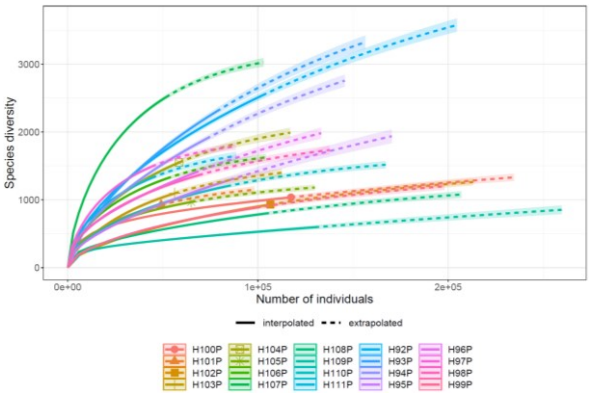

mothur Herleman C5

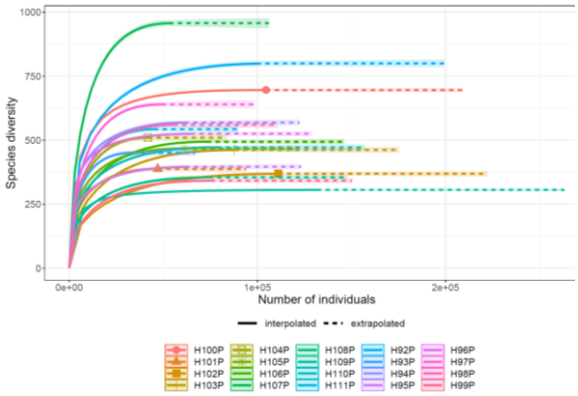

DADA2 Herleman C5

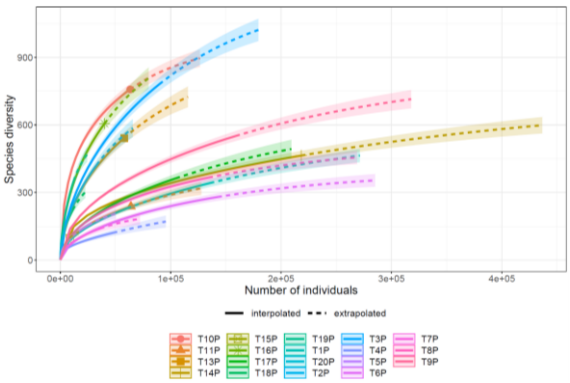

mothur Turner C1

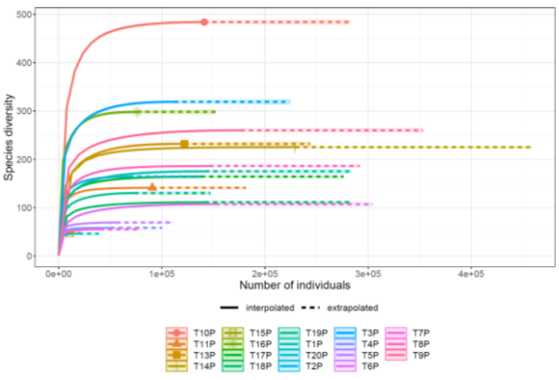

DADA2 Turner C1

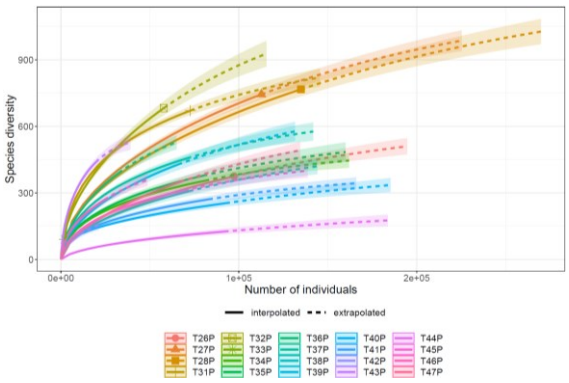

mothur Turner C2

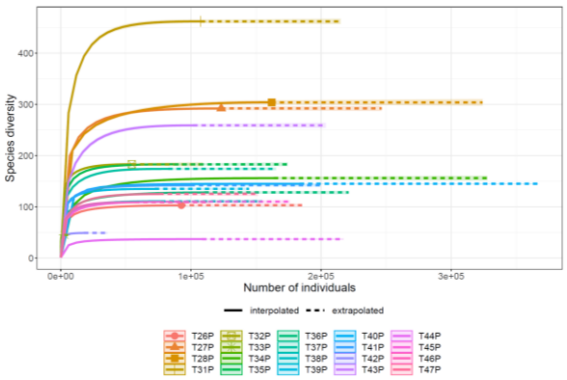

DADA2 Turner C2

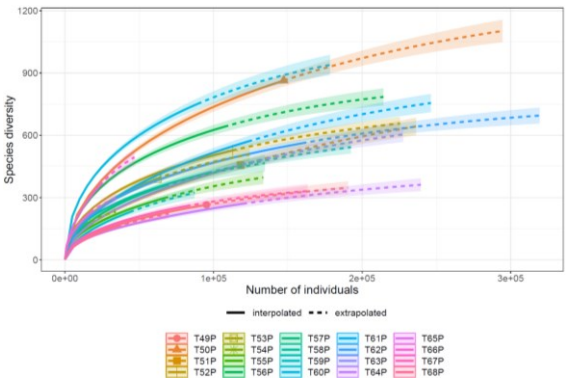

mothur Turner C3

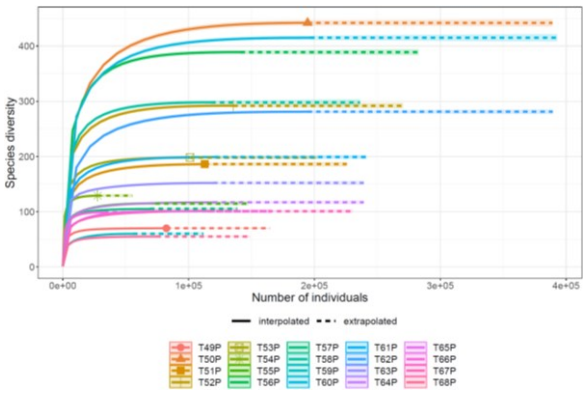

DADA2 Turner C3

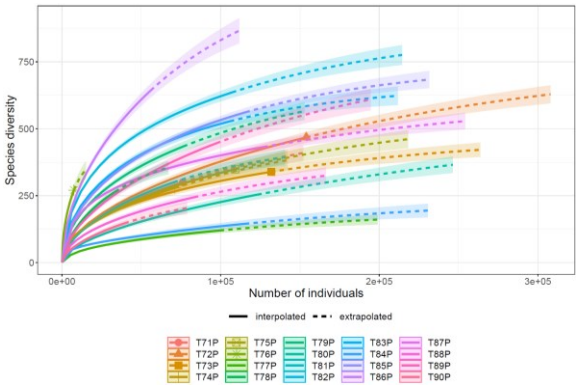

mothur Turner C4

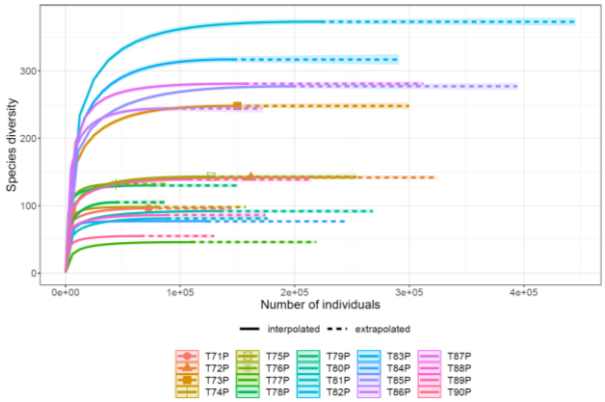

DADA2 Turner C4

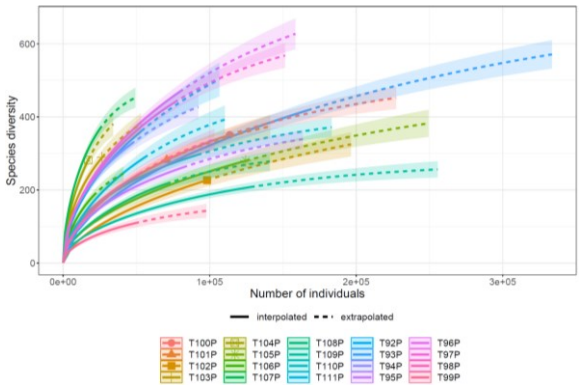

mothur Turner C5

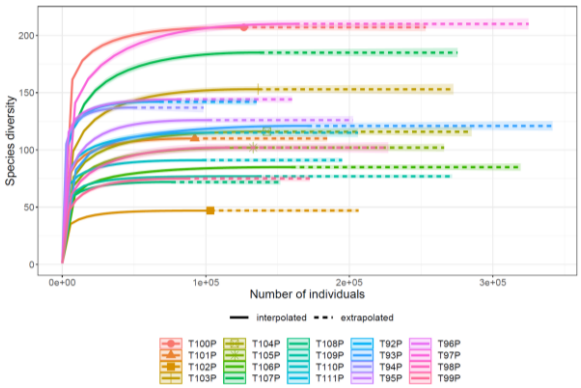

DADA2 Turner C5

8.2 Melting Curves

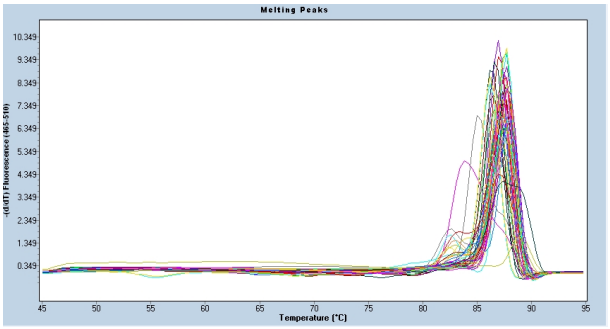

Melting curve of 46 plankton samples. Cyanobacterial primers with overhangs were used. Annealing temperature was 65°C. No $MgCl_2$ was added.

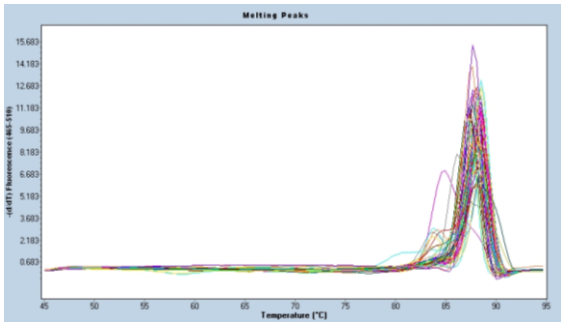

Amplification curve of 46 plankton samples. Cyanobacterial primers with overhangs were used. Annealing temperature was 65°C and 1.5 µM $MgCl_2$ was added.

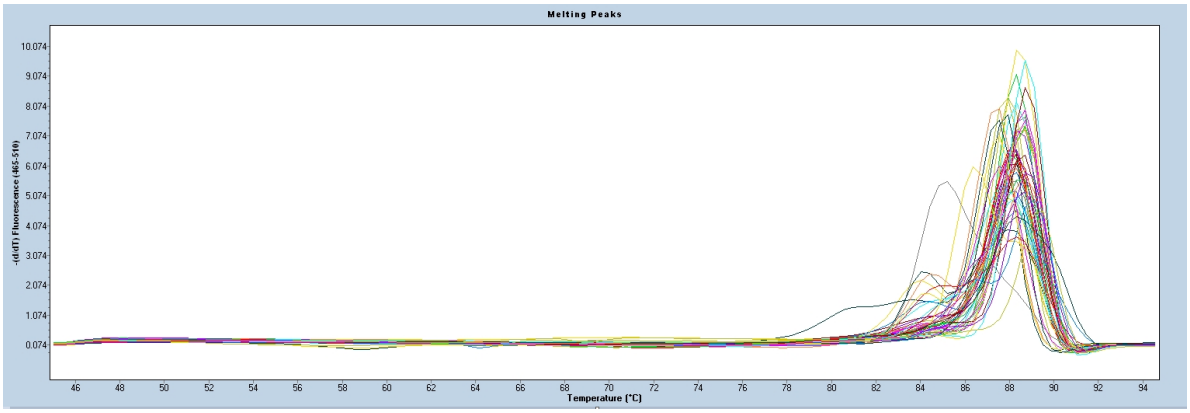

Amplification curve of 46 plankton samples. Cyanobacterial primers with overhangs were used. Annealing temperature was 62°C and 1.5 µM $MgCl_2$ was added.

8.3 Metadata

8.3.1 Abiotic and Biotic factors

TEMP = Temperature, O_2 = Oxygen, COND = Conductivity, SECCHI = Secchi depth, TCL = Total Chlorophyll, CCL = Cyanochloropyll, TP = Total Phosphorus, NO_2-N = Nitrite nitrogen, NH_4-N = Ammonium nitrogen, NO_3-N = Nitrate nitrogen, NA = not measured

SAMPLE ID	DATE	EVENT	TEMP [°C]	O_2 [%]	COND [µS cm^{-1}]	pH	SECCHI [m]	TCL [µg Chl-a L^{-1}]	CCL [µg Chl-a L^{-1}]	TP [µg L^{-1}]	NO_2-N [µg L^{-1}]	NH_4-N [µg L^{-1}]	NO_3-N [µg L^{-1}]	ENTEROCOCCI [CFU $100ml^{-1}$]	E.COLI [CFU $100ml^{-1}$]
1	2.6.	1	17.1	105.1	472	8.3	195	2.5	2.22	8.77	0	0.073	0.196	NA	NA
2	2.6.	1	17.9	122.4	388	8.356	NA	0.42	0.38	10.98	0	0.079	0.259	NA	NA
3	2.6.	1	17.1	97	418	8.05	160	1.45	0.41	10.22	0	0.057	0.488	NA	NA
4	2.6.	1	16.3	95	NA	8.3	170	2.8	0	16.1	NA	NA	NA	15	15
5	2.6.	1	17.1	114	NA	8.5	180	6.3	0	8	NA	NA	NA	15	15
6	2.6.	1	16.9	83	NA	8.3	180	5.8	0	NA	NA	NA	NA	15	30
7	2.6.	1	17.2	83	NA	7.8	80	28.9	10.7	NA	NA	NA	NA	15	15
8	2.6.	1	17	129	NA	8.2	120	3.9	0	NA	NA	NA	NA	15	15
9	2.6.	1	18.8	119	NA	9	60	78.9	27.6	39.5	NA	NA	NA	15	15
10	2.6.	1	18.6	101	NA	7.1	200	0.1	0	NA	NA	NA	NA	15	15
11	2.6.	1	17.5	117	NA	8.8	80	48.6	41.3	47.5	NA	NA	NA	15	61
12	2.6.	1	17.5	125	NA	8.6	100	41.3	1.7	17.7	NA	NA	NA	15	15
13	3.6.	1	16.6	108	NA	8.2	160	3.1	0	5.9	NA	NA	NA	15	580
14	3.6.	1	16.6	98	NA	7.9	200	2.2	0	13.7	NA	NA	NA	15	15
15	3.6.	1	16.8	100	NA	8.3	160	5.9	0	NA	NA	NA	NA	15	15
16	3.6.	1	16.8	126	NA	8.4	120	13.9	4.2	NA	NA	NA	NA	15	15
17	3.6.	1	16.1	122	NA	8.8	160	6.7	0.2	NA	NA	NA	NA	15	15
18	3.6.	1	18.5	143	NA	9.2	100	12.5	1.5	15.8	NA	NA	NA	15	15
19	3.6.	1	17.1	118	NA	8.4	120	12.5	1.5	NA	NA	NA	NA	15	15
20	3.6.	1	16.1	130	NA	9.3	40	19.9	14	NA	NA	NA	NA	61	15
21	13.6.	2	24.7	91.6	455	7.711	NA	0.75	0.09	6.39	0	0.041	0.231	NA	NA
22	13.6.	2	25.7	107.1	455	7.71	NA	1.5	0.13	6.45	0	0.045	0.22	NA	NA

22	13.6.	2	25.7	107.1	455	7.71	NA	1.5	0.13	6.45	0	0.045	0.22	NA	NA
23	13.6.	2	23.7	90.8	439	7.799	NA	0.8	0.52	9.3	0	0.052	0.218	NA	NA
24	13.6.	2	24.4	113	412	8.217	NA	1.76	0.55	11.96	0	0.06	0.201	NA	NA
25	15.6.	2	21.8	93.9	346	8.336	220	0.46	0.46	6.28	0	0.068	0.198	NA	NA
26	15.6.	2	22.4	104.7	463	8.19	190	6.01	3.16	10.2	0	0.039	0.2	NA	NA
27	15.6.	2	21.3	105	371	7.498	NA	0.42	0.42	9.61	0	0.095	0.212	NA	NA
28	15.6.	2	22	94.4	398	8.102	170	2.61	0.89	9.65	0	0.072	0.364	NA	NA
29	17.6.	2	22.0	134	404	9.646	300	2.15	1.22	6.09	0	0.027	0.207	NA	NA
30	18.6.	2	21.1	97	312	9.212	220	2.3	1.16	8.34	0	0.017	0.209	NA	NA
31	16.6.	2	19.4	106	NA	8.1	200	4.6	0.3	21.2	NA	NA	NA	15	15
32	16.6.	2	18.4	109	NA	8	200	2.5	2.5	NA	NA	NA	NA	15	15
33	15.6.	2	21.8	109	NA	8.5	170	9.2	0	0	NA	NA	NA	15	15
34	15.6.	2	21.2	106	NA	8.4	200	0.8	0	17.4	NA	NA	NA	309	15
35	16.6.	2	21.2	140	NA	8.7	110	36.9	0	16.2	NA	NA	NA	15	15
36	16.6.	2	20.6	87	NA	7.8	70	19.2	1.2	NA	NA	NA	NA	15	15
37	16.6.	2	21.3	165	NA	8.2	140	3.1	0	NA	NA	NA	NA	15	15
38	16.6.	2	22.5	137	NA	9	20	96.8	15.1	52.4	NA	NA	NA	15	15
39	16.6.	2	21	149	NA	9.3	40	71.7	17.3	NA	NA	NA	NA	15	15
40	16.6.	2	21.7	114	NA	7.8	300	2.8	0	NA	NA	NA	NA	110	30
41	16.6.	2	22.8	127	NA	8.5	80	39.6	12.3	60	NA	NA	NA	15	15
42	17.6.	2	20.1	104	NA	8.5	160	15.1	0.8	NA	NA	NA	NA	15	15
43	17.6.	2	10.6	89	NA	8	100	10.6	5	NA	NA	NA	NA	195	110
44	17.6.	2	19.2	136	NA	9.7	140	15.1	0.8	NA	NA	NA	NA	15	15
45	17.6.	2	20	142	NA	10	100	21.6	2	NA	NA	NA	NA	15	15
46	17.6.	2	18.8	124	NA	8.8	120	15.6	4	NA	NA	NA	NA	15	15
47	17.6.	2	18.2	107	NA	7.7	40	56.6	40	57.4	NA	NA	NA	15	272
48	7.7.	3	23.4	106.8	352	8.305	210	2.76	0.92	9.51	0.012	0.022	0.401	NA	NA
49	7.7.	3	24.6	133.4	431	8.443	160	16.61	6.41	13.7	0.003	0.014	0.288	NA	NA

50	7.7.	3	22.3	103.3	355	8.105	NA	4.2	0.88	14.4	0.006	0.044	0.312	NA	NA
51	7.7.	3	22.9	103.6	397	8.098	170	16.18	3.01	21.7	0.009	0.054	0.374	NA	NA
52	6.7.	3	23.2	130	NA	8.5	140	20.6	0	32.4	NA	NA	NA	15	15
53	6.7.	3	22.7	134	NA	8.4	60	53.8	9.2	59.8	NA	NA	NA	15	30
54	6.7.	3	23.6	185	NA	8.3	140	9	0	18.2	NA	NA	NA	15	15
55	6.7.	3	25.2	278	NA	8.8	40	128.3	8.8	89.5	NA	NA	NA	15	15
56	6.7.	3	23.7	218	NA	7.4	300	7.8	0	12.9	NA	NA	NA	15	15
57	6.7.	3	21.4	278	NA	9.1	60	101.7	29.6	81.3	NA	NA	NA	15	160
58	6.7.	3	24.2	111	NA	8.5	180	8	1.9	19.5	NA	NA	NA	15	15
59	6.7.	3	24.6	123	NA	8.4	160	3.3	1.5	12.3	NA	NA	NA	15	15
60	7.7.	3	21.6	110	NA	8.1	200	5.5	0.2	10.3	NA	NA	NA	15	30
61	7.7.	3	17.9	97	NA	7.9	200	9.9	0.8	13.8	NA	NA	NA	15	15
62	6.7.	3	23.5	122	NA	8.6	40	38.1	19.4	45.2	NA	NA	NA	15	15
63	8.7.	3	22.4	145	NA	8.5	160	17.4	3.6	NA	NA	NA	NA	30	15
64	8.7.	3	18.8	112	NA	8.5	1.4	NA	NA	NA	NA	NA	NA	15	30
65	8.7.	3	22	121	NA	8.9	130	6	0	NA	NA	NA	NA	46	46
66	8.7.	3	22.7	107	NA	9.5	100	4.7	1.5	71	NA	NA	NA	15	15
67	8.7.	3	21.9	113	NA	9.8	100	20.9	5.7	NA	NA	NA	NA	15	15
68	8.7.	3	21.9	109	NA	7.5	40	31.8	19.1	57	NA	NA	NA	15	15
69	16.7.	3	21.90	67.4	333	8.147	210	4.93	2.59	2.83	0	0.056	0.2	NA	NA
70	28.7.	4	26.17	126.3	362	8.218	195	6.8	2.42	6.17	0.003	0.27	0.29	NA	NA
71	28.7.	4	26.53	133.2	432	8.414	175	2.23	0.5	4.32	0.01	0.034	0.41	NA	NA
72	28.7.	4	24.97	119.4	333	7.971	NA	11.29	1.74	6.05	0.009	0.039	0.23	NA	NA
73	28.7.	4	25.13	123.8	373	8.327	175	4.01	1.08	9.03	0.012	0.06	0.37	NA	NA
74	28.7.	4	26	156	NA	8.7	80	18.1	1.6	31.3	NA	NA	NA	30	272
75	27.7.	4	20.5	113	NA	8.2	70	46.2	11.8	50.6	NA	NA	NA	15	15
76	27.7.	4	23.5	158	NA	8.6	140	10.1	0	11.7	NA	NA	NA	15	15
77	27.7.	4	24.5	119	NA	8.4	40	90.5	18.4	66.5	NA	NA	NA	15	45

78	27.7.	4	24.3	124	NA	7.8	210	8	0	0	NA	NA	NA	15	15
79	27.7.	4	23.6	160	NA	9.6	30	80.3	27.4	61.2	NA	NA	NA	15	15
80	27.7.	4	22.9	108	NA	8.6	100	8.2	5.9	20.8	NA	NA	NA	15	15
81	27.7.	4	24.7	124	NA	8.5	120	4.6	1.3	11.7	NA	NA	NA	15	15
82	28.7.	4	22.5	137	NA	8.2	200	5.8	0.4	10.2	NA	NA	NA	15	127
83	28.7.	4	21.1	120	NA	8.1	200	6.9	0.5	12.6	NA	NA	NA	15	15
84	27.7.	4	23.8	163	NA	8.7	40	80.9	37.1	23.2	NA	NA	NA	15	15
85	29.7.	4	24.5	130	NA	8.4	180	15.2	0.9	24.9	NA	NA	NA	15	15
86	29.7.	4	15.5	66	NA	7.1	200	16	2	27.7	NA	NA	NA	15	15
87	29.7.	4	25.2	145	NA	9.1	200	2.6	0	0	NA	NA	NA	15	15
88	29.7.	4	24.5	167	NA	10.1	100	42.4	14.3	32.7	NA	NA	NA	15	15
89	29.7.	4	22.9	128	NA	7.6	200	18.8	2.5	20.9	NA	NA	NA	15	61
90	29.7.	4	24.8	135	NA	8.2	60	53.1	17.2	47	NA	NA	NA	30	15
91	18.8.	5	24.63	91.9	369	7.988	200	0.78	0.55	6.17	0.002	0.072	0.21	NA	NA
92	18.8.	5	25.27	108.6	437	8.227	180	2.07	0.53	5.69	0.002	0.046	0.2	NA	NA
93	18.8.	5	23.70	87.1	320	7.822	NA	0.49	0.08	9.9	0.01	0.098	0.31	NA	NA
94	18.8.	5	23.87	104.2	387	8.224	186	0.69	0.25	9.26	0.003	0.057	0.2	NA	NA
95	18.8.	5	25.5	125	NA	8.4	120	25.7	5.7	26	NA	NA	NA	15	15
96	18.8.	5	22.1	88	NA	7.8	60	69.5	26.6	78.1	NA	NA	NA	15	15
97	18.8.	5	23.2	92	NA	8.2	120	54	3.9	12.4	NA	NA	NA	15	15
98	18.8.	5	23.2	92	NA	8.2	40	111	10.6	81.8	NA	NA	NA	46	15
99	18.8.	5	24.1	142	NA	8.7	160	17.5	0.7	0	NA	NA	NA	15	15
100	18.8.	5	22.9	136	NA	9	40	60.5	29.1	70.5	NA	NA	NA	61	127
101	17.8.	5	24.3	107	NA	8.5	100	26.2	19.3	22.5	NA	NA	NA	15	15
102	17.8.	5	25.9	127	NA	8.4	100	6.2	1.3	11.5	NA	NA	NA	15	15
103	18.8.	5	23.2	137	NA	8	120	43.5	0	0	NA	NA	NA	15	94
104	18.8.	5	20.2	105	NA	8	200	14.8	0	11.6	NA	NA	NA	160	127
105	18.8.	5	24.4	96	NA	8.6	30	101.5	70.7	11.2	NA	NA	NA	30	15

106	20.8.	5	22.4	120	NA	8.4	140	64.9	4.3	41.9	NA	NA	NA	15	15
107	20.8.	5	20.4	95	NA	7.7	140	15.4	1.4	45.7	NA	NA	NA	30	109
108	20.8.	5	24.7	129	NA	9	220	20.8	0.6	20.9	NA	NA	NA	15	15
109	20.8.	5	23.1	145	NA	10	80	70	45.9	34.5	NA	NA	NA	30	15
110	20.8.	5	26.0	131	NA	8.3	100	33.7	12	28.5	NA	NA	NA	15	15
111	20.8.	5	25.6	125	NA	7.7	40	29.3	13.2	41.1	NA	NA	NA	45	30
112	10.9.	6	18.27	75.6	477	7.318	NA	1.35	0.24	8.37	0.007	0.262	0.36	NA	NA
113	10.9.	6	18.23	77	477	7.745	NA	2.56	0.37	8.03	0.006	0.261	0.35	NA	NA
114	10.9.	6	19.23	68.7	397	7.735	NA	2.33	0.68	8.3	0.005	0.328	0.21	NA	NA
115	10.9.	6	21.13	91.5	377	8.055	NA	10.68	1.42	9.8	0.005	0.248	0.2	NA	NA
116	15.9.	6	23.67	128.6	355	8.357	210	3	1.11	8.22	0.005	0.239	0.21	NA	NA
117	15.9.	6	23.83	134.1	424	8.421	190	4.34	2.16	8.8	0.005	0.1387	0.2	NA	NA
118	15.9.	6	22.63	125.8	316	8.229	NA	0.36	0.27	9.48	0.007	0.224	0.24	NA	NA
119	15.9.	6	23.20	105.8	381	8.058	160	7.95	1.79	9.5	0.003	0.261	0.21	NA	NA
120	15.9.	6	22.73	89.1	318	8.642	NA	4.03	1.78	10.5	0.003	0.278	0.21	NA	NA

8.3.2 Toxins

MC = microcystin, ANA = anatoxin, NOD = nodularin, CYR = cylindrospermopsin, NA = not measured

SAMPLE ID	**MC LR (CELL BOUNDED) [µg L^{-1}]**	**MC LR (FREE) [µg L^{-1}]**	**MC RR (CELL BOUNDED) [µg L^{-1}]**	**MC RR (FREE) [µg L^{-1}]**	**MC YR (CELL BOUNDED) [µg L^{-1}]**	**MC YR (FREE) [µg L^{-1}]**	**MC ASPDHBRR (CELL BOUNDED) [µg L^{-1}]**	**MC ASPDHBRR (FREE) [µg L^{-1}]**	**ANA (CELL BOUNDED) [µg L^{-1}]**	**ANA (FREE) [µg L^{-1}]**	**NOD (CELL BOUNDED) [µg L^{-1}]**	**NOD (FREE) [µg L^{-1}]**	**CYR (CELL BOUNDED) [µg L^{-1}]**	**CYR (FREE) [µg L^{-1}]**
1	0	0	0	0	0	0	0	0	0	0	0	0	0	0
2	0	0	0	0	0	0	0	0	0	0	0	0	0	0
3	0	0	0	0	0	0	0	0	0	0	0	0	0	0
4	0	0	0	0	0	0	0	0	0	0	0	0	0	0
5	0	0	0	0	0	0	0	0	0	0	0	0	0	0
6	NA	NA	NA	NA	NA	NA	NA	NA	NA	NA	NA	NA	NA	NA

7	NA	NA	NA	NA	NA	NA	NA	NA	NA	NA	NA	NA	NA	NA
8	NA	NA	NA	NA	NA	NA	NA	NA	NA	NA	NA	NA	NA	NA
9	0	0	0	0	0	0	0	0	0	0	0	0	0	0
10	NA	NA	NA	NA	NA	NA	NA	NA	NA	NA	NA	NA	NA	NA
11	0	0	0	0	0	0	0	0	0	0	0	0	0	0
12	0	0	0	0	0	0	0	0	0	0	0	0	0	0
13	0	0	0	0	0	0	0	0	0	0	0	0	0	0
14	0	0	0	0	0	0	0	0	0	0	0	0	0	0
15	NA	NA	NA	NA	NA	NA	NA	NA	NA	NA	NA	NA	NA	NA
16	NA	NA	NA	NA	NA	NA	NA	NA	NA	NA	NA	NA	NA	NA
17	NA	NA	NA	NA	NA	NA	NA	NA	NA	NA	NA	NA	NA	NA
18	0	0	0	0	0	0	0	0	0	0	0	0	0	0
19	NA	NA	NA	NA	NA	NA	NA	NA	NA	NA	NA	NA	NA	NA
20	NA	NA	NA	NA	NA	NA	NA	NA	NA	NA	NA	NA	NA	NA
21	0	0	0	0	0	0	0	0	0	0	0	0	0	0
22	0	0	0	0	0	0	0	0	0	0	0	0	0	0
22	0	0	0	0	0	0	0	0	0	0	0	0	0	0
23	0	0	0	0	0	0	0	0	0	0	0	0	0	0
24	0	0	0	0	0	0	0	0	0	0	0	0	0	0
25	0	0	0	0	0	0	0	0	0	0	0	0	0	0
26	0	0	0	0	0	0	0	0	0	0	0	0	0	0
27	0	0	0	0	0	0	0	0	0	0	0	0	0	0
28	0	0	0	0	0	0	0	0	0	0	0	0	0	0
29	0	0	0	0	0	0	0	0	0	0	0	0	0	0
30	0	0	0	0	0	0	0	0	0	0	0	0	0	0
31	0	0	0	0	0	0	0	0	0	0	0	0	0	0
32	0	0	0	0	0	0	0	0	0	0	0	0	0	0
33	0	0	0	0	0	0	0	0	0	0	0	0	0	0

34	0	0	0	0	0	0	0	0	0	0	0	0	0	0
35	0	0	0	0	0	0	0	0	0	0	0	0	0	0
36	NA	NA	NA	NA	NA	NA	NA	NA	NA	NA	NA	NA	NA	NA
37	NA	NA	NA	NA	NA	NA	NA	NA	NA	NA	NA	NA	NA	NA
38	0	0	0	0	0	0	0	0	0	0	0	0	0	0
39	0	0	0	0	0	0	0	0	0	0	0	0	0	0
40	0	0	0	0	0	0	0	0	0	0	0	0	0	0
41	0	0.25	0	0	0	0.35	0	0	0	0	0	0	0	0
42	NA	NA	NA	NA	NA	NA	NA	NA	NA	NA	NA	NA	NA	NA
43	NA	NA	NA	NA	NA	NA	NA	NA	NA	NA	NA	NA	NA	NA
44	NA	NA	NA	NA	NA	NA	NA	NA	NA	NA	NA	NA	NA	NA
45	0	0	0	0	0	0	0	0	0	0	0	0	0	0
46	NA	NA	NA	NA	NA	NA	NA	NA	NA	NA	NA	NA	NA	NA
47	0	0	0	0	0	0	0	0	0	0	0	0	0	0
48	0	0	0	0	0	0	0	0	0	0	0	0	0	0
49	0	0	0	0	0	0	0	0	0	0	0	0	0	0
50	0	0	0	0	0	0	0	0	0	0	0	0	0	0
51	0	0	0	0	0	0	0	0	0	0	0	0	0	0
52	0	0	0	0	0	0	0	0	0	0	0	0	0	0
53	0	0	0	0	0	0	0	0	0	0	0	0	0	0
54	0	0	0	0	0	0	0	0	0	0	0	0	0	0
55	0	0	0	0	0	0	0	0	0	0	0	0	0	0
56	0	0	0	0	0	0	0	0	0	0	0	0	0	0
57	0	0	0	0	0	0	0	0	0	0	0	0	0	0
58	0	0	0	0	0	0	0	0	0	0	0	0	0	0
59	0	0	0	0	0	0	0	0	0	0	0	0	0	0
60	0	0	0	0	0	0	0	0	0	0	0	0	0	0
61	0	0	0	0	0	0	0	0	0	0	0	0	0	0

62	0.1	2.01	0	0.28	0.12	2.89	0	0	0	0	0	0	0	0
63	0	0	0	0	0	0	0	0	0	0	0	0	0	0
64	NA	NA	NA	NA	NA	NA	NA	NA	NA	NA	NA	NA	NA	NA
65	NA	NA	NA	NA	NA	NA	NA	NA	NA	NA	NA	NA	NA	NA
66	0	0	0	0	0	0	0	0	0	0	0	0	0	0
67	NA	NA	NA	NA	NA	NA	NA	NA	NA	NA	NA	NA	NA	NA
68	0	0	0	0	0	0	0	0	0	0	0	0	0	0
69	0	0	0	0	0	0	0	0	0	0	0	0	0	0
70	0	0	0	0	0	0	0	0	0	0	0	0	0	0
71	0	0	0	0	0	0	0	0	0	0	0	0	0	0
72	0	0	0	0	0	0	0	0	0	0	0	0	0	0
73	0	0	0	0	0	0	0	0	0	0	0	0	0	0
74	0	0	0	0	0	0	0	0	0	0	0	0	0	0
75	0	0	0	0	0	0	0	0	0	0	0	0	0	0
76	0	0	0	0	0	0	0	0	0	0	0	0	0	0
77	0	0	0	0.1	0	0	0	0	0	0	0	0	0	0
78	0	0	0	0	0	0	0	0	0	0	0	0	0	0
79	0	0.58	0	0.42	0	0	0	0.13	0	0	0	0	0	0
80	0	0	0	0	0	0	0	0	0	0	0	0	0	0
81	0	0	0	0	0	0	0	0	0	0	0	0	0	0
82	0	0	0	0	0	0	0	0	0	0	0	0	0	0
83	0	0	0	0	0	0	0	0	0	0	0	0	0	0
84	0	1.54	0	0	0	1.23	0	0	0	0	0	0	0	0
85	0	0	0	0	0	0	0	0	0	0	0	0	0	0
86	0	0	0	0	0	0	0	0	0	0	0	0	0	0
87	0	0	0	0	0	0	0	0	0	0	0	0	0	0
88	0	1.33	0	1.82	0	0	0	0.35	0	0	0	0	0	0
89	0	0.11	0	0	0	0	0	0	0	0	0	0	0	0

90	0	0.1	0	0.29	0	0	0	0	0	0	0	0	0	0
91	0	0	0	0	0	0	0	0	0	0	0	0	0	0
92	0	0	0	0	0	0	0	0	0	0	0	0	0	0
93	0	0	0	0	0	0	0	0	0	0	0	0	0	0
94	0	0	0	0	0	0	0	0	0	0	0	0	0	0
95	0	0	0	0	0	0	0	0	0	0	0	0	0	0
96	0	0	0	0	0	0	0	0	0	0	0	0	0	0
97	0	0	0	0	0	0	0	0	0	0	0	0	0	0
98	0	0	0	0	0	0	0	0	0	0.11	0	0	0	0
99	0	0	0	0	0	0	0	0	0	0	0	0	0	0
100	0	0.17	0	0.25	0	0	0	0	0	0	0	0	0	0
101	0	0	0	0	0	0	0	0	0	0	0	0	0	0
102	0	0	0	0	0	0	0	0	0	0	0	0	0	0
103	0	0	0	0	0	0	0	0	0	0	0	0	0	0
104	0	0	0	0	0	0	0	0	0	0	0	0	0	0
105	0	1.4	0	0.42	0	0.82	0	0	0	0	0	0	0	0
106	0	0	0	0	0	0	0	0	0	0	0	0	0	0
107	0	0	0	0	0	0	0	0	0	0	0	0	0	0
108	0	0	0	0	0	0	0	0	0	0	0	0	0	0
109	0	0.8	0	1.02	0	0.16	0	0.26	0	0	0	0	0	0
110	0	0	0	0	0	0	0	0	0	0	0	0	0	0
111	0	0.12	0	0.28	0	0	0	0	0	0	0	0	0	0
112	0	0	0.13	0	0	0	0	0	0	0	0	0	0	0
113	0	0	0	0	0	0	0	0	0	0	0	0	0	0
114	0	0	0	0	0	0	0	0	0	0	0	0	0	0
115	0	0	0	0	0	0	0	0	0	0	0	0	0	0
116	0	0	0	0	0	0	0	0	0	0	0	0	0	0
117	0	0	0	0	0	0	0	0	0	0	0	0	0	0

118	0.11	0	0	0	0	0	0	0	0	0	0	0	0	0
119	0	0	0	0	0	0	0	0	0	0	0	0	0	0
120	0	0	0	0	0	0	0	0	0	0	0	0	0	0